Aalto University
School of Chemical
Engineering

Sugam Shukla

FLUIDIZED BED DRYING OF WATER SOLUBLE POLYMER

Master's Programme in Chemical, Biochemical and Materials Engineering
Major in Chemical and Process Engineering

Master's thesis for the degree of Master of Science in Technology submitted for inspection, Espoo, 29.03.2019

Thesis Supervisor: Prof. Ville Alopaeus (Aalto University)
1st Thesis Advisor: Dr. Marko Laakkonen (Kemira Oyj)
2nd Thesis Advisor: Dr. Wenli Zhao (Aalto University)

Aalto University
School of Chemical
Engineering

Aalto University, P.O. BOX 11000, 00076
AALTO
www.aalto.fi

Abstract of Master's Thesis

Author:	Sugam Shukla
Title of thesis:	Fluidized Bed Drying of Water Soluble Polymer
Degree Programme:	Master's Programme in Chemical, Biochemical and Materials Engineering
Major: Chemical and Process Engineering	**Code:** CHEM3034
Thesis Supervisor:	Professor Ville Alopaeus
Thesis Advisors:	Dr. Marko Laakkonen and Dr. Wenli Zhao
Date: 29.03.2019	**Number of pages:** 97+48 **Language:** English

ABSTRACT

The objective of this thesis was to study the effect of various operating parameters on fluidized bed drying of water soluble polyacrylamide-gel (PAM-gel). The elucidated information about PAM-gel, synthesis and drying of PAM and application of dry-polyacrylamide (DPAM) is in the introductory part. Conventional fluid bed dryers (FBDs) and alternative technology in fluidized bed drying is also discussed in the later sections. This study focuses on the effect of varying operating parameters on fluidized bed drying of PAM-gel. It was necessary to determine the equilibrium moisture content (EMC) for DPAM to examine the effect of operating parameters on drying process.

Moreover, analysis were based on data obtained from the in-built data logger of lab-scale batch fluidized bed drying equipment. Various operating parameters such as residence time, airflow, feed particle size, bed load and inlet temperature were studied by analysing the difference between moisture content and particle size distribution before and after the drying process. Analysis confirmed that neither cutting oil nor particle size had any effect on EMC, as expected. Furthermore, examination of operating parameters displayed some operating parameters exhibit direct and some effect indirectly the drying process of PAM-gel in FBDs.

Keywords: Equilibrium Moisture Content (EMC), Fluidized Bed Dryers (FBDs), Polyacrylamide-Gel (PAM-gel), Dry-Polyacrylamide (DPAM)

ACKNOWLEDGEMENTS

I express my sincere gratitude to my supervisor, Prof. Ville Alopaeus, who have given me this opportunity along with his guidance during the thesis. His immense support and liberty to pursue the topic for this thesis kept up my motivation.

This thesis was carried out in the Polymer Synthesis Lab at Kemira R&D Center, Espoo as part an ongoing project. Hence, I would like to extend my thanks to Kemira Oy for their technical as well as financial support. I would also like to thank Dr. Marko Laakkonen (1st advisor) and Dr. Jonni Ahlgren, without their guidance and support it would have not been possible to carry out such a big task with such great ease. In addition, I am highly obliged to the entire staff of Kemira R&D center including top to the bottom in organizational hierarchy. Special thanks to all the lab technicians for all their help, which not only have helped me in having a better understanding of operating the lab equipment with proper work safety but also for creating such a pleasant and friendly working environment.

I would also like to thank Dr. Wenli Zhao (2nd Advisor) alongside with Dr. Marko Laakkonen, for their comments, discussions and valuable inputs into this work. I extend him my best wishes for his career as well as future endeavors.

Last but not the least, my warmest gratitude to the entire staff of Aalto University and the entire student community for their encouragement and support during my studies.

Espoo, March 29, 2019

Sugam Shukla

TABLE OF CONTENTS

LIST OF FIGURES

LIST OF TABLES

NOMENCLATURE

T_g	glass transition temperature	°C or K
γ_c	critical surface tension	dyn/cm
$\bar{X}^*$	average equilibrium moisture content	dry basis
p_v	partial vapour pressure	Pa
T	Temperature	°C or K
p_v^*	equilibrium vapour pressure	Pa
ψ	relative moisture content	dimensionless
p_{ov}^*	saturation vapour pressure of water at given temperature	Pa
m_{sw}	mass of wet sample	kg
m_w	mass of moisture	kg
m_s	mass of sample	kg
X	moisture content	dimensionless
N_w	drying rate	kg/(m².s)
A_s	surface area	m²
τ	time	s, min or h
X_c	critical moisture content	dry basis
X^*	equilibrium moisture content	dry basis
j_q	heat flow density	W/m²
h	heat transfer coefficient	W/(m².K)
T_G	temperature of gas	°C or K
T_W	wet bulb temperature	°C or K
N_{w_c}	critical drying rate	kg/(m².s)
ΔH	sum of heat of evaporation plus heat of moisture	J/kg
K	mass transfer coefficient	kg/(m².s.Pa)
Y_W	moisture content of saturated air at temperature T_W	dry basis
Y_G	moisture content of air	dry basis
u_{mf}	minimum fluidization gas velocity	m/s
q	rate of heat transfer	W

h_p	heat transfer coefficient of particle	W/(m².K)
A_p	surface area of particle	m²
T_p	temperature of particle	K
T_g	temperature of gas	K
k_g	thermal conductivity of gas	W/(m.K)
d_p	particle diameter	m
Nu_p	Nusselt number of particle	dimensionless
Pr_g	Prandtl number of gas	dimensionless
Re_p	Reynolds number of particle	dimensionless
h_w	heat transfer coefficient of wall	W/(m².K)
a_w	surface area of wall in contact	m²
T_b	bed temperature	K
T_w	wall temperature	K
h_c	convective heat transfer coefficient	W/(m².K)
d_t	column diameter	m
ρ_s	particle density	kg/m^3
ρ_g	gas density	kg/m^3
g	acceleration due to gravity	m/s^2
μ_g	gas viscosity	N.s/m^2
ε	void fraction	dimensionless
h_r	radiative heat transfer coefficient	W/(m².K)
σ	Stefan-Boltzmann constant	W/m^2 K^4
e_b	bed emissivity, (0.9 approx.)	dimensionless
e_w	wall emissivity (0.9 ~ 1.125 approx.)	dimensionless
X	free moisture content	dry basis
D	diffusivity	m²/s
r	radial dimension of particle	m
$\bar{X}$	average moisture content	dry basis
V_p	particle volume	m³
X_o	initial moisture content	dry basis

X_{eq}	equilibrium moisture content	dry basis
D_{eff}	effective diffusivity	m²/s
r_{sph}	sphere radius	m
$\dot{m}$	mass rate of evaporation of water per unit volume of bed	kg/(m³.s)
ε_{mf}	void fraction for minimum fluidization	dimensionless
ε_{bb}	void fraction for bubble fluidization	dimensionless
Y_{bb}	absolute humidity	kg/kg
k_c	mass transfer coefficient across bubble boundary	m/s
t_R	residence time	s, min or h
M_s	mass of solids	kg
λ	latent heat of vaporization	J/kg
G_g	gas mass flow rate	kg/s
c_{pg}	heat capacity at constant pressure	J/(kg.K)
T_{in}	inlet temperature	°C or K
T_{out}	outlet temperature	°C or K
D	diffusivity	m²/s
K_1	6.089613, constant	hPa
K_2	7.33502, constant	dimensionless
K_3	230.3921, constant	°C
K_4	2.16679, constant	g.K/J
P_{ws}	water vapor saturation pressure over water	hPa
$P_{ws(@T)}$	water vapor saturation pressure at given temperature	hPa
RH	relative humidity	%
P_w	vapor pressure	hPa
H_{abs}	absolute humidity of inlet air at process temperature	g/m³
$V_{air(@20°C)}$	volume of air at 20°C	m³
C_1	0.0187, constant	m³/s
C_2	0.1338, constant	m³/s
$v_{\%}$	blower process value	%
t_i	time of logged data	s

$V_{air(@T)}$	volume of air at process temperature	m^3
N_{evap}	net evaporation rate	g/s
H_{air}	absolute humidity of air at the end of the drying process	g/m^3
$\acute{N}_{evap}$	net scaled evaporation rate	g/s
X_{solid}	moisture content in solid phase	g
X_{gas}	moisture content in gas phase	g
X_{cum}	unscaled cumulative moisture content	g
$\acute{X}_{cum}$	scaled cumulative moisture content	g

1 INTRODUCTION

Several classes of water soluble and hydrophilic polymers, containing polyacrylamides, comprising some of the most salient synthetic polymeric materials, are applied to improve the quality of life in modern society. Since, government regulations are becoming more and more restricted day by day, hydrophilic polymers come to play an important role. They are applied to enhance the quality of end-product, efficiency of process and better effluent streams treatment and makes the business more profitable for the customer by reducing cost. Polyacrylamide, abbreviated as PAM, is a polymer made by free radical polymerization of acrylamide subunits. However, acrylamide homo-polymers are not water-soluble but cationic and anionic co-monomers lead to water-soluble polymer. Acrylamide polymers fall into three main categories: nonionic, anionic and cationic.

As, for PAMs, one of the major area of application is in solid-liquid separations as flocculants and dewatering aids for a very broad range of processes. Pioneering technologies for synthesizing cationic polymers with a vast range of charge levels, novel structures and from low to very high molecular weights. These synthesizing processes of cationic PAMs have embarked on to settle down majority of present market exigency. The largest volume of application for PAM in paper-mills is in wet-end processes. Conventionally, high molecular weight PAMs have been used in mineral processing industry. These anionic PAMs are used as flocculants in the coal mining processes. Using PAMs as modifiers have reflected higher selectivity and yield of the end product.

Other areas for significant application of PAM includes soil conditioning and erosion control, drag reduction, sugar processing, additives in cosmetics and also as superabsorbent [1], [2], [3], [4], [5], [6], [7].

The solid polyacrylamides, completely dry PAM (DPAM) is a brittle white solid. In contrast to the monomer, it is nontoxic. DPAMs are available commercially, as spherical beads and as non-dusting powders. These DPAMs may contain small quantity of additives that helps in the stability as well as dissolution of DPAM in water. Typically, these DPAMs are dried under mild conditions and generally contains 5~15% water which is directly dependent on their ionicity. DPAMs are particularly

hygroscopic, especially cationic DPAMs. However, increase in hygroscopic property is equivalent to the increase in ionic character of DPAM [1].

The physical properties of DPAM is tabulated below in **Table 1-1**. The polymerization temperature is considered responsible for the tacticity (viz. the stereo-chemical arrangement of units in the main chain of a polymer) as well as for the linearity of the polymer chain. At low temperatures, syndiotacticity (viz. the substituent units have alternate position along the main chain of polymer) is more favorable [8]. At below 50°C, linear polymer chains are obtained. However, the formation of branching initiates when the temperature is increased slightly above this mark [9].

Table 1-1. Physical Properties of Solid Polyacrylamides

S. No.	Property	Value	Reference
1.	Density	1.302 g/cm^3 (@ 23°C)	[10]
2.	Glass-transition temperature (T_g)	195°C	[11]
3.	Critical surface tension (γ_c)	52.3 dyn/cm (@20°C)	[12]
4.	Chain structure	Mainly heterotactic linear or branched, some head-to-head addition	[13], [14], [15], [16]
5.	Crystallinity	Amorphous (high molecular weight)	[17]
6.	Solvents	Water, ethylene glycol, formamide	[18]
7.	Non-solvents	Ketones, hydrocarbons, ethers, alcohols	[19]
8.	Gases evolved on combustion in air	H_2, CO, CO_2, NH_3, NO_x	[20]

2 POLYMERIZATION OF POLYACRYLAMIDE

2.1 Synthesis and drying of Polyacrylamide

There are three classifications of PAM, based on the charge type as mentioned above viz. anionic, cationic and non-ionic PAM. Depending upon the charge type of PAM, different monomers are used for the polymerization.

There are many quality and performance parameters to be considered for commercial grade finished material such as [1]:

- Very low to very high molecular weights
- Low insoluble content
- Low residual monomer content
- Fast dissolution rate
- Ease of handling
- Minimal dusting for dry solids
- Product uniformity
- Long term storage stability to ensure the performance consistency
- High solids to reduce shipping cost

Some of the widely used commercial processes are discussed below:

Solution Polymerization: Solution polymerization of polyacrylamides is carried out in an aqueous solution, either adiabatically or isothermally, for commercial production. Process development is conducted at control of molecular weight and heat released during exothermic reaction ensuring low amount of residual monomer, amount of polymer solids and that the final product is fluid and pumpable.

Acrylamide monomer solution is prepared and deaerated by sparging it with an inert gas (such as nitrogen) to reduce oxygen content in solution. Often stainless steel batch reactors or glass continuous stirred tank reactors are used for solution polymerization. Usually, a chelating agent is added in the solution to complex auto-polymerization inhibitors such as copper or other metals if they are present. The polymerization can be initiated by adding several free radical initiator systems at various concentrations (varying from 0.001 ~ 10 wt. % on monomer) by either using one or the combination of free radical initiator systems. Usually, the polymerization rate rely upon reaction conditions, but typically lies in between 1.2 – 1.6 order of monomer concentration and

0.5 order of initiator concentration. The heat released during polymerization can be removed via using external cooling system. For adiabatic processes, the rise in temperature needs to be meticulously estimated beforehand to avoid thermal runaway. Inorganic salts and chain transfer agents can be used to enhance reaction rate as well as to reduce the amount of insolubles in the final product. Monomer to polymer conversions can be up-to 99.5% in 4-6 hours of polymerization time with molecular weight ranging from one thousand to four million and solid contents can range from 2-30%. The process needs to be coupled with further thermal drying of the product to be in powder or granular form. Drum drying can be performed for short residence time in the dryer in order to avoid chain degradation and formation of insolubles. The resulting granules can undergo further milling and sieving to produce a uniform product. However, excessive care must be taken for fine particles to avoid dusting problems and production loss [1].

Inverse Emulsion Process: This process is widely used to avoid high solution viscosities while producing high molecular weight water soluble polymers. In this polymerization method, the aqueous monomer solution is emulsified in an oil containing surfactants. It helps in homogenizing the mixture to form a water-to-oil inverse emulsion, and then polymerizing the monomers in the emulsion. An illustrated process for this inverse emulsion polymerization, in which the polymerization is carried out and results in fine particles small enough to avoid the settling and can produce the final product which is ready for commercial application without any further modification [1]. In addition, commercial manufacturing process via inverse emulsion polymerization of polyacrylamide has also been reviewed in past two decades [21]. As a result, current commercial production via inverse emulsion polymerization include new monomers, result in high solid concentrations, providing self-inverting water/oil emulsions, application of new emulsifiers to improve stability and seek to attain specific physical and chemical properties e.g. chemical modification of the PAM backbone.

Moving Belt Polymerization: Dry polyacrylamides are generally preferred over the solution, wherever the transportation distances are long in order to avoid increased logistics cost for the final product. Wide number of continuous processes have been developed over the past several years for producing dry polyacrylamides that consist

of polymerization of aqueous acrylamide on a moving belt and then the resulting polymer under goes further drying and milling for more uniform and high quality end product [1]. In general at the end of the belt the polymer gel is obtained which is then further sliced into smaller granules and then dried in the oven. Often after drying, the dried polymer is passed through another grinder to retain desired particle size for uniform end product for enhanced handling and application.

Various advancement are introduced in the discussed moving belt process. In some cases, for a higher solids polymerization is carried out by cooling the initial monomer solution till some monomers crystallizes and forms a slurry. Then this slurry is introduced on the moving belt for polymerization. This helps in controlling the heat released during the reaction. By using the heat generated during the polymerization for the latent heat for fusion of monomers, which otherwise inhibits the formation of solid content during the polymerization. Further changes in the geometry of the moving belt has been reviewed and its impact on the polymerization is been observed, e.g. a concave belt, flattened at the end results in improved release of the polymer from the moving belt [1].

2.2 Applications of Dry-polyacrylamide

Dewatering: One of the major area of application of DPAM is in polyelectrolyte dewatering of solid-liquid separations in aqueous media which can be enhanced by the flocculation of small suspended particles into larger ones, and hence increasing the separation efficiency. DPAM is widely used as flocculants in various other industries such as mineral processing, pulp and papermaking industry etc. [3], [22].

Paper Manufacturing: Another wide application of polyacrylamide in paper manufacturing industry is, as the wet-end additives to enhance the water removal from cellulose web. This results in improvement to retain white pigments, clay fillers in the sheet, enhanced dry tensile strength and promotes sheet uniformity. Due to increase in demand of writing and copy papers over past few decades, which must exhibit good print characteristics. Hence, for improved surface strength and sizes along with increased print quality, polyacrylamides have been widely used in paper manufacturing. It also helps in improving burst and crush strengths as well [1].

Enhanced Oil Recovery: One of the main benefits of using polyacrylamide over conventional brine solution is that it increases injection fluid viscosity and push oil at the higher yield out of oil well. In addition, it is also preferred because of its low cost when compared conventionally used xanthan gum. Polyacrylamides exhibit high temperature limit and lesser vulnerability towards bacterial degradation. However, polyacrylamides are more susceptible to shear. A significant reduction in the thickening properties of saline water is observed when polyacrylamides are used instead of conventional xanthan gum. This results in increased activity along with improved injectability and compatibility with saline formation of waters hence, reducing the cost [23]. Polyacrylamides have a very wide range of application in the oilfields other than making complex with the metal ions for more permeable zones prior to water flooding in the oil recovery. Some of the uses of polyacrylamides in oilfield applications include cement additive for fluid loss control in well-cementing operations, viscosity control additives for drilling muds and brine, and as fracturing fluids [1].

Mineral Processing: In mineral processing industry, most of the water-soluble polymers are used as flocculants and flotation modifiers including polyacrylamide. Non-ionic polyacrylamides are very effective and widely used for the insoluble gangue in acid leaching of copper and uranium [24], [25], for thickening of iron ore slimes [26], and also, for gold flotation tailings [27].

Super-absorbents: Polyacrylamide is extensively used in industrial applications with copolymers of metal salts of acrylic acid or some other monomers. These hydrogel forming systems may result in high gel strength viz. measured by shear modulus. Sometimes, dry polyacrylamide is conjugated with inorganic water-insoluble powder to improve gel strength [1].

3 MOISTURE CONTENT EQUILIBRIUM AND MEASURING METHODS

3.1 Introduction

When PAM-gel is stored in bulk temperature, moisture content, inter-particle gas composition etc. make the handling and logistics of the material becomes very difficult. Hence, the concept of equilibrium moisture content (EMC) plays a significant role in understanding the drying process and material's potential to deteriorate.

As per definition, the equilibrium moisture content can be defined as the moisture content of the product which is in equilibrium with the surrounding air at a constant temperature. The relative humidity of air as in equilibrium is known as equilibrium relative humidity [28].

3.2 Determination of Moisture Content

- Determination of the moisture content of Solid Materials

In general, it appears quite straightforward to determine the moisture content of a solid material, however the results determined may not be sufficiently accurate as the solid may not only undergo moisture loss but also under various chemical changes, such as, oxidation, decomposition, destructive distillation etc. when subjected to heating and this may not only change the materials' chemical properties as well as physical properties too. Hence, it is important to bifurcate between adsorbed moisture and bond moisture.

Once the selection is made, depending upon the technique to determine the moisture content, one must consider the desired accuracy, the procedure, investigation length and complexity of the required measuring instruments and equipment.

- Direct Methods

In general, this method involves drying of the material with or without blow through of air, or drying in a vacuum chamber or in a vacuum desiccator. The sample preparation involves the particle size of 1–2 mm^3 and of known mass nearly 4–5 g is placed in a preciously dried and weighed glass chamber, and subjected to a temperature of 102–105°C. While performing the mass measurement of the dried sample must be

carried out at the ambient temperature and hence, the dried sample must be left within the desiccator for cooling down. When the difference between the two consecutive sample measurements is less than ±0.05%, then the drying process considered to be complete. In reference to literature reviewed, it was observed that this process is faster when performed at higher temperatures are 130–150°C. However, this rapid drying can cause a deviation in results obtained nearly by 0.5–1.0%, due to less residence time of material in the dryer. Hence, this method of rapid drying must only be applied when an approximate determination of moisture content is required.

Also, when 102–105°C air is blown through the drying chamber then the length of the experiment can be shortened [30].

- Indirect Methods

Industrial measurements may require faster technique to determine the moisture content. There are generally three such electrical methods available for the determination of moisture content which are widely used are discussed later. Also, some other quick moisture content determination methods are available however, these are chemical methods developed mainly for the most recent and frequent cases, when the moisture is just water, such as Karl-Fischer analysis based on the chemical reaction of iodine in the presence of water [31], the distillation method, in which the moisture is determined by the distillation with toluene, and the extraction method, which is carried out with absolute ethanol.

For the description of moisture transport mechanism of wet material, various factors are essentially needed such as distribution of moisture content of the dried material and its charge type and density during the drying process must be known. Generally, these measurements are performed at the laboratory conditions with two main widespread methods given below:

- For rapid determination of moisture content of individual element, mechanical disintegration of the material via compressing the sample [32].
- Special adaptation with specific changes and advancement in one of these electrical method such as moisture determination based on the change of the ohmic DC resistance, a measurement of di-electric

constant of material (electrostatic capacitance), and a measurement of the loss in an AC field [33].

- Determination of the moisture content of Gases

Among various methods available for the determination of moisture content of gases, some of them are widely used such as: determination of the absolute value of moisture content by gravimetric or barometric method (direct method), measurement of wet particles in the air by determining the dry and wet bulb temperature and dew point temperature (indirect method), and measurement of a property of the wet gas which depends on the moisture content, such as absorptivity of the gas to electromagnetic waves.

One of the most commonly used indirect method is determining the dry and wet bulb temperatures as well as the dew point temperature, even though it requires a bit more expensive instrument. Still in some cases, on using this indirect method does not result in the sufficient accuracy for determination of moisture content of the wet gas. Whenever high accuracy is required, it is always suggested to opt for one of the absolute methods to determine the moisture content of the wet gas.

The absolute determination of moisture content of gases can be carried out by the absorption method, in which the gas is allowed to flow through a silica-gel bed or allowing it to be absorbed methanol and then determining the water content by Karl-Fischer titration method [31], [34].

3.3 Experimental determination of the sorption equilibrium characteristics of materials

- Interpretation of the Equilibrium Moisture Content of Materials

A major part of solid particle contains a large number of capillaries, micro- and macro-pores, cells and micelles of multitude dimensions and shapes. The potential sites for moisture can be determined by the structural build-up of these materials.

The characteristic of binding moisture of these materials are affected by the internal structural build-up. Hence, the structurally identical material must be used for which the measurements have been carried out, to the material which the equilibrium characteristics is to be determined.

Even though the materials may estimate the equilibrium moisture of content by moisture adsorption or by desorption via drying. The value of equilibrium vapour pressure commonly depends upon the way used for the estimation of equilibrium content, for capillary-porous material. This is generally called as *sorption hysteresis* because of this reason it is necessary to know the difference in between adsorption equilibrium moisture and desorption equilibrium moisture.

As a result of the interaction in between the material and the surroundings, equilibrium moisture content can be developed and mathematically, can be given as $\bar{X}^* = \bar{X}^*(p_v, T)$. Changes in the moisture content in the material is due to these conditions (p_v, T) occurring at the surface of the material. With steady state limit conditions and adequate long time, an internal moisture diffusion balance starts to take place until the equilibrium moisture content is achieved. A steady internal moisture distribution exists, in an equilibrium state. Although to attain such conditions, an infinite time is needed theoretically, however a practicable approach can be accepted up-to an acceptable approximation via a number of procedures and methods with a finite time period [28].

- Interpretation of the Equilibrium Vapour Pressure

The equilibrium vapor pressure is defined as the vapor pressure at which the material of a given moisture content at a specific temperature is at sorption equilibrium (i.e. it neither lose nor take up any moisture). Mathematically, it can be represented as $p_v^* = p_v^*(T)_{\bar{X}}$.

It is important to have the knowledge of the equilibrium vapor pressure at a constant temperature while studying drying of any material. Hence, when T and p_v^* are constants, in such case the equilibrium relative vapor content was applied in drying as a characteristic of the vapor pressure and can be given as by the equation below [28]:

$$\psi = \frac{p_v}{p_{ov}^*}$$

where, ψ = Relative moisture content

p_v = Partial vapor pressure (in Pa)

p_{ov}^* = saturation vapor pressure of water at a given temperature (in Pa)

3.4 Lumped approach for drying experiments

At constant operating conditions such as constant temperature, humidity and velocity, the mass of a sample kept in the airflow must be measured as a function of time, in order to determine the drying rate. If the aim of the experiment is to obtain data in order to scale up the process, then these aspects must be taken into consideration such as, that the sample must not be too small and the operating conditions of drying should be almost identical as to the industrial unit [29], [35].

- In laboratory, sample placing must be done in a similar way as of industrial unit.
- Drying surface to non-drying surface ratio must be identical.
- Radiative heat transfer conditions must be of the same manner.
- Moisture content, temperature, velocity and the flow direction of drying gas (generally air) must be identical to the sample when compared with industrial process.

It is always suggested to perform a wide range of experiments with multitude of material samples of varying particle size and other variable parameters, just to determine the dry matter content of the sample. For drying process to take place in constant drying conditions, temperature, velocity and moisture content of the drying air must remain constant.

As it is known from definition that the wet mass of the sample is given as:

$$m_{sw} = m_w + m_s$$

and the moisture content is given as:

$$X = \frac{m_w}{m_s}$$

hence, from both the above equations it can be deduced that,

$$\frac{m_{sw}}{m_s} = 1 + X$$

And now on rearranging this equation

$$X = \frac{m_{sw} - m_s}{m_s}$$

So from the above correlation it is clear, that in order to possibly plot the moisture content of any given sample as a function of time, it is must to calculate the drying wet mass as a function of time and of the bone-dry mass of the sample (Figure 3-1).

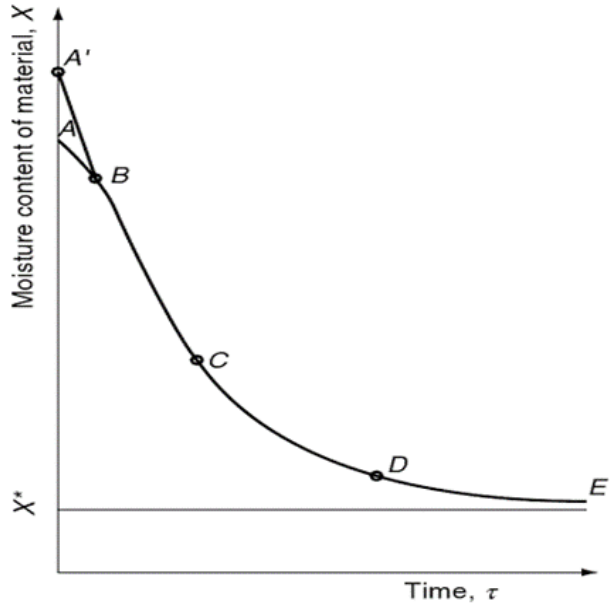

Figure 3-1. Batch, convection drying curve [28]

The curve can then be directly applied for determining the time of drying greater of masses to an adequate moisture content, when subject to identical conditions. However, for better data analysis and results it is suggested to plot the drying rate curve against the moisture content. For such plot, the drying rate is defined as

$$N_W = -\frac{1}{A_s}\frac{dm_{sw}}{d\tau} = \frac{m_s}{A_s}\frac{d\bar{X}}{d\tau}$$

where, A_s is the contact surface of the drying gas and the dried material, and a cross section of perpendicular to the air flow for drying process through circulation. With the determination of weight loss curve, and equation obtained above, it is easier to plot the drying rate curve against moisture content as shown in Figure 3-2. In the plot AB

and A'B show the preheating regime. At the beginning, solids are usually cold and hence, follow the regime AB. However, if the solids are preheated initially then plot follows path A'B. At point B the surface temperature of solid particle rises to its equilibrium value. The regime BC is known as the constant drying rate period and at point C the corresponding moisture content is known as critical moisture content, X_C. After the critical moisture is attained the plot follows the falling rate period CE which is divided into two parts CD and DE. The first falling rate period is at regime CD and usually it is linear. The wetted area is continuously decreasing during the first falling rate until point D. After point D, the second falling rate period begins and the rate of drying falls even more rapidly until it reaches point E and attains equilibrium moisture content X^*.

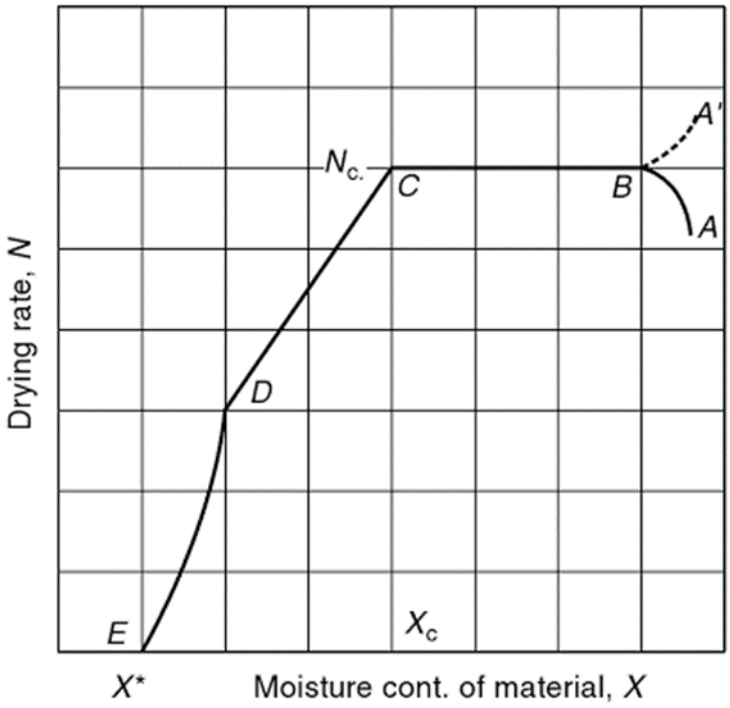

Figure 3-2. Drying rate curve [28]

It is possible to extrapolate within limits of the other operating conditions, if the drying rate is known for the one set of constant drying conditions [35]. **Figure 3-3** exhibits the variation of drying surface temperature with time whilst **Figure 3-4** summarizes all the characteristic parameters of the drying process.

Transport coefficient can also be determined via drying experiment to achieve appropriate results. During constant drying, the temperature of the drying surface is in

a purely convective drying, the so-called wet bulb temperature. With this value, the steady state of heat flux, mathematically, can be given as:

$$j_q = h(T_G - T_W)$$

where j_q can be determined by using the constant drying rate and can also be represented as:

$$j_q = N_{W_c} \Delta H$$

Thus,

$$h = N_{W_c} \left(\frac{\Delta H}{T_G - T_W} \right)$$

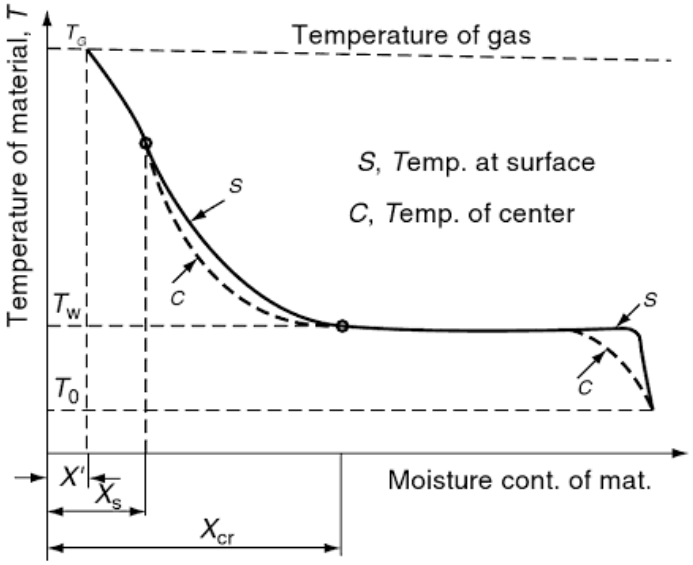

Figure 3-3. Temperature curves of a wet material at the surface and the middle of the sample [28]

In terms of mass transfer coefficient,

$$N_{W_c} = K(Y_w - Y_G)$$

where, Y_W is the moisture content of the saturated air at temperature T_W, the coefficient of evaporation or mass transfer can be given as:

$$K = \frac{N_{W_c}}{Y_W - Y_G}$$

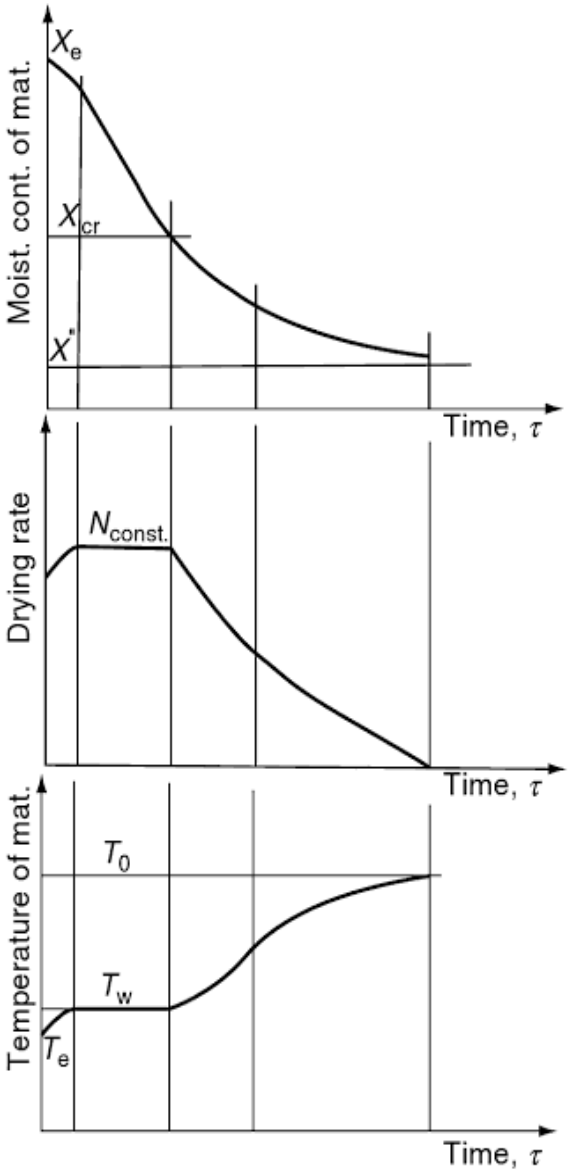

Figure 3-4. Characteristic functions of a convective drying [28]

The heat and mass transfer coefficients on the gas side, under constant drying conditions, may be considered constant during the entire drying process while characterizing the steady state.

Internal heat and moisture diffusivities affects greatly when the drying rate is at the falling rate period. Hence, it is also necessary to determine these coefficients. During the falling drying rate period which contributes to the continuous decrease in vapor diffusivity of the material at the surface layer, the transport coefficients on the gas side might also change [36].

4 FLUIDIZED BED DRYING

4.1 Introduction

For the drying of wet particulate and granular materials that can be fluidized, fluidized bed dryers (FBD) are widely used. In addition, FBDs are also used for slurries, pastes and suspensions that consist of the bed of inert solids that can be fluidized. An FBD is operated at superficial gas velocities higher than the minimum fluidization velocities. The minimum fluidized velocity for any system is obtained experimentally. There are various analytical methods and mathematical correlations can be applied to determine or estimate the minimum fluidized bed velocity. Figure 4-1 exhibits various regimes of a bed of particles from fixed bed to bubbling bed at different gas velocities.

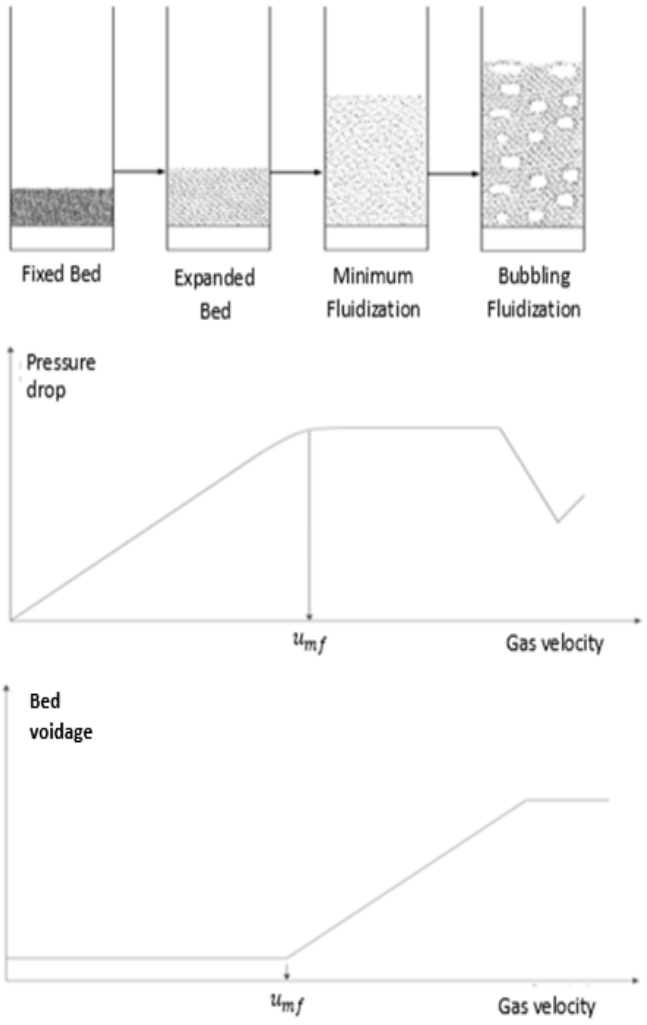

Figure 4-1. Various regimes of a bed of particles at different gas velocities [72]

The graphs show the bed pressure drop and bed voidage under various regimes. It is also important to consider that these correlations have some certain limitations such as particle size, column dimensions and other operating parameters. Hence, many correlations may only be applicable for a certain range of operating conditions. However, the initial moisture content of the particle is not included in many of the correlations, which is also another operating parameter which may affect the dryer performance, as particles with higher initial moisture content need higher minimum fluidization velocity when compared with the dry particles for the same bed height [37].

4.2 Advantages and limitations of fluidized bed drying

There are various advantages of fluidized bed drying such as high rate of moisture removal, high thermal efficiency, easy material transport inside the dryer, ease of control, and low maintenance cost. However, there are also some recognizable limitations to fluidized bed drying as well, such as high pressure drop, high electrical power consumption, for some particulate products poor fluidization quality, non-uniform product quality for certain types of FBDs, erosion of pipes and vessels, entrainment of fine particles , attrition or pulverization of particles, along with agglomeration of fine particles [38].

In addition to drying, fluidized bed have a wide range of application in various industries when conjugated with various unit processes such as mixing, de-dusting, granulation, coating, cooling, chemical reactions, incineration, combustion, gasification etc. When one or more processes combined in one unit along with fluidized bed drying, then more than one process can be carried out in the same unit. However, which will be the advantageous process to combine with fluidized bed drying not only depends on the operating parameters and operating condition but also on feed-stock characteristics as well [39].

4.3 Heat transfer in fluidized bed drying

Depending upon the operating conditions heat transfer in fluidized bed can result of conduction, convection and radiation. Contribution to the heat transfer coefficient by respective modes of heat transfer depends solely upon particle classification, flow

conditions, fluidization regimes, type of distributor, operating temperature and pressure. The conventional equation of heat transfer can define the heat transfer between a single particle and gas phase:

$$q = h_p A_p (T_p - T_g)$$

In general, heat transfer rate is highly dependent on number of particles. Moreover, heat transfer rate obtained for this system is high due to the large interfacial surface area of all the particles. In addition, thermal equilibrium is reached quickly due to the high heat capacity of the bed. Often isothermal conditions are assumed while designing FBDs.

As mentioned above heat transfer coefficient, h_p, is a function of dryer geometry, operating parameters and particulate characteristics. Hence, from the use of following correlations depending upon the particle's Reynolds number, Re_p, heat transfer coefficient can be estimated [40]:

$$h_p = \frac{k_g}{d_p} Nu_p$$

For $0.1<Re_p<50$, $Nu_p = 0.0282\, Re_p^{1.4} Pr_g^{0.33}$, and for $50<Re_p<10^4$, $Nu_p = 1.01 Re_p^{0.48} Pr_g^{0.33}$

To improve drying through conduction mode, single or multiple heater tubes or flat channels can be immersed either vertically or horizontally. Empirical correlation for different geometry and operating conditions usually beg to differ.

The heat transfer coefficient for surface-to-bed, $h_w = q/a_w\,(T_b - T_w)$, is dependent on the immersed object surface area that is in contact with the material. The heat transfer coefficient constitutes two element, convective as well as radiative, if the temperature is really high. In the mentioned correlation, a_w is the wall surface area (m^2), T_w is the wall temperature (K) and T_b is the bed temperature (K).

The convective heat transfer coefficient, h_c, can be estimated using the following correlation [41]:

$$\frac{h_c d_t}{k_g} = 420 \left(\frac{\rho_s}{\rho_g} Pr_g \frac{\mu_g^2}{g\rho_s^2 d_p^3}\right)^{0.3} Re_t^{0.3} \quad \text{if } \frac{\rho_s}{\rho_g} Re_p \geq 2550$$

$$\frac{h_c d_t}{k_g} = 0.66 Pr_g^{0.3} \left(\frac{\rho_s(1-\varepsilon)}{\rho_g \varepsilon}\right)^{0.44} Re_t^{0.44} \quad \text{if } \frac{\rho_s}{\rho_g} Re_p \leq 2050$$

$$Re_t = \frac{d_t \rho_g u_g}{\mu_g}$$

and

$$Re_p = \frac{d_p \rho_g u_g}{\mu_g}$$

The radiative heat transfer coefficient, h_r (W/m^2 K) can be estimated using following correlation [42]:

$$h_r = \left(\frac{e_b e_w}{e_b + e_w - e_b e_w}\right) \frac{\sigma(T_b^4 - T_w^4)}{(T_b - T_w)}$$

Generally, if the temperature is lower than 700°C, then the radiative heat transfer is insignificant. Since most of the drying processes are carried out in temperatures less than 700°C, hence radiative heat transfer is usually neglected [42].

Effect of various operating parameter on particle's heat transfer coefficient is given in Table 4-1.

Table 4-1. Effect of operating parameters on Particle Heat Transfer Coefficient

Parameter	Effect on heat transfer coefficient, *h*	Ref.
Particle		
Diameter, d_p	For fine particles, h is higher; for coarse particles, h is lower	[43]
Shape	Higher for rounded and smooth surface particles	[44], [45]
Specific heat, c_p	$h \propto c_p^n$, where $0.25 < n < 0.8$	[46], [47]

Thermal conductivity, k_p	No influence for small *Biot Number*	[48], [49]
Gas		
Velocity, u_g	Increases above u_{mf} to a maximum value at an optimum velocity, u_{opt} and decreases thereafter	[43]
Density, ρ_g	Increases with increasing, ρ_g	[44], [45]
Viscosity, μ_g	Increases with decreasing, μ_g	[46], [47]
Specific heat, c_g	At moderate pressure and velocity, no information is available	[50], [51]
	At high pressure, increases with increasing, c_g	
Thermal conductivity, k_g	$h \propto k_g^n$, where $0.5 < n < 0.66$	[48], [52]
	h increases as bed temperature increases, due to increase in k_g	
Fluidized Bed		
Bed height, H_b	No influence	[46], [53]
Bed diameter, d_b	No information available	
Bed temperature, T_b	Gas-convective; increases for small particles; decreases for coarse particles	[54]
Bed pressure, P_b	No influence on particle-convective heat transfer	[55]
	Gas-convective heat transfer increases	
Heat transfer surface		
Length, L	No influence	[56]
Tube diameter, d_{tube}	Increases with decreasing, d_{tube}	[51]

4.4 Mathematical models of fluidized bed drying

Many mathematical models for fluidized bed drying are available. However, all these mathematical models are based on various assumptions. Although, the several mathematical model discussed in this literature were already verified in the referred literature [72]. In this section, some of those mathematical models are discussed.

4.4.1 Diffusion Model

In the diffusion model, drying of single particles in a fluidized bed is assumed which is fully controlled by the internal moisture diffusion inside the particle. Whilst for the purpose of analysis of particulate drying, equivalent diameter of a sphere can be used to study diffusion model [57], [58].

The main assumptions of this model are:-

- The solid particles are spherical, isotropic, uniform size and homogeneous. The mixing is perfect while performing fluidized bed drying.
- All the physical properties of the dry solid particle remain constant over the time period of drying.
- Solid shrinkage as well as temperature gradient inside the solid particle are negligible.
- The internal moisture diffusion guides the drying kinetics. In such a manner that bed air humidity and solid surface moisture are in equilibrium.
- Air is homogeneous and perfectly mixed. Bed and the exhaust air are in thermal equilibrium.
- FBD is perfectly insulated.

With the following equation moisture transport can be defined. The diffusivity is assumed to be constant:

$$\frac{\partial X}{\partial t} = D\left[\left(\frac{\partial^2 X}{\partial r^2}\right) + \frac{2}{r}\left(\frac{\partial X}{\partial r}\right)\right]$$

where, X is the free moisture content, i.e., in excess than the equilibrium value, D is the diffusivity (m^2/s), and r is the radial dimension of particle (m).

Once the diffusivity is determined, numerical analysis can be applied to the diffusion equation, to find out the moisture content profile inside the solid particle. Average moisture content $\bar{X}$, can be determined from the following equation:

$$\bar{X} = \frac{4\pi}{V_p}\int_0^{r_p} r^2 X dr$$

where, V_p is the particle volume (m^3). It is important to note that to solve these equations numerically moisture content and temperature-dependent diffusivity values can be used.

4.4.2 Empirical Model

The drying process mechanism is different in each drying period. Hence, in empirical model, the entire drying process is divided into specific drying period as the mechanism for each drying period is different.

The Fick's diffusion equation's solution results in the moisture content in form of exponential function for the drying time. Following equation gives the solution of Fick's diffusion when particles are solid sphere [59], [60], [61]:

$$\frac{X - X_{eq}}{X_o - X_{eq}} = \frac{6}{\pi^2}\sum_{n=1}^{\infty}\frac{1}{n^2}e^{-n^2\left(\frac{\pi^2 D_{eff} t}{r_{sph}^2}\right)}$$

where r_{sph} is the sphere radius (m), D_{eff} is the effective diffusivity (m^2/s). Also, subscript "o" and "eq" indicates initial and equilibrium states respectively.

As the general solution of the diffusion equation results in a long series of exponential functions. Hence, experimental data obtained from FBD can be correlated as an exponential function. As per this, many empirical exponential equations have been proposed, however only few are discussed in the later part.

A simple exponential equation which assumes that the difference between average and equilibrium moisture content is directly proportional to the drying rate [62]. The equation is as given below:

$$\frac{X - X_{eq}}{X_{ind} - X_{eq}} = e^{-kt}$$

where subscript "ind" indicates the induction period. However another exponential equation which is a modified version of the previous equation [63]. This equation is also analogous to the theoretical diffusion equation solution for an infinite slab [59], [64]. On comparing equation above equations, it can be deduced that, $b = D_{eff}\pi^2/r_{sph}^2$ [65]:

$$\frac{X - X_{eq}}{X_{ind} - X_{eq}} = ae^{-bt}$$

Since previous equation leads to over-predict and under-predict the early and later stages of drying respectively. Hence, some empirical modification is carried out in the later equation, by introducing another exponent y [66]. This modified equation is most widely used because majority of the experimental data can be fitted very easily and very well with the following equation:

$$\frac{X - X_{eq}}{X_{ind} - X_{eq}} = e^{-xt^y}$$

Another equation which includes the first two terms from the Fick's second law of diffusion can also be used. The advantage of this equation over others is that it can be used regardless of the solids geometry [67]:

$$\frac{X - X_{eq}}{X_{ind} - X_{eq}} = a_1 e^{-b_1 t} + a_2 e^{-b_2 t}$$

It is important to note that all the constants in the equations mentioned above are empirically obtained. Also, these constants depend on the type of materials, operating conditions as well as dryer dimensions. In order to use any of these above equations for the fluidized bed dryer design, experimental investigation on drying kinetics must be performed to obtain drying constant for the particular material prior to dryer design.

4.4.3 Dynamic Model

For a batch fluid bed dryer, the solid phase may be considered as well mixed, in order to be described as input output model with the accumulation term. However, in contrast the gas phase changes it parameters as it travels through the bed as shown in Figure 4-2 below:

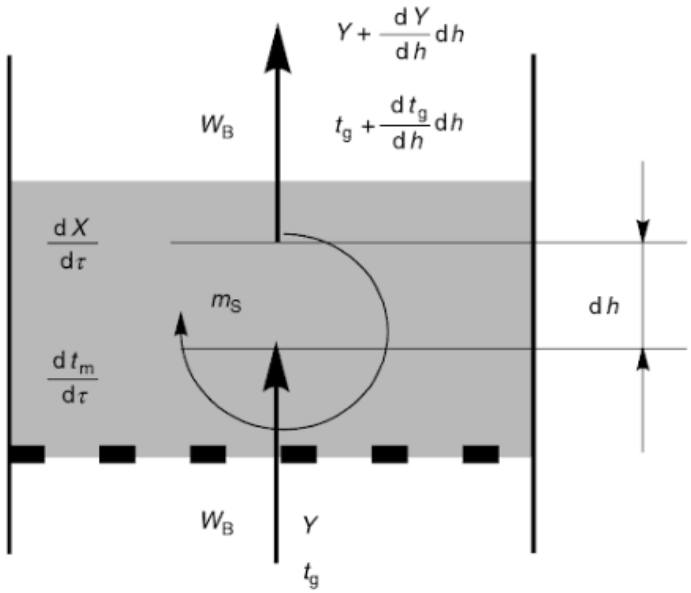

Figure 4-2. Schematic diagram of a batch fluid bed dryer [81]

Hence, gas phase is described as Distributed Parameter Model with no accumulation and solid phase is presented in Lumped Parameter Model with accumulation. Following equations represent the model with mentioned conditions:

$$\frac{dX}{d\tau} = -\frac{a_V}{(1-\varepsilon)\rho_S}\frac{1}{H}\int_0^H w_D dh$$

$$\frac{dY}{dh} = \frac{S}{W_B} w_D a_V$$

$$\frac{dt_m}{d\tau} = \frac{a_V}{(1-\varepsilon)\rho_S}\frac{1}{c_S + c_{A1}X}\frac{1}{H}\int_0^H [q - ((c_A - c_{A1})t_m + \Delta h_{v0})w_D]dh$$

$$\frac{dt_g}{dh} = -\frac{S}{W_B} a_V \frac{1}{c_B + c_A Y} [q + c_A(t_g - t_m) w_D]$$

Second and fourth equation are for the gas phase which only calculates the distribution of Y and t_g along the bed height, as they are needed to calculate q and w_D. However, first and third equations can be solved by using an ODE solver to get the values of X and t_m.

4.4.4 Single-phase Model

Heat and mass balances are used as it is assumed that there is partial mixing of all the particles. For the single-phase model the equations are generalized and is in as for continuum equations for moisture balance and energy balance as represented in **Figure 4-3**.

$$-M_s \frac{d\bar{X}}{dt} = G_g(Y_{out} - Y_{in})$$

where M_s is the hold-up mass of dry solid in bed (kg), $\bar{X}$ is the average moisture content (kg/kg), G_g is the mass flow rate of dry air (kg/s), and Y is the air humidity (kg(water vapor)/kg(dry air)).

$$M_s c_{ps} \frac{dT}{dt} = G_g(c_g + Y_{in} c_v)(T_{in} - T_{out}) - G_g(Y_{out} - Y_{in})\lambda$$

where c_p is the heat capacity of solids at constant pressure at the FBD (kJ/(kg.K)) and λ is the latent heat of vaporization (kJ/kg). Subscript "s" indicates wet solid, "g" indicates dry air, and "v" denotes the water vapor. However, above energy balance equation does not involve the sensible heat of the water in solids [58].

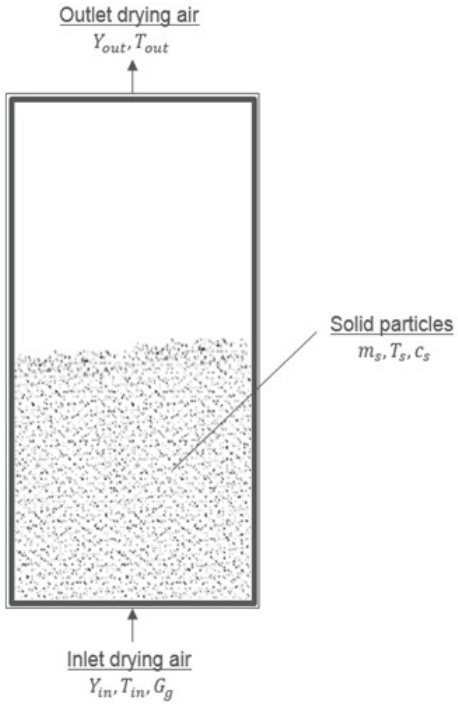

Figure 4-3. Schematic diagram of the single phase model of fluidized bed dryer [72]

4.4.5 Two-Phase Model

In a two-phase model, when compared with the single phase model, comprises of a bubble phase (dilute phase) and an emulsion phase (dense phase). A schematic diagram of a simple two phase model is given in Figure 4-4.

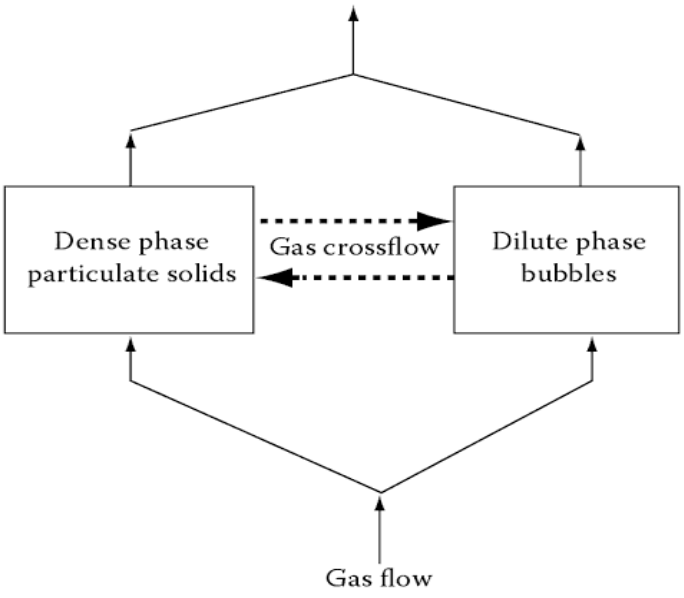

Figure 4-4. Schematic diagram of a two-phase model for fluidized bed drying [72]

Following are the major assumptions for the two-phase model:

- All the gas in excess of minimum fluidization velocity flows through the bed as bubbles [68].
- The emulsion phase remains stagnant at the minimum fluidization conditions [69].
- The bubble phase is particle free, the gas in the bubble phase as well as suspension phase flows as plug flow.
- Suspended particles are perfectly mixed.
- Solids s are added and removed from the system at a constant rate.
- Heat and mass transfer takes place between solid particles and the surrounding suspension gas.
- The bubble fraction is dependent on the bed height and calculated accordingly [70].
- There is no entrainment of solids.

The mass balance of liquid in the dense-phase particles can be expressed as follows:

$$\dot{m} = -\rho_p(1-\varepsilon_{mf})(1-\varepsilon_{bb})\frac{d\bar{X}}{dt}$$

Mass balance of liquid in the bubble phase can be written as below [71]:

$$\rho_g \varepsilon_{bb}\frac{dY_{bb}}{dt} + \rho_g \frac{V_{g\cdot bb}}{V_b t}(Y_{bb}-Y_{in}) = \frac{6K_c\rho_g\varepsilon_{bb}}{d_{bb}}(Y_d - Y_{bb})$$

The coupled mass and energy balance in dense phase consisting of particles and interstitial gas phases can be given as by the following equation:

$$\rho_p(1-\varepsilon_{mf})(1-\varepsilon_{bb})(c_{ps}-c_{pl}\bar{X})\frac{dT_p}{dt}$$
$$= \rho_g \frac{V_{g\cdot d}}{V_b t}(c_{pg}+Y_{in}c_{pv})(T_{g\cdot in}-T_P) - \Delta H_{evap}\times[\rho_g\frac{V_{g\cdot d}}{V_b t}(Y_d - Y_{in})$$
$$-\frac{6K_c\rho_g\varepsilon_{bb}}{d_{bb}}(Y_{bb}-Y_d)]$$

This coupled mass and energy balance equation mentioned above can be used to determine the temperature change of the particle in the dense (or emulsion) phase as a function of average moisture content $\bar{X}$. Also, solving this above equation results in the solids temperature at different drying times. This average moisture content can be estimated based on any of the above equations depending upon various operating parameters, the mathematical model which is being applied, dense phase and bubble phase humidity, enthalpy of vaporization, bubble diameter and mass transfer coefficient of bubble boundary [72].

4.5 Effect of operating parameters on fluidized bed drying

4.5.1 Bed Height

Such materials which exhibit high internal moisture mobility such as silica gel, ion-exchange resigns etc. most of the drying takes place at the distributor plate. Usually for such materials, bed height does not have any direct effect on its drying rate. If the bed height is increased beyond a particular value leads to no effect on drying rates. In contrast, for materials with resistance to drying within the material, the drying rate decreases with increase in bed height [72].

4.5.2 Particle Size

For sand-like particles the residence time required for removal of a given amount of moisture, directly proportional to the square of the particle diameter, whilst all the other operating conditions remain constant. However, for aeratable particles which are finer and exhibits smooth fluidization before entering the bubbling fluidization regime, this effect is much smaller [72].

4.5.3 Gas Velocity

This operating parameter has a very dominant effect on the drying rate via removing surface moisture and hence, drying rate increases with increase in velocity. However, for materials with high internal resistance to the moisture transfer towards surface, gas

velocity has no significant effect on the drying rate. High internal moisture resistance dominates at the end of the falling rate period of drying [72].

4.5.4 Bed Temperature

With high external heat fluxes for the material can result in increase in bed temperature. This is a complex effect which depends on the relative significance of both the external as well as the internal resistances to moisture transfer. High external heat fluxes leads to higher moisture diffusivities resulting in higher drying rate [72].

4.6 Types of fluidized bed dryers: Classification and Selection

Fluidized bed dryers are widely used for drying of wet powders, granules, pellets and other bulk solids because of the versatility and heat transfer efficiency of dryers as well as the low cost of their typical heat source [80].

In accordance with respective processes, products, operational safety and environmental requirement, various types of FBDs have been studied, developed and operated over several decades for industrial application. While making a logical and cost-effective equipment selection, it is essential to have the knowledge about the specific characteristics of various FBDs. However, in many process based instances, there is a possibility that different FBDs may result in similar performance and that too at the same cost [72].

The major classification in FBDs are of two types: conventional and modified fluidized bed dryers. In order to overcome difficulties and disadvantages some novel fluidized bed dryers are the modification over the conventional FBDs. However, it is not necessary that modified FBDs will have better performance and cost effective when compared with their conventional counter-part. It may also be possible that modified FBDs have lower product quality, or reduced energy efficiency or drying performance. Various types of fluidized bed dryers classified on their specific characteristics are tabulated below in **Table 4-2**.

Since there is a wide range of FBDs available only those FBDs concerning more to their application related to the DPAM process have been discussed in detail further in this section.

Table 4-2. Classification of Fluidized bed dryers [72]

Criterion	Types of Dryer	Sub-classification
Processing mode/feed and discharge	• Batch FBDs (well-Mixed) • Semi-continuous FBDs • Continuous	• Well-Mixed FBDs • Plug Flow FBDs • Single-stage FBDs • Multi-stage FBDs • Hybrid /Combined FBDs
Particulate flow regime	• Well-mixed FBDs • Plug Flow FBDs • Circulating FBDs • Hybrid	• Multistage FBDs (well-mixed/plug flow) • Hybrid/Combined FBDs
Operating pressure	• Low (for heat-sensitive products, low pressure strategy) • Near atmospheric (most common) • High (5 bars, superheated steam FBDs)	
Fluidization gas flow	• Continuous FBDs • Pulsed FBDs	
Fluidizing gas temperature	• Constant • Time-dependent	• Step down • Step up • Periodic (zigzag) • Combined
Heat supply	• Convective • Convective/conduction (immersed FBDs) or • Continuous • Intermittent (multiple variable strategy)	

Fluidization action	• By gas flow (pneumatic) • By jet flow • With mechanical assistance • With external field	• Ordinary FBDs • Circulating FBDs • Spouted FBDs • Recirculating FBDs • Jetting FBDs • Vibration (vibrated FBDs) • Agitation (agitated FBDs) • Rotation (centrifugal FBDs) • Microwave-radio frequency field (MW-RF FBDs) • Acoustic field • Magnetic field
Fluidized material	• Particulate solid (most common) • Paste/slurry	• Group A and B (most common, conventional FBDs) • Group C (vibrated FBDs, agitated FBDs) • Group D (vibrated FBDs, baffled FBDs, spouted FBDs) • Spray onto a bed of inert particles (inert solids FBDs) • Spray onto absorbent particles (silica gel, biomass) • Spouted FBDs
Fluidizing medium	• Heated air/flue gases/direct combustion gas • Superheated steam/vapor • Dehumidified cool air (heat pump FBDs) • Air below freezing point of liquid being removed (fluidized bed freeze dryers)	

4.6.1 Static Fluidized Bed Dryer

Operation: In a static fluidized bed dryer (Figure 4-5), the fluidized material bed is usually deep and the material behaves like a liquid, flowing from a height in the dryer to a low level. A static dryer has multiple drying zones. The air supplied to the system is usually by two air heaters and that the hybrid heat panels are in the drying chamber. The liquid- like flow in the drying chamber's highest point, i.e. at the feed inlet, towards the lowest point of the drying chamber, i.e. at the outlet, is a result of the heated air flow through an air distributor plate. This not only fluidizes the material but

also promotes the liquid-like flow in the drying chamber. The material bed in the static dryer must be completely fluidized in order to be dried and flow towards dryers' outlet as the material bed is deep (usually more than a foot). Due to deep bed size of material, it significantly reduces the overall size of the dryer and hence, its airflow requirements. Design of such static dryer for a specific application depends upon the material retention time, which can be determined by developing a drying curve for the material. The longer retention time required by the material, the greater advantage static FBD have over a vibrating FBD unit.

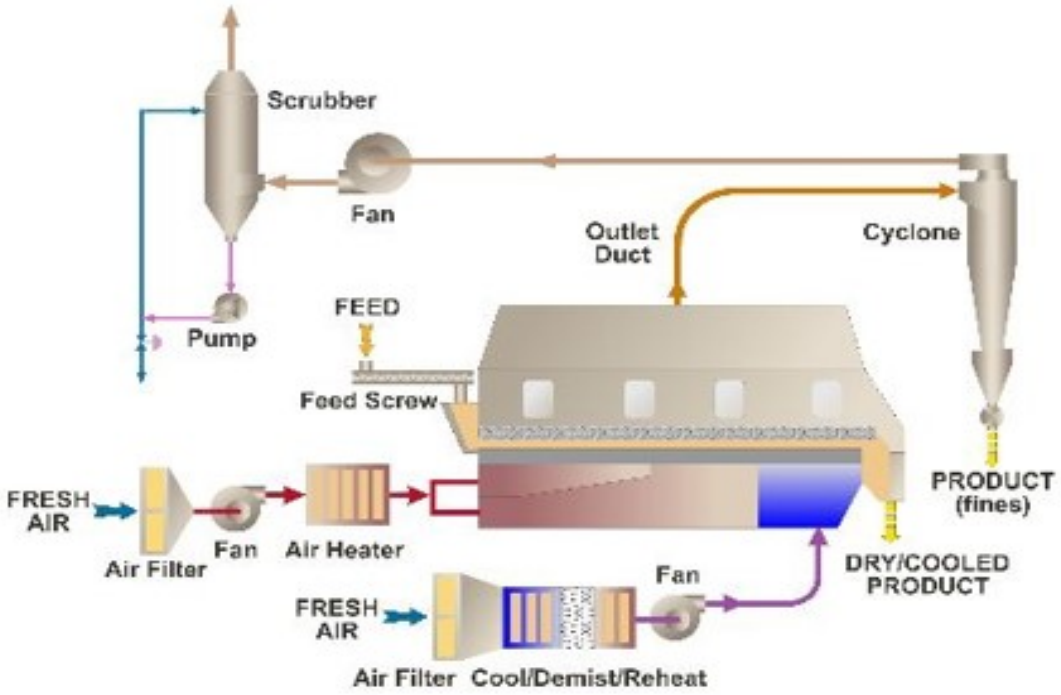

Figure 4-5. Static fluidized bed dryer [80]

Another major difference in the static FBD and vibrating FBD unit is that the static FBD unit has a back-mixing zone the feed inlet. At the feed inlet, the wet material is distributed by a rotating spreader called a feed distributor. Spreading the wet material over the partially dried fluidized material achieves a uniform material moisture content and temperature profile throughout the entire drying chamber. It promotes and assist the dryer to handle a wide range of moisture levels in the feed materials.

Applications: Usually, static FBDs have vast range of application, such as for polymers, ceramics, and inorganic materials. Static FBDs are suitable for such materials which have narrow size distributions and with particle size ranging from 50

μm to ½ inch. Static FBDs are not suited for particles which have a high length-to-diameter ratio because the air flowing through the air distributor plate will channel through the material. This condition tends to become established if the local pressure drop through the bed-distributor system decreases with increased fluid velocity [80].

4.6.2 Vibrating Fluidized Bed Dryer

Operation: In vibrating FBD (Figure 4-6), the heated air flows vertically through a perforated conveying pan, bubbling upward through a shallow material bed (usually few inches) of wet material on a vibrating conveyor. As the dryer completely depends on the conveyor's vibratory action for transporting the material towards the outlet. Due to this characteristic, the dryer allows to control the airflow velocity to dry materials with a wide particle size distribution without much affecting the conveying as well as performance. In contrast to static FBD, vibrating FBD does not require material to be completely airborne to be successfully dried up. It also helps in minimizing fines carryover to the downstream air-material separation equipment.

In the vibrating FBD, the system exhibit a plug flow of material through the dryer. As the vibrating conveyor moves material and allowing first-in first-out flow and hence, lowering the material retention time when compared with the static FBD. Another advantage of the vibrating FBD over static FBD unit is that it can have both a drying zone as well as a cooling zone.

Applications: Major area of application for the vibrating FBD are food products, specialty chemicals and extrudates. The dryer is suitable for handling a wide range of particle size range from particle smaller than 50 μm up to about ½ inch. The dryer is ideal for handling food and other products with sanitary requirements because this unit can be equipped with a removable top cover that will allow fast access for cleaning the internals [80].

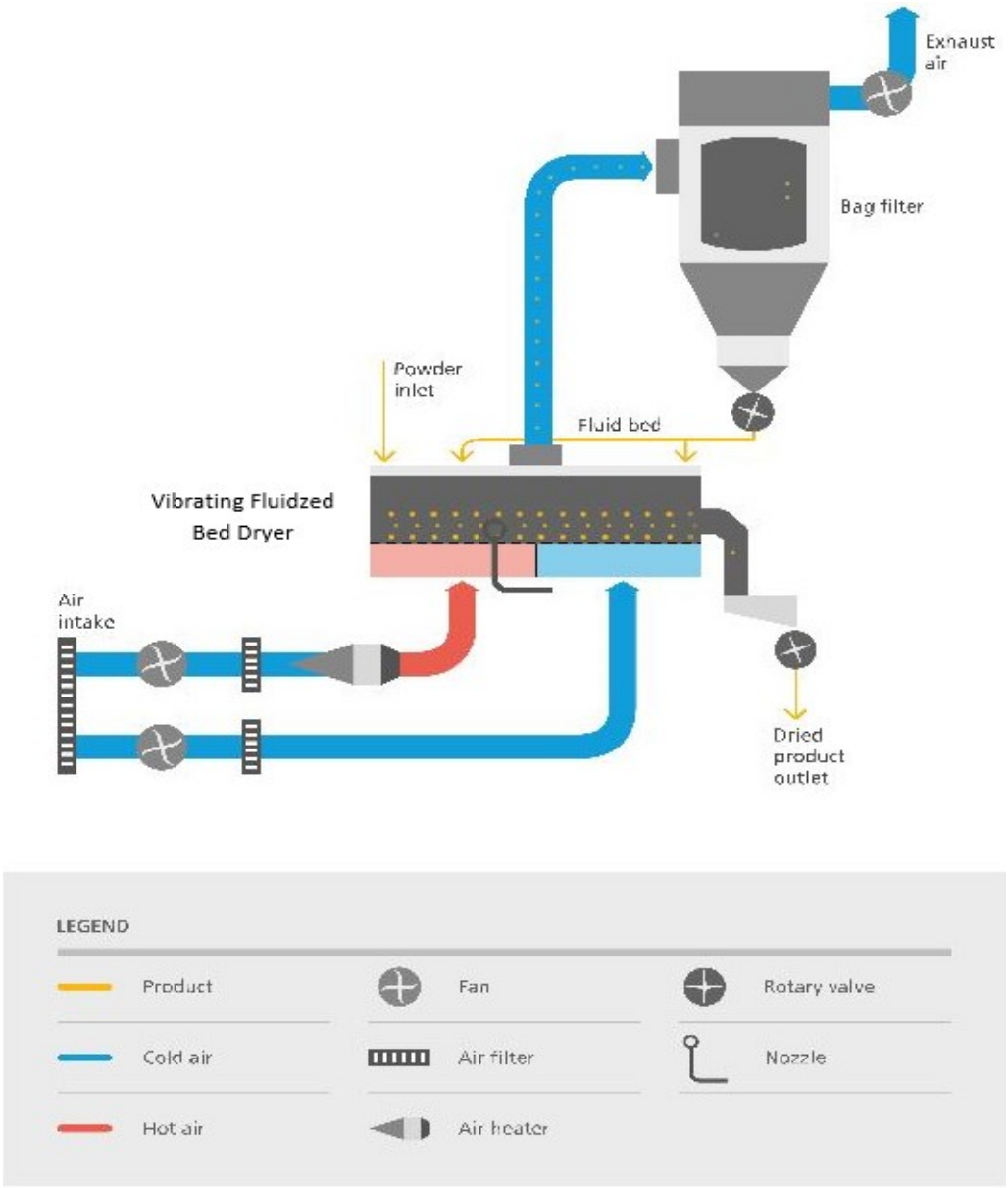

Figure 4-6. Vibrating fluidized bed [80]

4.6.3 Alternative Technology in Fluidized Bed Dryer

- Contact Fluidized Bed Dryer

Operation: The contact FBD (Figure 4-7) is applied where drying of wet-powder, chemical bulk product is required for a very large-scale. This hybrid advancement is compact in design with high heat transfer efficiency and low airflow throughput.

The wet material is fed into the back-mixing section of the dryer. Here the evaporation of the free moisture initiates, this promotes the direct fluidization of the material. The feed distributor ensures the uniformity by back-mixing of the wet material maintain

the homogeneity of the wet material and hence thereby increasing its performance. The plug flow of this semi-dried material allows to control the retention time for the wet material. This drying zone can also be coupled with the cooling section by equipping the dryer with the internal cooling panels depending upon the product requirement.

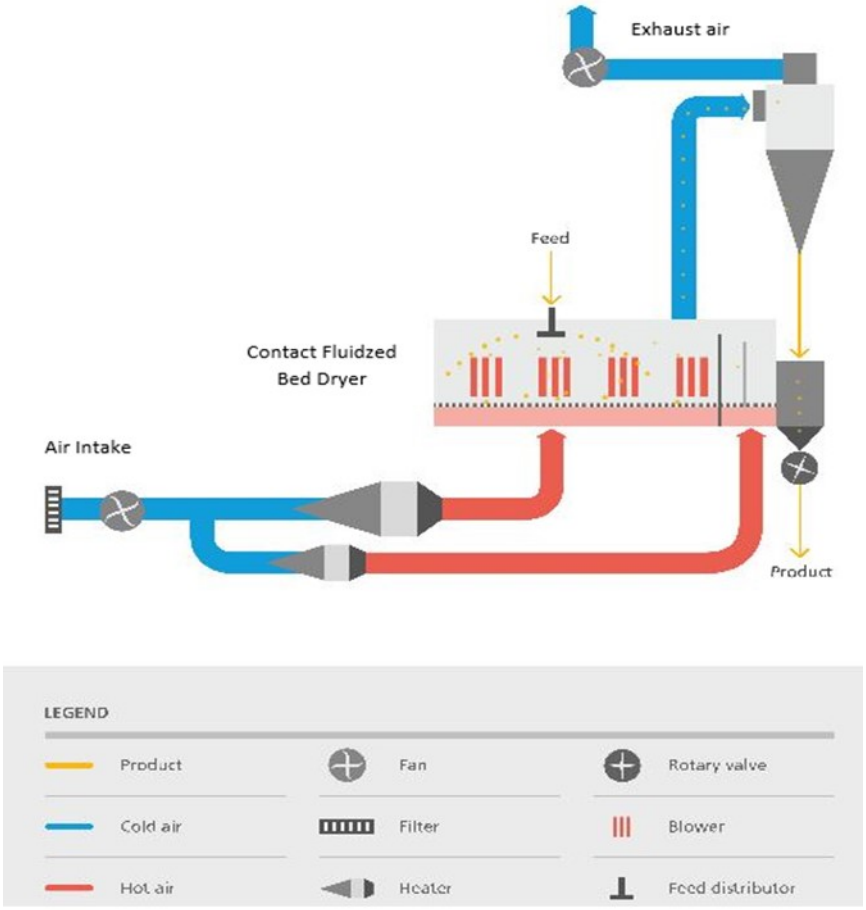

Figure 4-7. Contact fluidized bed dryer [80]

The airflow required for the fluidization of the wet material is distributed through a perforated air distributor plate to ensure evenly distribution of gas over the entire bed. This not only promotes the effective emptying of the FBD at shut-down but also accompanies good transport of lumps too.

The heating panels submerged into the fluidized material enhances the thermal efficiency as well as the heat transfer efficiency resulting in better drying of the product. This is a hybrid design which is highly effective for transferring the heat from the panel to the wet material via contact as well as through fluidizing air hence called as contact FBD.

Application: This hybrid FBD is a modification over the static FBD and allows its application for powders wetted with organic solvents, polymers and also to the food products. The average particle size range lies between 50 µm to 800 µm. Due to combination of back-mixing and plug flow section it allows gentle drying with longer residence time. As heating panels are used for increasing the drying performance hence it requires lower specific amount of air flow [80].

5 DESIGN PROCEDURE AND EQUATIONS

The design procedure and design equations for batch and continuous fluidized bed dryers vary widely for both constant rate period and falling rate period. In this section, the discussion is just confined to the drying of solid particulates.

5.1 Residence Time

If the particles are small in size, physically very porous and wet enough to contain free moisture, then the rate of drying remains constant throughout the drying process. However, if solid particulates initially contain surface moisture, then as soon as the surface moisture is removed resulting in constant drying rate, falling rate of drying will occur after a short period of constant rate drying. In such case the design calculation constitutes two parts: one for the constant rate drying and the other one for the falling rate drying. From Table 5-1, a list of equations for the residence time for various types of FBDs as well as for different mode of operations such as batch drying and continuous drying [72].

Table 5-1. Equations to determine Residence time for Drying [72]

	Remarks	**Drying Time Required**
Batch Drying		
1. Constant rate Period	**Only surface moisture present**	$t_R = \frac{(X_0 - X)M_s\lambda}{G_g c_{pg}(T_{in} - T_{out})}$
2. Falling rate Period	**(i) From diffusion model**	$\frac{X - X_{eq}}{X_0 - X_{eq}} = \frac{6}{\pi^2}\sum_{n=1}^{\infty}\frac{1}{n^2}e^{[-(n\pi)^2 Dt/R^2]}$ **is obtained by trial and error**
	(ii) Simplified equation	$t_R = \frac{M_s c_{ps}}{G_g c_{pg}}\ln\left(\frac{T_P - T_{in}}{T_{P0} - T_{in}}\right)$
	(iii) Empirical formulation	$t_R = \frac{1}{k}\ln\left(\frac{X_{crl} - X_{eq}}{X - X_{eq}}\right)$
Continuous Drying		

(a) Well- mixed	**Design curve [73]:** $\bar{X} = \int_0^\infty X(t)E(t)dt$	
1. Constant rate period	**Only surface moisture**	$t_R = \frac{X_0 - \bar{X}}{k}$
2. Falling rate period		$t_R = \frac{1}{k}\left(\frac{X_{in} - X_{eq}}{X_{out} - X_{eq}} - 1\right)$ [74]
3. Batch Drying Curve	(1) Obtain a record of the changing bed temperature T_b during constant inlet air temperature run. (2) Divide the constant inlet air temperature batch drying curve $X(t)$ into increments of length, ΔX. For each increment note the time Δt_{T_1} required to accomplish that amount of drying at constant bed temperature of T_1 (3) Calculate the time Δt_{T_2} required to accomplish the same increment of drying at constant bed temperature T_2 by the use of the following equation: $\frac{\Delta t_{T_1}}{\Delta t_{T_2}} = \frac{[(p_{sat} - p_{in})(\bar{X} - X_e)]_{T_1}}{[(p_{sat} - p_{in})(\bar{X} - X_e)]_{T_2}}$ [75], [76] (4) Build up the constant bed temperature batch drying by increments (5) Obtain drying equation for each curve (6) Obtain residence time from the design curve $t_R = \frac{SA}{f^* G\beta}\left(\frac{X_{in} - X_{out}}{X_{out} - X_{eq}}\right)$ [77], [78] where, S the bed loading, A is the bed area, $f^*$is the ratio of bed loading and flux of gas flow rate G/A, at constant temperature T_1	
(b) Plug flow		
1. Batch drying curve	**Residence time distribution function is** $E(t) = \frac{1}{2\sqrt{\pi B}} exp\left[-\frac{1 - (t/\tau_m)^2}{4B}\right]$ where, $B = \frac{D\tau_m}{L^2}$ and $D = \frac{3.71\times10^{-4}(u - u_{mf})}{u_{mf}^{1/3}}$; $D = \frac{1.49[0.01(H_b - 0.05) + 0.00165\rho_s(u - u_{mf})]u^{0.23}}{u_{mf}^{2/3}}$ [77] Note that validity of Reay's correlation for particle diffusivity has only been confirmed for bed depths up to 0.10 m. There	

	is some evidence in the literature that D may be an order of magnitude larger in much deeper beds [79]. Shallow bed is recommended if the objective is a close approach to plug flow behaviour of solid particles in the bed.

5.2 Sizing of Bed

Sizing of the bed is directly dependent on the hold-up mass balance for the fluidized bed dryers. The direct correlation of cross-sectional area of the fluidized bed can be given in terms of the solids flow rate (dry basis), bed density, and bed height are specified and particle residence time is determined from previous equations, and must be used to calculate the cross sectional area given by the following equation [72]:

$$A = \frac{F_s t_R}{\rho_b H_b}$$

5.3 Gas Flowrate

Gas flow rate (dry basis) can be determined from the following equations. The operating gas velocity, u_g, is defined as 2-3 times of the minimum fluidization velocity of the gas, generally for the fluidized bed drying. However, the appropriate operating gas velocity can be estimated from the laboratory-scale fluidized bed as far as the gas velocity results in good fluidization quality. The gas flow rate (dry basis) can be calculated from the following equation [72]:

$$G_g = \rho_g u_g A$$

5.4 Mass-Balance

A generalized mass balance equation can be coined for a given fluidized bed drying system with solid particulates as follows [72]:

$$F_s(X_{in} - X_{out}) = G_g(Y_{out} - Y_{in})$$

In the above equation, F_s, is the solid flow rate (kg/s), G_g, is the gas flow rate (kg/s), X, is the moisture content of the solid (kg/kg), Y is the absolute humidity of the gas (kg/kg).

5.5 Heat-Balance

For a single phase model for the heat balance equation results in the energy balance equation given below [72]:

$$F_s H_{s.in} + G_g H_{g.in} + Q_h = F_s H_{s.out} + G_g H_{g.out} + Q_w$$

In the above equation, Q_h and Q_w are the rate of heat input from the immersed tubes (kJ/s) and the rate of heat loss from the wall of the fluidized bed dryer (kJ/s), and H is the enthalpy (kJ/kg). It is important to note that the enthalpy of the solids at the inlet and outlet can be obtained from the following equations respectively.

$$H_{s.in} = (c_{ps} + X_{in} c_l) T_{s.in}$$

$$H_{s.out} = (c_{ps} + X_{out} c_l) T_{s.out}$$

In such cases, where the system exhibit a gas-vapor system, then in such case Mollier diagram can be used to determine the enthalpies of gas in and gas out, $H_{g.in}$ and $H_{g.out}$, respectively. Also, following equations can also be used to calculate the enthalpy for organic vapor-inert gas system provided as below:

$$H_{g.in} = (c_{pg} + Y_{in} c_l) T_{g.in} + Y_{in} \lambda$$

$$H_{g.out} = (c_{pg} + Y_{out} c_l) T_{g.out} + Y_{out} \lambda$$

A step by step flowchart for designing the fluidized bed dryer is given below in **Figure 5-1**. Also a simple guide for choosing a suitable fluidized bed dryer based on material properties is given in the **Figure 5-2**.

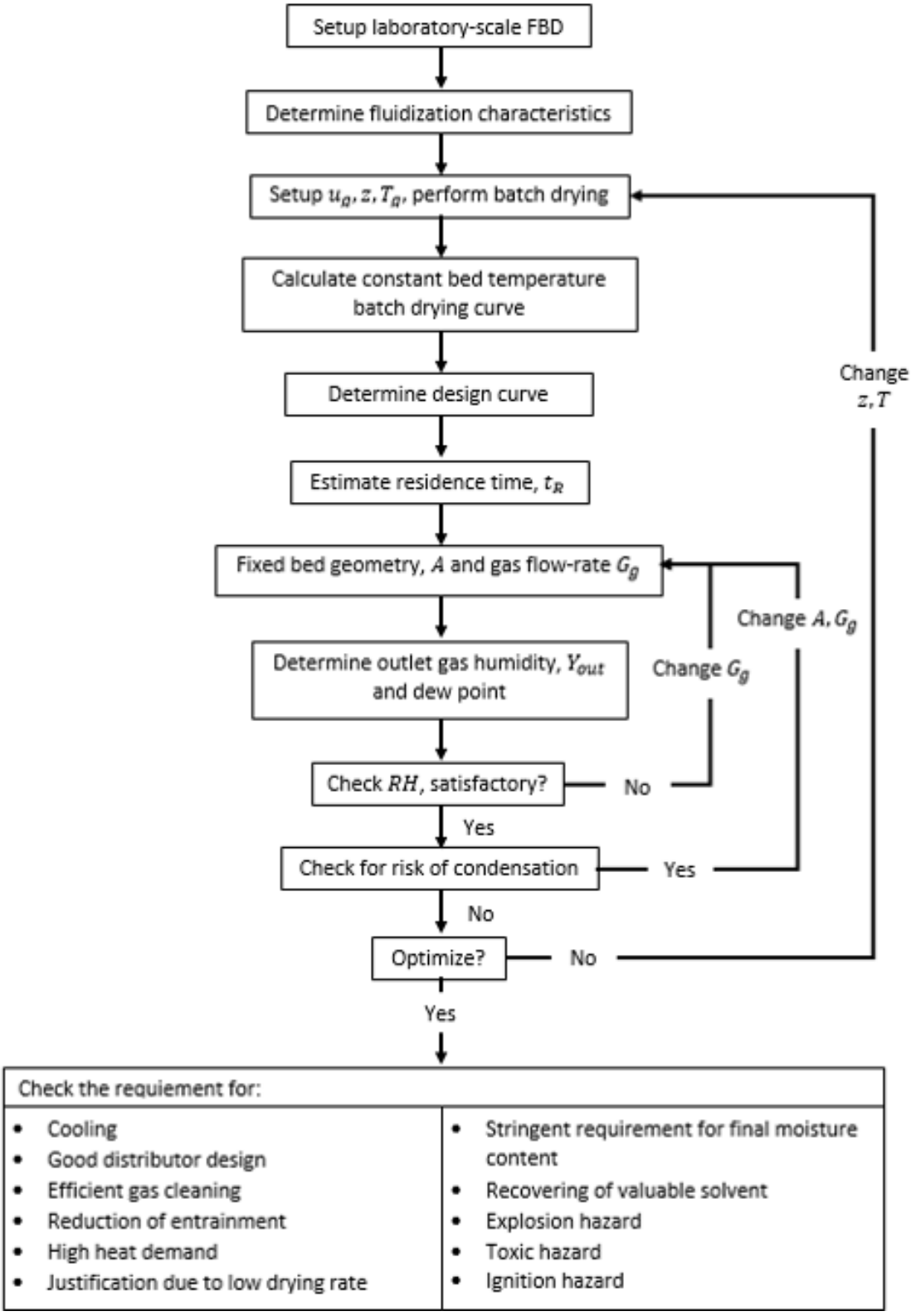

Figure 5-1. Design step starting from laboratory test [72]

Figure 5-2. Dryer selection [72]

6 AIM OF EXPERIMENTS

The experiments were carried out, aimed for two separate objectives as mentioned below:

- Determining the equilibrium moisture content of Dry-polyacrylamide

The equilibrium moisture content of the Dry-polyacrylamide at varying temperature and relative humidity combination must be examined for both with and without dosage of cutting oil at varying particle size distributions. Moreover, analysing effect of particle size distribution and of cutting oil dosage on equilibrium moisture content.

- Effect of different operating parameters on fluid bed drying of Polyacrylamide-gel

Raw data collection, using a logger software, of various operating parameters such as residence time, airflow, feed particles size, bed load and heater temperature, from a fluid bed dryer. Inspecting the effect of these varying operating conditions on drying of Polyacrylamide-gel by analysing the data. Identify, among these operating parameters, whether these have either directly or indirectly on drying process of it.

The samples and their preparation, procedures and results for both the objectives are elucidated in later sections.

7 EQUIPMENT, MATERIALS AND SOFTWARE

7.1 Equipment

- Meat Mincer

For mincing of the PAM- Gel, Koneteollisuus LM-10P was used. This meat mincer comes with range for aperture disk diameter (i.e. 3.0, 4.5 and 6.0 mm) for different output particle size which is one of the operating parameter for the fluid bed dryer.

- Fluid Bed Dryer

Sherwood tornado M501 fluid bed dryer was used for studying the effect of various operating parameters. The fluid bed dryer comes with an in-built data logger program which reads the reading through a Rotronic H/T (humidity and temperature) probe. It is a capacitive relative humidity sensor. However, the H/T probe has a limitation and can only measure up to 100°C as of outlet temperature. The equipment used is shown in Figure 7-1 along with the H/T probe and tub assembly used.

Figure 7-1. Fluid Bed Dryer with Humidity/Temperature probe and tub assembly

However, due to the limitation of H/T probe, comparison is done with another hygrometer viz. Rotronic Hygropalm HP22-A and having higher range from -100°C to 200°C and relative humidity 0% to 100%. The difference in the hygrometer reading was ~5°C higher at temperature reading and ~2% higher at relative humidity reading then of the H/T probe. This is due to the limitation of the H/T probe sensor which was causing this deviation and hence acted as a source of error. Comparison of Hygropalm Hygrometer and Conditioning Cabinet are presented in **Table 7-1** below:

Table 7-1. Comparison of Hygrometers

Conditioning Cabinet Hygrometer		Portable Hygropalm Hygrometer	
Temperature (°C)	**Relative Humidity (%)**	**Temperature (°C)**	**Relative Humidity (%)**
30.0	30.0	30.2	29.8
50.0	50.0	50.0	49.8
70.0	70.0	70.1	70.2

- Halogen Dryer

After the fluid bed dryer, the dried material was tested for the remaining moisture content. Mettler Toledo HR73 halogen moisture analyzer was used. The halogen dryer is used to determine the bone dry weight of the PAM-Gel and DPAM to analyze the total moisture removed under various operating conditions.

- Oven Dryer

Oven dryer used for drying the minced PAM-Gel. As of before grinding the PAM-Gel drying was essential for determining the equilibrium moisture content. The oven dryer used for this purpose was SalvisLab Thermocenter TC100.

- Grinding Mill

DPAM was then further grinded using Retsch ZM200 and it is an ultra-centrifugal mill. After grinding of the DPAM, grinded material was then passed through sieving.

- Sieve Trays

Sieving was performed by using 316 stainless steel VWR sieve trays of 150µm, 250µm and 1mm aperture size.

- Weigh Scale

For determining the weight of various raw material such as cutting oil, PAM-Gel and DPAM, Mettler PE3600 weigh scale was used.

- Conditioning Cabinet

Weiss WK111-340 conditioning cabinet was used to determine the equilibrium moisture content of the DPAM. Also, the effect of various particle sizes and addition of cutting oil was studied.

7.2 Materials

- Cationic Polyacrylamide Gel

Cationic polyacrylamide gel is used under this research and analytical work. It is used as a flocculant for primary clarification, sludge thickening and sludge dewatering applications in municipal areas for waste water treatment.

- Cutting Oil

Cutting oil reduces the adhesiveness among the minced PAM-Gel and used to avoid the agglomeration of the particles causing the fluidization difficult.

7.3 Software

- Sherwood Data Logging Software

Sherwood tornado M501 fluid bed dryer comes along with the compact disc of the data logging software. It is used for all the data logging and monitoring the operating parameters.

- ImageJ

ImageJ is used which is an image processing program, to analyze the particle size of the feed and dried product.

8 EXPERIMENTS

8.1 Determining the Equilibrium Moisture Content of Dry-polyacrylamide

8.1.1 Samples and their preparation

Three samples of DPAM without cutting oil dosage and three samples of DPAM with cutting oil dosage were used to measure the equilibrium moisture content. All the samples were in solid form, however varying from powder to granular form. The sample preparation is carried out as follows:

- Firstly, PAM-gel is grinded through meat grinder with 4.5 mm particle opening.
- Grinded PAM-gel is then divided in two halves.
- One of the halves is weighed and cutting oil is added into the grinded PAM-gel by a pre-defined ratio (i.e. 1 ml of cutting oil/100 g of PAM-gel)
- Then both sample lots are kept in an oven dryer at 60°C for 24 hours.
- Afterwards both DPAM granules (with and without cutting oil) are grinded using a grinding mill and sieved using sieve tray in three know particle size ranges (i.e. 150 µm – 250 µm, 250 µm – 1 mm and greater than 1 mm)

All three samples of with and without the cutting oil are of different size and these sample properties are mentioned in **Table 8-1**.

Table 8-1. Samples and their physical properties

Sample	Cutting Oil	Particle Size
S_1	without cutting oil	150 µm – 250 µm
S_2	without cutting oil	250 µm – 1 mm
S_3	without cutting oil	1 mm <
S_1'	with cutting oil	150 µm – 250 µm
S_2'	with cutting oil	250 µm – 1 mm
S_3'	with cutting oil	1 mm <

8.1.2 Procedure

For determining the equilibrium moisture content of DPAM and effect of cutting oil dosage along with the particle size involved following steps:

- All DPAM samples (with and without cutting oil) are then kept in a halogen dryer before putting them into the conditioning cabinet in order to find out the moisture present in the samples.
- All the samples are weighed to 2 g and kept in separate aluminium trays of known weight.
- The conditioning cabinet is set to a known temperature and relative humidity.
- After a known time interval (viz. 1, 2, 3, 4, 20, 22 and 23 hours) samples are weighed again and total moisture gained by each sample is calculated by subtracting the bone dry weight of the sample and weight of aluminum tray
- With such dataset obtained a graph between moisture content per bone dry weight material (Y-axis) is plot against relative humidity (X-axis) for different temperature profiles as presented in Figure 8-1 and Figure 8-2.

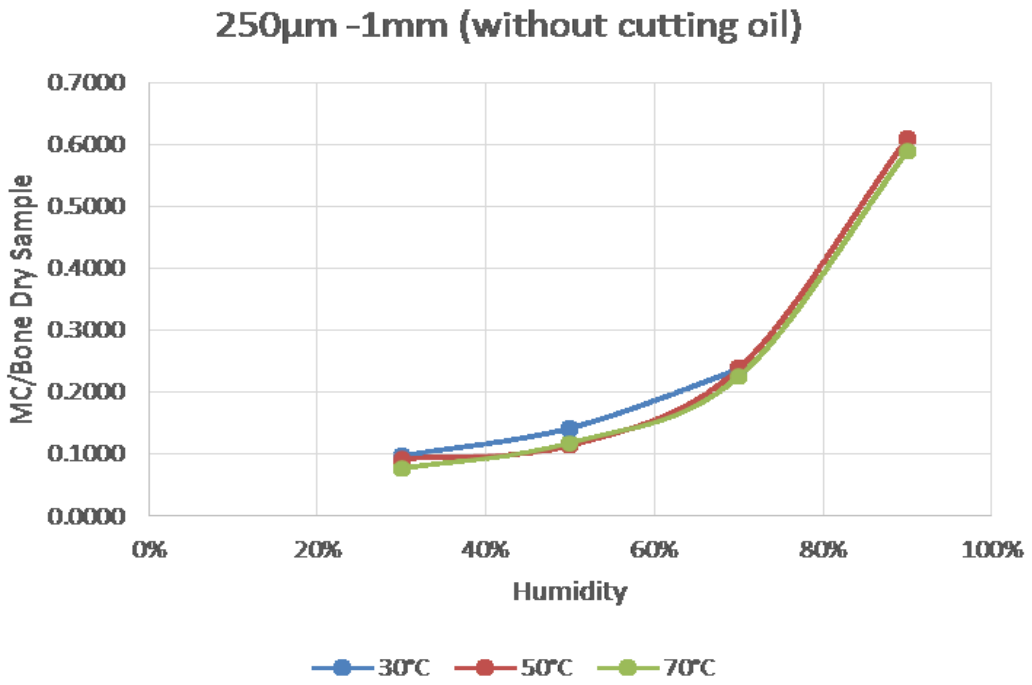

Figure 8-1. Equilibrium Moisture Content for Dry-polyacrylamide without cutting oil

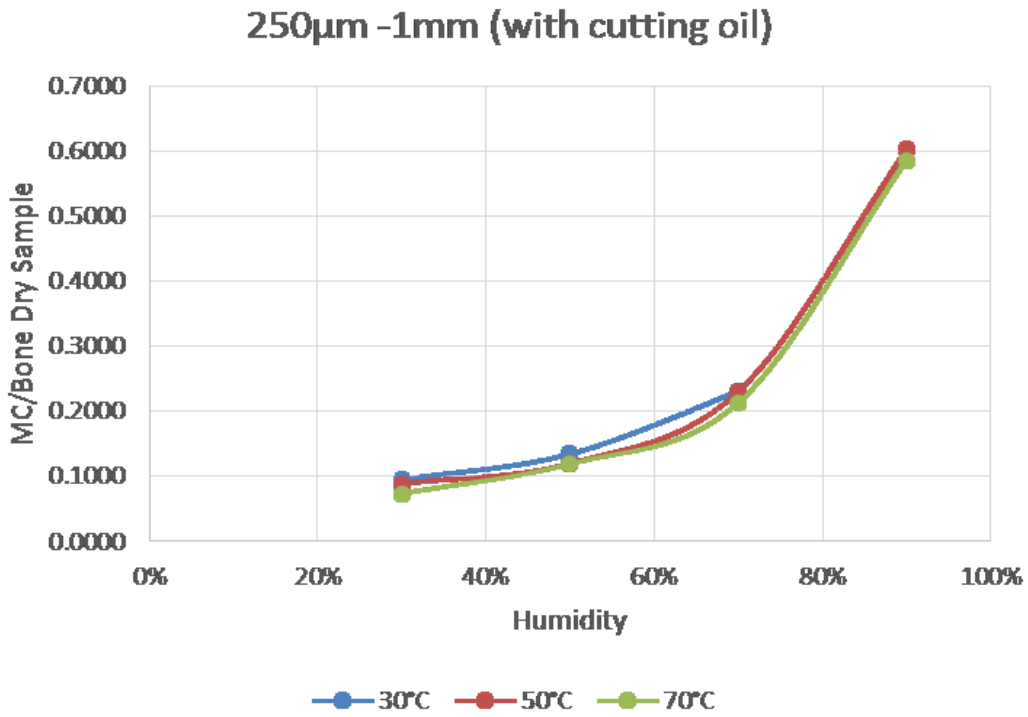

Figure 8-2. Equilibrium Moisture Content for Dry-polyacrylamide with cutting oil

8.1.3 Results

As from the Figure 8-1 and Figure 8-2, it is clear that there is no significant effect of cutting oil and particle size on the equilibrium moisture content (refer to Appendix A). In all the tested parameters' combination (viz. temperature and relative humidity) equilibrium for each and every sample were attained in between 22 ~ 24 hours in the conditioning cabinet (Figure 8-3 and Figure 8-4). Once the equilibrium moisture content is determined, the second phase of the experiment is carried out viz. effect of the fluid bed operating parameters on the drying of PAM-Gel.

Further EMC related findings are discussed in later chapter and other results are present in Appendix A.

The experimental data of equilibrium moisture content was also collected for 99% relative humidity at 30°C, 50°C and 70°C. However, due to the condensation of water droplets over the material as well as on the sampling aluminium tray were acting as error sources. Hence, the collected data at 99% relative humidity at different temperatures were not considered.

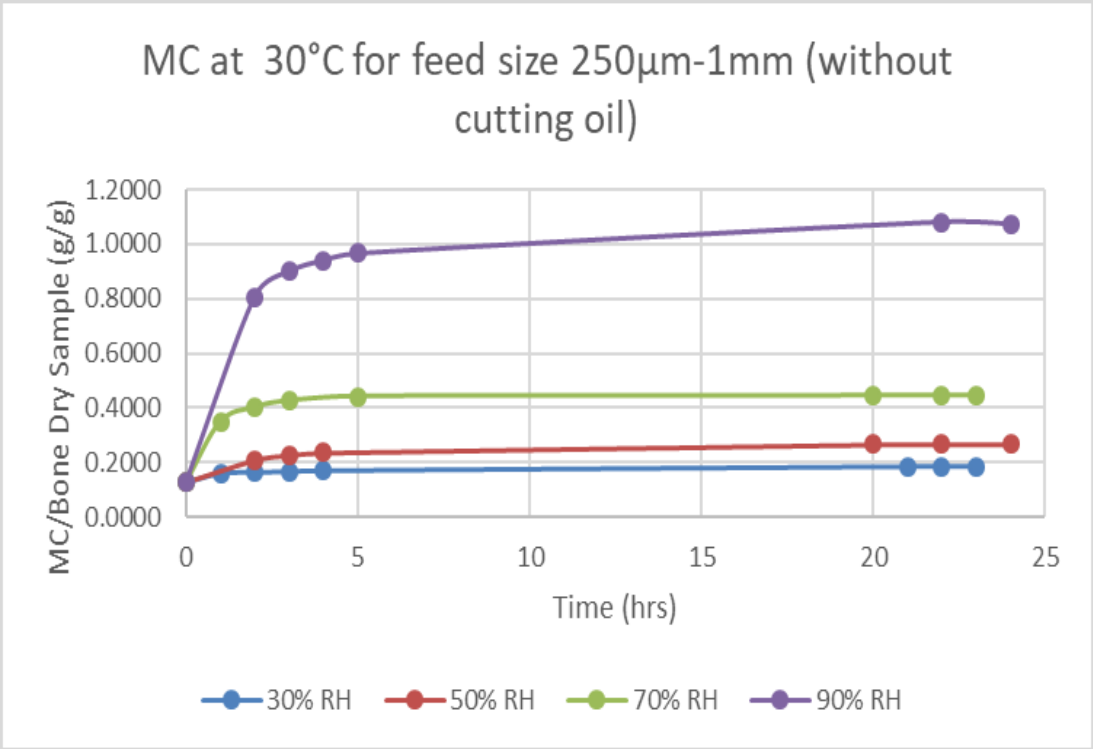

Figure 8-3. Moisture content for Dry-polyacrylamide without cutting oil

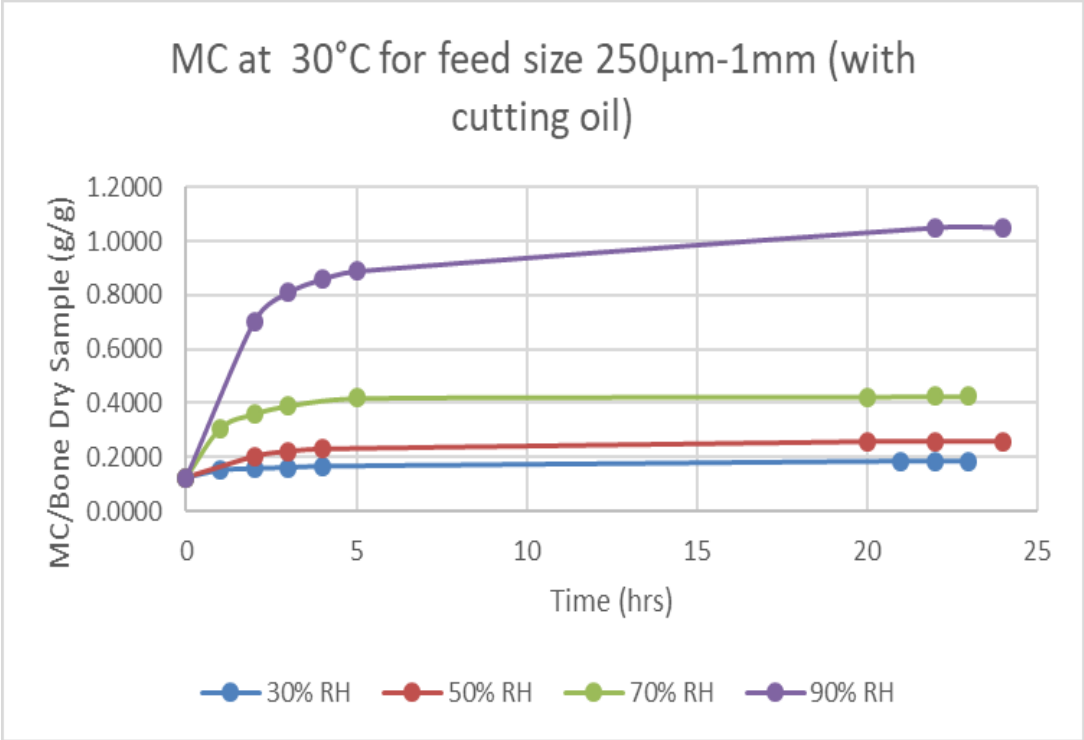

Figure 8-4. Moisture content for Dry-polyacrylamide with cutting oil

8.2 Effect of various Fluidized Bed Dryer operating parameters on drying of Polyacrylamide-gel

The tested operating parameters include:

- Residence Time
- Airflow Rate
- Feed Particle Size
- Inlet Temperature
- Bed Loading

The baseline operating parameters of all the experiments are mentioned in **Table 8-2** given below:

Table 8-2. Tested operating parameters and their baseline values

Operating Parameter	Baseline Value	Unit
Residence Time	80	min
Airflow Rate	0.0272	m^3/sec
Feed Particle Size	4.5	mm
Inlet Temperature	80	°C
Bed Load	300	g

In all the samples under observation the dosage of cutting oil is in a pre-defined ratio (i.e. 1 g of cutting oil/100 g of PAM-Gel).

In these sections below, an elucidated description of procedures and findings are discussed related to effect of each operating parameter separately. All the samples are prepared with the same procedure. Hence, common sample preparation and other information are provided in **Section 8.2.1** and **Section 8.2.2**. Detailed information about the tested parameters and number of samples are mentioned in their respective sub-sections.

8.2.1 Samples and their preparation

All the PAM samples are in gel form, granulated by using a meat grinder resulting in 4.5 mm feed particle size (excluding feed particle size as tested parameter). Number of samples may vary depending upon the tested parameters. The preparation of

samples includes following steps, disregarding the tested parameters in order to keep the consistency in feed material:

- Weigh the PAM-gel and add the cutting oil in a pre-defined ratio (i.e. 1 g of cutting oil per 100 g of PAM gel)
- Grind the PAM-gel in known feed particle size i.e. for most of the experiment is 4.5 mm, except feed particle size (viz. 3 mm, 4.5 mm and 6 mm)
- Make batches of known weight i.e. 300 g for most of the experiment with freshly grinded PAM-gel, except bed loading as tested parameter (viz. 100 g, 200 g, 300 g, 400 g, 500 g and 600 g)
- These are the samples to be tested for the effect for varying operating parameters

8.2.2 Procedure

In all the experiments and data analysis same procedure was followed and only one set of experiment is explained and elucidated description is provided. All the remaining results and observations are presented in **Appendices B**, **C**, **D**, **E**, **F**, **G**, **H** and **I**. The tested operating parameter in this section is residence time (viz. 80 min). All the other parameters are kept to their baseline values and are provided in the sections below:

Halogen Dryer

- Take a small yet appropriate amount of freshly prepared sample and run the test on the halogen dryer to determine the moisture content in the sample
- The operating parameters for the halogen dryer are presented in **Table 8-3**.
- Once the run is complete, the reading displayed denotes the moisture content by the sample.

Table 8-3. Halogen dryer operating parameters for determining the moisture content of the sample

Operating Parameter	Baseline Value	Unit
Residence Time	120	min
Inlet Temperature	105	°C
Sample Weight	2.5	g

The reason to choose halogen dryer over the conventional oven dryer is that it is a less time consuming process with better accuracy and repeatability of the measurements. Although, a comparison between oven dryer and halogen dryer is tabulated and presented below in Table 8-4.

Table 8-4. Comparison between Oven and Halogen Dryer

Operating Parameter	**Oven Dryer**		**Halogen Dryer**	
Sample Type	PAM-gel	DPAM	PAM-gel	DPAM
Temperature (°C)	105	105	105	105
Residence Time (hrs.)	8	8	2	2
Sample Weight (g)	2.5	2.5	2.5	2.5
Moisture Content (%)	69.10	6.52	68.66	6.43

Fluid Bed Dryer

- Firstly, ensure all the connections are fastened properly, to avoid false air into the system.
- Run the FBD without the PAM-gel for 10 min. at the mentioned operating parameters as to match the heater set value and process value. However, it is important to mention that the inlet temperature of the FBD never achieves the heater set value. Inlet temperature is always lower than the heater set value.
- Afterwards, add 300 g of the freshly prepared PAM-gel in FBD tub assembly.
- Start the data logging for the residence time, airflow rate, outlet temperature, relative humidity.
- Once, the data logging initiates run the FBD system for each testing residence time.

ImageJ (Particle Size Distribution)

- A small amount of feed/dried product is distributed evenly over a black surface.
- Scale is kept on one side of sample (in order to compare the pixel size).

- Picture is captured in .jpeg format and then processed using the ImageJ analyser.
- Firstly, image which is to be analysed is opened and straight line tool is selected from the toolbar and is used to determine 10mm scale length in terms of pixel length by keeping angle at 0.0 and the 10mm scale length in pixel length is then obtained (**Figure 8-5**).
- Now, the image is cropped using rectangular selection tool to reduce the excess background and only up to where the particles are visible. This helps in further image processing steps (**Figure 8-6**).
- Moreover, now change Image Type by tab selection Image → Type → 8-bit (**Figure 8-7**)
- Then threshold is under Image → Adjust → Threshold. It is ensured that the most of the particle are between the threshold (**Figure 8-8**)
- After threshold is adjusted, the image colour is inverted by opting Edit → Invert in the tool bar (**Figure 8-9**).
- Now, particles are analyzed by **Analyze → Analyze Particles**. While performing particle analysis, **Size** is set in pixel² for the smallest particle in the image to infinity with **Circularity** from 0.00 to 1.00. In the **Show** tab, nothing is opted in order to analyze the entire particle area (**Figure 8-10**) and results are then saved in .xlsx format for calculations in later **Section 9**.

8.2.3 Results

All the results for the effect of fluid bed operating parameters are discussed in the later sections.

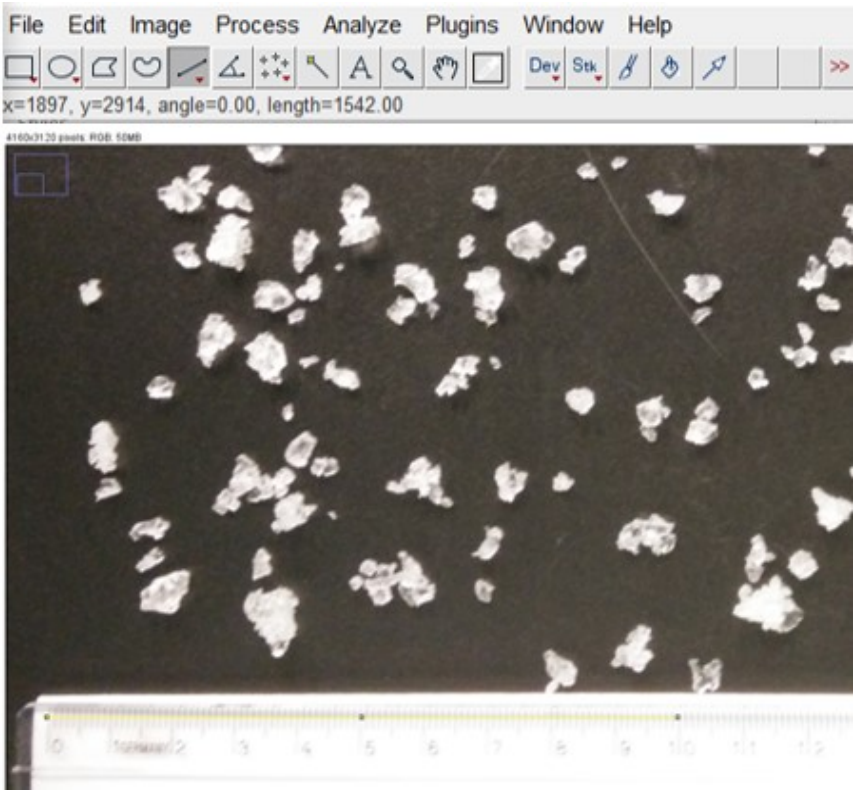

Figure 8-5. Particle Identification (Step-1)

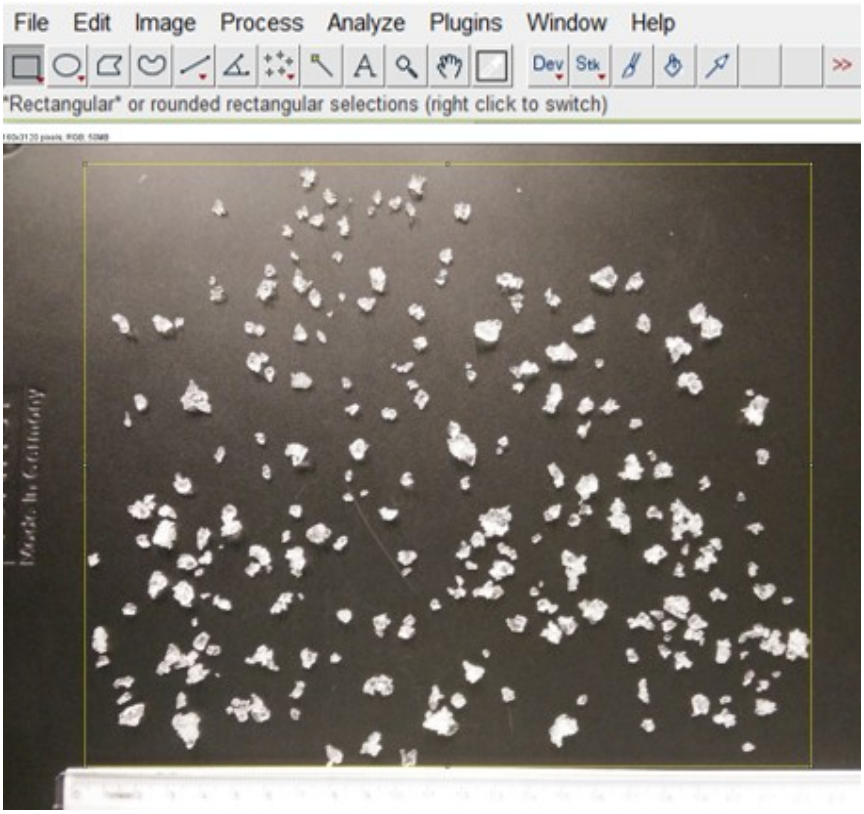

Figure 8-6. Particle Identification (Step-2)

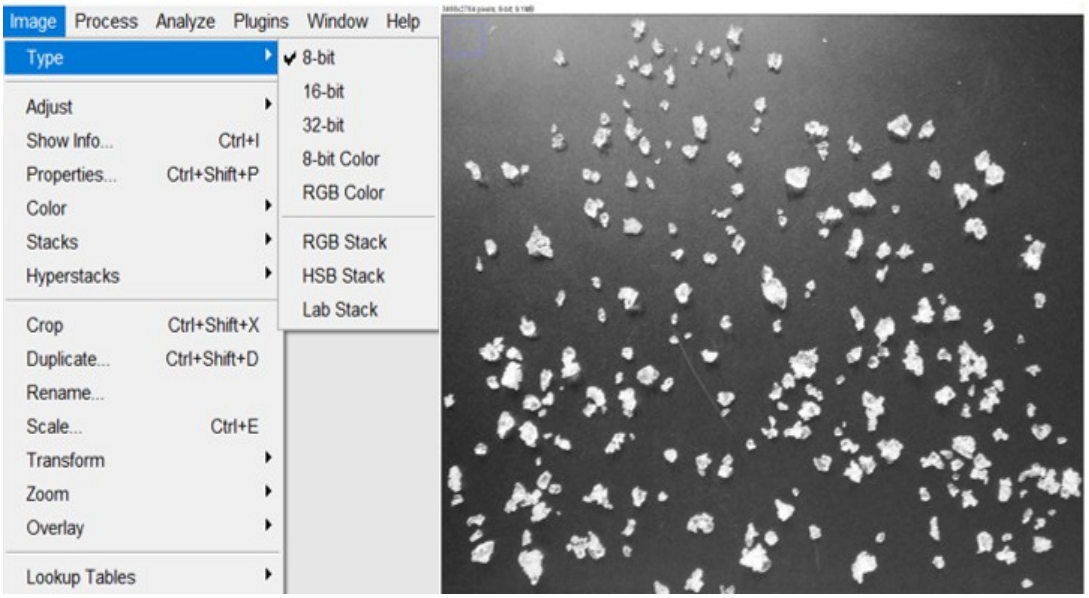

Figure 8-7. Particle Identification (Step-3)

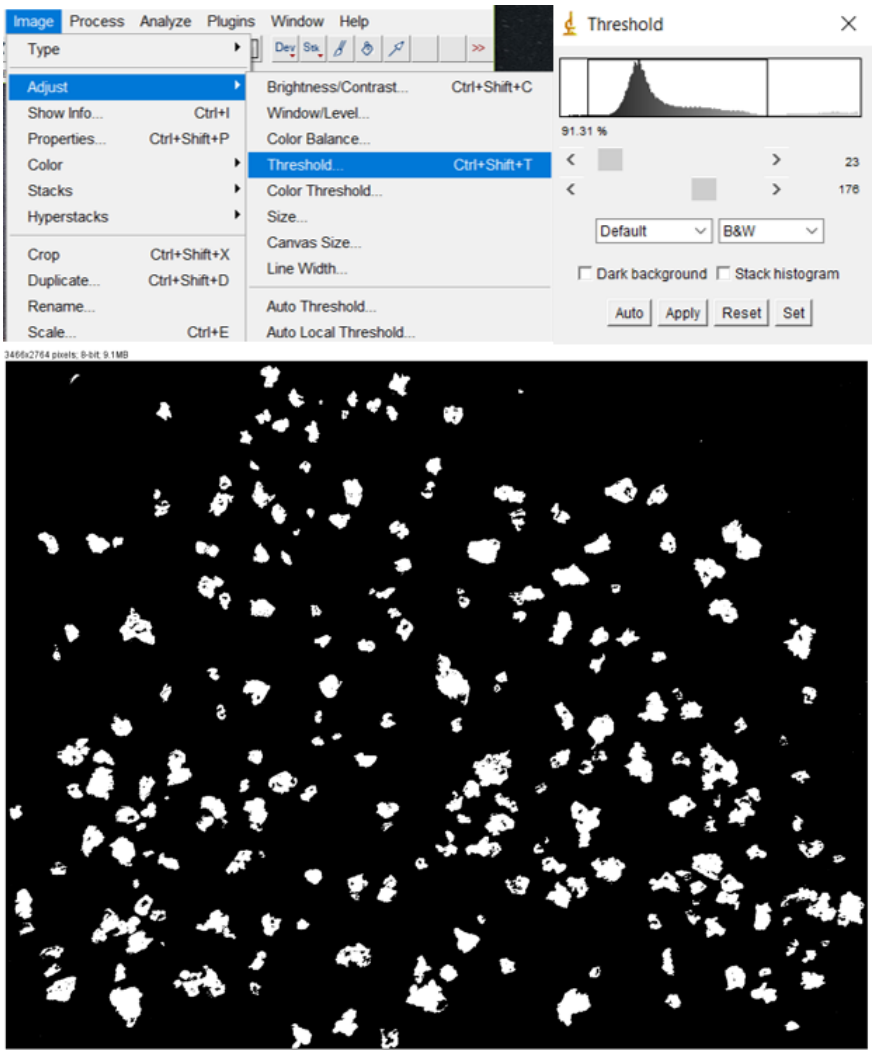

Figure 8-8. Particle Identification (Step-4)

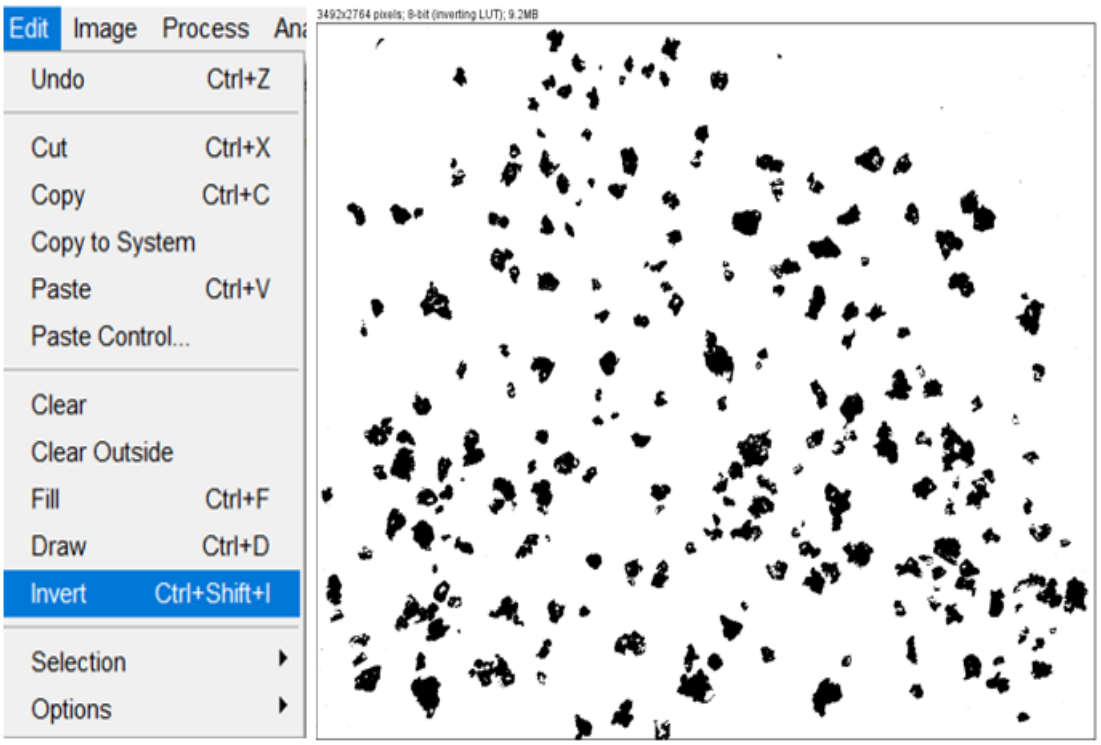

Figure 8-9. Particle Identification (Step-5)

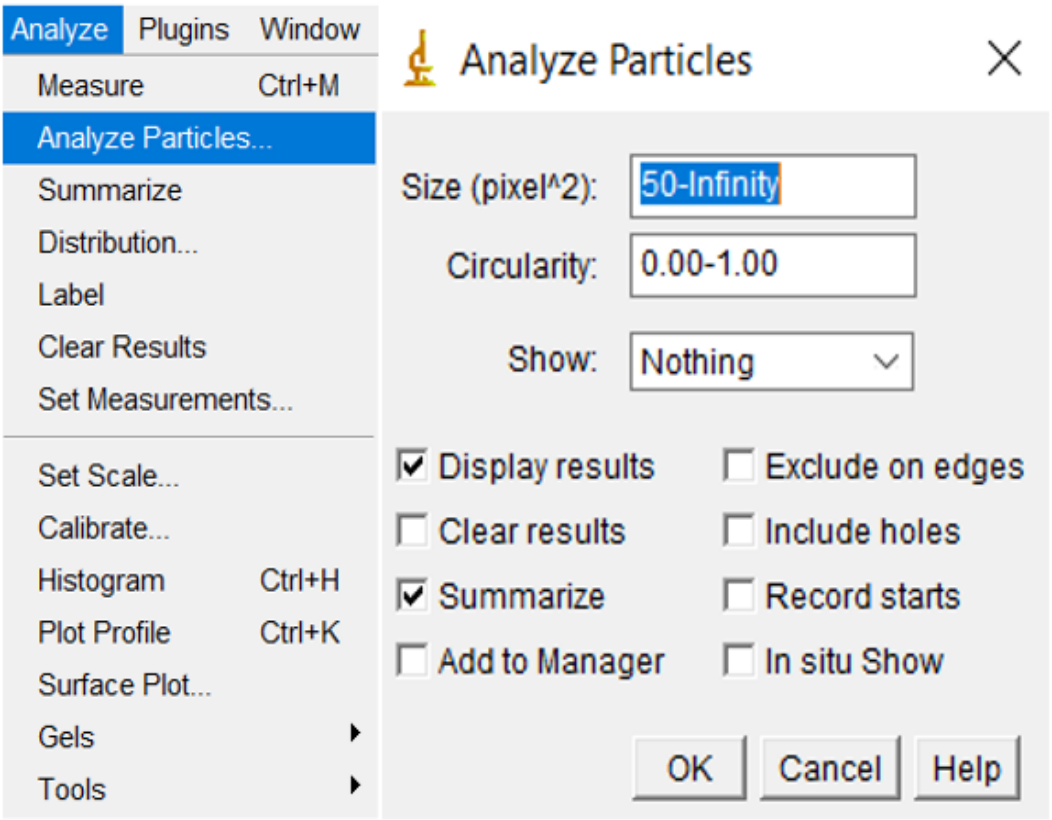

Figure 8-10. Particle Identification (Step-6)

9 CALCULATIONS

Fluid Bed Dryer

For calculating absolute humidity from relative humidity which is a temperature dependent property following procedure and mathematical formula is used for conversion.

Firstly, water vapor saturation pressure is calculated using following correlation [82]

$$P_{ws} = K_1 \cdot 10^{\left(\frac{K_2 T}{T+K_3}\right)}$$

where, K_1 = 6.089613 (constant) (hPa)

K_2 = 7.33502 (constant) (dimensionless)

K_3 = 230.3921 (constant) (°C)

After this vapor pressure is calculated using following equation:

$$P_w = P_{ws(@T)} \cdot \frac{RH}{100}$$

Then absolute humidity is calculated from the equation [82] provided below:

$$H_{abs.} = K_4 \cdot P_w / T$$

where, K_4 = 2.16679 (gK/J) (constant)

After calculating the absolute humidity net airflow conversion from percentage to volume is carried out using the conversion table provided with the FBD user manual and by using that conversion data following equation was obtained at ambient pressure:

$$V_{air(@20°C)} = ((C_1 \cdot v_{\%} + C_2)/60) \times (t_i - t_{i-1})$$

where, C_1 = 0.0187 (m^3/s) (constant)

C_2 = 0.1338 (m^3/s) (constant)

Since the airflow-rate conversion is provided at 20°C by the manufacturer of FBD, hence conversion at the required temperature is calculated by using the ideal gas law as provided below:

$$V_{air(@T)} = V_{air(@20°C)} \cdot \frac{T + 273.15}{20 + 273.15}$$

Now, for calculating net evaporation rate, the equation has been derived using gas phase material balance and provided below,

$$N_{evap} = V_{air(@T)} \cdot \frac{H_{abs} - H_{air}}{t_i - t_{i-1}}$$

After the calculation of the net evaporation rate, the second scaling of data is performed. The reason for the second scaling is that total evaporation moisture calculated from gas phase is more than total moisture calculated from solid phase, which means mass balance does not conserve. Therefore, based on the total evaporation moisture from solid phase is used to scale the evaporation rate again to hold the mass balance.

In order to obtained the scaled data following equation has been used,

$$N_{evap}^{'} = N_{evap} \cdot \frac{X_{solid}}{X_{gas}}$$

X_{solid} is calculated by subtracting the moisture present in dried product with moisture present in the feed. Similarly, X_{gas} is calculated as the overall cumulative moisture content by multiplying the net evaporation rate with the time of logged data (only the maximum value is taken into the consideration). In **Table 9.1**, average deviation in X_{solid} and X_{gas} for various dryer operating condition is presented.

Table 9-1. Average Deviation in X_{solid} and X_{gas}

Operating Parameters	Feed Particle Size (mm)	Deviation (g)	Deviation (%)
Residence Time	4.5	39.24	16.02
Airflow	3.0 / 4.5	48.81 / 45.35	19.59 / 17.29
Particle Size	3.0 / 4.5 / 6.0	24.12 / 35.97 / 59.13	10.71 / 14.87 / 21.95
Bed Load	4.5	48.54	15.05
Inlet Temperature	3.0 / 4.5 / 6.0	31.96 / 61.12 / 59.13	13.43 / 22.33 / 21.95

The elucidated results for deviation between X_{solid} and X_{gas} are given in **Appendix B**. As per due to limitation of the H/T probe the values of X_{solid} and X_{gas} is not coherent.

Hence, the deviation is measure and presented. However, no specific trend is followed by deviation in X_{solid} and X_{gas}. In addition, X_{gas} is scaled and used for material balance as it conserves the mass balance.

Particle Size Distribution

ImageJ is used to analyze particle and for particle identification. As the area of the particle is calculated by ImageJ. Same procedure for calculation is carried out for the feed and for the dried product. Following calculation have been performed to determine the particle size distribution.

- Initially, unitary method is applied to determine the length of 1 pixel in mm.
- Then 1 x 1 pix^2 is converted into the mm^2.
- Now the area (in pix^2) obtained from the image processing and analysis is converted into mm^2.
- After the area is obtained (in mm^2), diameter (in mm) of the equivalent circle is calculated for each particle.
- By the diameter obtained, volume is calculated for each particle (in mm^3)
- Now, the total volume of the entire sample is calculated by summing up individual volume of the particle.
- Also, in between >0 mm to maximum diameter with 1 mm interval, volume is summed up for each diameter range respectively.
- All the data for particle size range and volume fraction are then tabulated (**Table 9-2**).

ImageJ software for particle identification and analyses, surely provide reproducible results with reasonable accuracy for small samples. It is ensured while particle analysis is performed that images used are clear and in .jpeg format. It is fast and simple as well as cost effective, when compared with high end equipment required for entire population size distribution rather than small samples. Although, this method provide plausible results, there is wide scope of making manual errors such as Size range for particles to be analyzed and can lead to calculation errors.

Furthermore, in **Table 9-3**, **Table 9-4** and **Table 9-5**, logged, calculated (unscaled) and calculated (scaled) data is tabulated, respectively. In the table vSV (airflow rate) and HeatSV (heater temperature) are the set values. Time, vPV, HeatPV, TempPV

(inlet temperature) and RH% (relative humidity) are the logged data. However, P_{ws}, P_w, H_{abs}, V_{air}, $V_{air(@20°C)}$, $V_{air(@T)}$, N_{evap}, X and X_{cum} are the calculated unscaled data and $\dot{N}_{evap}$, $\dot{X}$ and $\dot{X}_{cum}$ are calculated scaled data.

Table 9-2. Particle Size Distribution for Feed

Particle Size Range (mm)	Volume (mm^3)	Volume Fraction
0-1	5.80	0.0004
1-2	63.59	0.0048
2-3	380.30	0.0286
3-4	978.07	0.0735
4-5	1980.47	0.1488
5-6	2719.41	0.2043
6-7	2426.23	0.1823
7-8	2465.04	0.1852
8-9	1888.83	0.1419
9-10	402.04	0.0302

Table 9-3. Logged data for Fluid Bed Dryer

Min.	Sec.	vSV (%)	vPV (%)	HeatSV (C)	HeatPV (C)	TempPV (C)	RH (%)
0	0	80	80	80	79.1	31.2	27
0.17	10.2	80	80	80	72.1	31.2	37.4
0.33	19.8	80	80	80	66.8	31.4	43.8
0.5	30	80	80	80	69.1	31.5	46.5
0.67	40.2	80	80	80	73.6	31.7	43.2
0.83	49.8	80	80	80	77.8	32.4	42
1	60	80	80	80	80.3	33.4	43.7
1.17	70.2	80	80	80	81.1	34.4	47.8
1.33	79.8	80	80	80	80.5	35	50.6
1.5	90	80	80	80	79.5	35.3	50.9
1.67	100.2	80	80	80	78.7	35.3	51
1.83	109.8	80	80	80	78.4	35.2	50.7
2	120	80	80	80	78.9	35.2	51
2.17	130.2	80	80	80	79.3	35	50.7
2.33	139.8	80	80	80	79.8	35	51.2
2.5	150	80	80	80	80	35	51.2
2.67	160.2	80	80	80	80.1	35	51.5
2.83	169.8	80	80	80	79.8	35	50.6
3	180	80	80	80	80	35	50.2
3.17	190.2	80	80	80	80	35.1	50.3
3.33	199.8	80	80	80	80.1	35.1	49.9
3.5	210	80	80	80	79.9	35.1	50.2
3.67	220.2	80	80	80	79.9	35.2	50.2
3.83	229.8	80	80	80	79.9	35.3	49.2
4	240	80	80	80	79.9	35.3	49.2
4.17	250.2	80	80	80	79.9	35.3	48
4.33	259.8	80	80	80	80	35.5	45.4
4.5	270	80	80	80	80.1	35.6	43.2
4.67	280.2	80	80	80	80	35.9	41
4.83	289.8	80	80	80	79.9	36.2	39
5	300	80	80	80	80	36.7	36.9

Table 9-4. Calculated and unscaled data for Fluid Bed Dryer

Min.	P_{ws}	P_w	H_{abs}	V_{air}	V_{air} (@ 20°C)	V_{air} (@ T)	N_{evap}	X	X_{cum}
0	45.7	12.3	8.8	0.03	0.0	0.0	0.0	0E+00	0E+00
0.17	45.7	17.1	12.2	0.03	0.3	0.3	0.3	3E+00	3E+00
0.33	46.2	20.2	14.4	0.03	0.3	0.3	0.3	3E+00	6E+00
0.5	46.4	21.6	15.4	0.03	0.3	0.3	0.4	4E+00	9E+00
0.67	47.0	20.3	14.4	0.03	0.3	0.3	0.3	3E+00	1E+01
0.83	48.9	20.5	14.6	0.03	0.3	0.3	0.3	3E+00	2E+01
1	51.7	22.6	16.0	0.03	0.3	0.3	0.4	4E+00	2E+01
1.17	54.6	26.1	18.4	0.03	0.3	0.3	0.4	4E+00	2E+01
1.33	56.5	28.6	20.1	0.03	0.3	0.3	0.5	5E+00	3E+01
1.5	57.4	29.2	20.5	0.03	0.3	0.3	0.5	5E+00	3E+01
1.67	57.4	29.3	20.6	0.03	0.3	0.3	0.5	5E+00	4E+01
1.83	57.1	29.0	20.4	0.03	0.3	0.3	0.5	5E+00	4E+01
2	57.1	29.1	20.5	0.03	0.3	0.3	0.5	5E+00	5E+01
2.17	56.5	28.6	20.1	0.03	0.3	0.3	0.5	5E+00	5E+01
2.33	56.5	28.9	20.3	0.03	0.3	0.3	0.5	5E+00	6E+01
2.5	56.5	28.9	20.3	0.03	0.3	0.3	0.5	5E+00	6E+01
2.67	56.5	29.1	20.5	0.03	0.3	0.3	0.5	5E+00	7E+01
2.83	56.5	28.6	20.1	0.03	0.3	0.3	0.5	5E+00	7E+01
3	56.5	28.4	19.9	0.03	0.3	0.3	0.5	5E+00	8E+01
3.17	56.8	28.6	20.1	0.03	0.3	0.3	0.5	5E+00	8E+01
3.33	56.8	28.3	19.9	0.03	0.3	0.3	0.5	5E+00	9E+01
3.5	56.8	28.5	20.0	0.03	0.3	0.3	0.5	5E+00	9E+01
3.67	57.1	28.7	20.2	0.03	0.3	0.3	0.5	5E+00	1E+02
3.83	57.4	28.3	19.9	0.03	0.3	0.3	0.5	5E+00	1E+02
4	57.4	28.3	19.9	0.03	0.3	0.3	0.5	5E+00	1E+02
4.17	57.4	27.6	19.4	0.03	0.3	0.3	0.5	5E+00	1E+02
4.33	58.1	26.4	18.5	0.03	0.3	0.3	0.4	4E+00	1E+02
4.5	58.4	25.2	17.7	0.03	0.3	0.3	0.4	4E+00	1E+02
4.67	59.4	24.3	17.1	0.03	0.3	0.3	0.4	4E+00	1E+02
4.83	60.3	23.5	16.5	0.03	0.3	0.3	0.4	4E+00	1E+02
5	62.0	22.9	16.0	0.03	0.3	0.3	0.4	4E+00	1E+02

Table 9-5. Calculated and scaled data for Fluid Bed Dryer

Mins.	$\dot{N}_{evap}$	$\dot{X}$	$\dot{X}_{cum}$
0	0E+00	0E+00	0E+00
0.17	2E-01	2E+00	2E+00
0.33	2E-01	2E+00	4E+00
0.5	2E-01	2E+00	6E+00
0.67	2E-01	2E+00	8E+00
0.83	2E-01	2E+00	1E+01
1	2E-01	3E+00	1E+01
1.17	3E-01	3E+00	2E+01
1.33	3E-01	3E+00	2E+01
1.5	3E-01	3E+00	2E+01
1.67	3E-01	3E+00	3E+01
1.83	3E-01	3E+00	3E+01
2	3E-01	3E+00	3E+01
2.17	3E-01	3E+00	4E+01
2.33	3E-01	3E+00	4E+01
2.5	3E-01	3E+00	4E+01
2.67	3E-01	3E+00	5E+01
2.83	3E-01	3E+00	5E+01
3	3E-01	3E+00	5E+01
3.17	3E-01	3E+00	6E+01
3.33	3E-01	3E+00	6E+01
3.5	3E-01	3E+00	6E+01
3.67	3E-01	3E+00	7E+01
3.83	3E-01	3E+00	7E+01
4	3E-01	3E+00	7E+01
4.17	3E-01	3E+00	8E+01
4.33	3E-01	3E+00	8E+01
4.5	3E-01	3E+00	8E+01
4.67	3E-01	3E+00	8E+01
4.83	3E-01	3E+00	9E+01
5	3E-01	3E+00	9E+01

10 OBSERVATIONS

10.1 Net Evaporation Rate

In the Figure 10-1, net evaporation rate is presented (i.e. scaled net evaporation rate). As it can be observed from the graph that there is a small drop in the evaporation rate at initial 1~2 min. That is because the bed is not completely fluidized and it takes 1~2 min for the bed to be perfectly fluidized. In addition, the particles initially are at the room temperature and hence, during 1~2 min at the beginning of the experiment, particles are heating up.

Later during the experiment it is evident that the convective drying ends in between 5~8 minutes and diffusion takes control over the convective drying. During the diffusive drying the evaporation rate is quite low when compared with the convective drying.

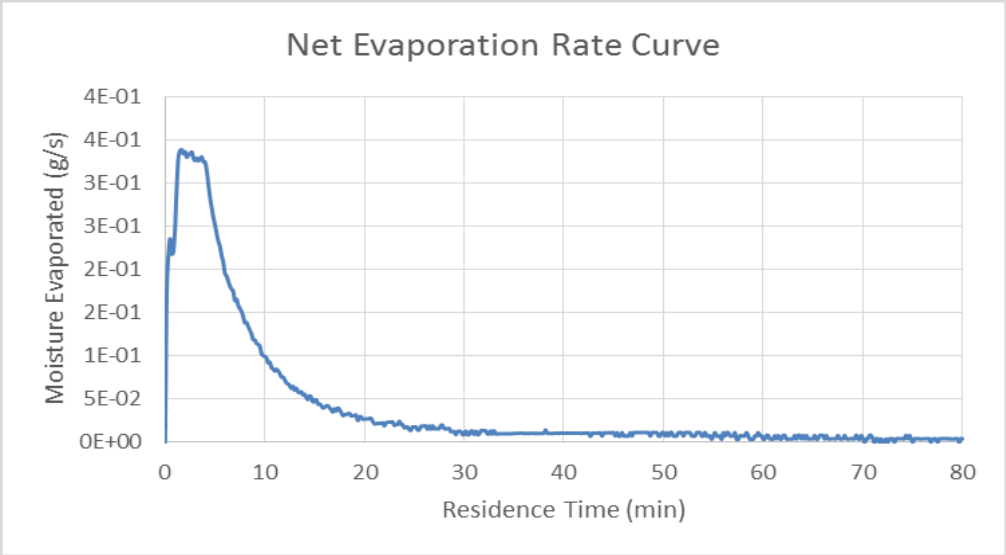

Figure 10-1. Net evaporation rate curve for residence time = 80 min

10.2 Particle Size Distribution

PAM Gel particles when undergo drying process, tends to shrink and exhibit significant volume reduction. In Figure 10-2, the particle size distribution is presented in terms of volume fraction for both feed and dried product. In the presented experimental result, the average particle diameter of PAM Gel before drying is 3.68 mm while after drying the average particle diameter reduces to 2.67 mm. This shrinkage in particle size leads to the volume reduction of the bed up to 60%~62%

approximately, which is nearly as same as the amount of moisture evaporated from the particle for the presented case. The particle size distribution of feed and feed product for different operating conditions are presented in **Appendices E**, **F**, **G**, **H** and **I**.

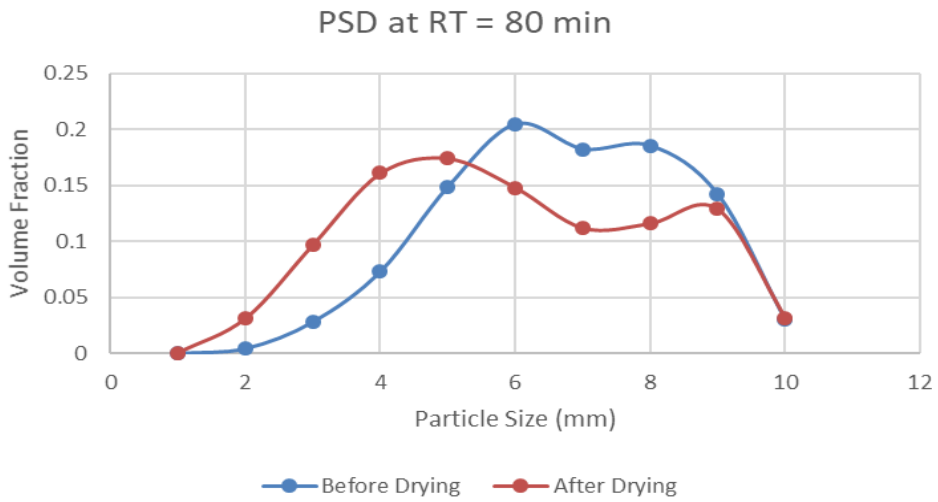

Figure 10-2. Particle size distribution of PAM Gel as feed before and after drying with operating conditions as Residence Time = 80 min, Airflow = 0.0273 m³/s, Feed Particle Size = 4.5 mm, Actual Inlet Temperature = 68°C and Bed Load =300 g

As each case is analysed for the shrinkage in particle size, it was observed that shrinkage is directly related to the moisture removed from the feed. The moisture removed at varying residence time is shown in **Figure 10-3** and refer to **Appendix C** for moisture removal at other varying operating conditions.

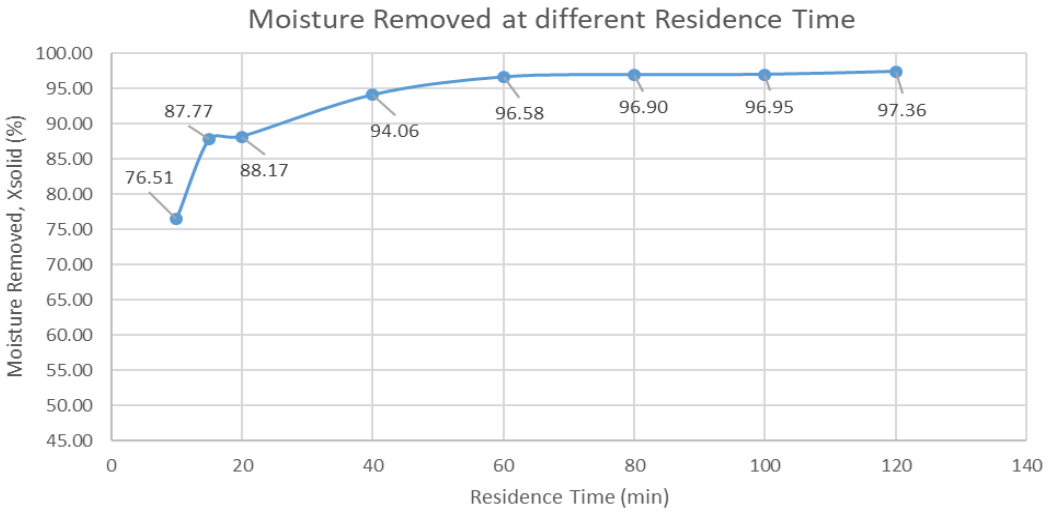

Figure 10-3. Moisture removed at different Residence Time at constant Airflow = 0.0273 m³/s, Feed Particle Size = 4.5 mm, Actual Inlet Temperature = 68°C and Bed Load =300 g

10.3 Inlet Temperature

Another observation while performing the experiments was that the inlet air temperature is always lower than the heater set temperature of the fluid bed dryer (**Appendix D**). Hence, for two different set-points of heater temperature versus inlet air temperature, along with the constant airflow rate have been as shown in **Figure 10-4.** The difference in the set point and actual inlet temperature is always the same and always repeatable. The plausible reason for the difference in heater temperature and actual inlet temperature is due to the residence time of inlet air in the heater. The deviation is always repeatable and is of nearly ~2°C. The difference is slightly affected by the airflow by 2°C±0.5. The actual inlet temperature is used for absolute humidity calculations is used for closing the material balance.

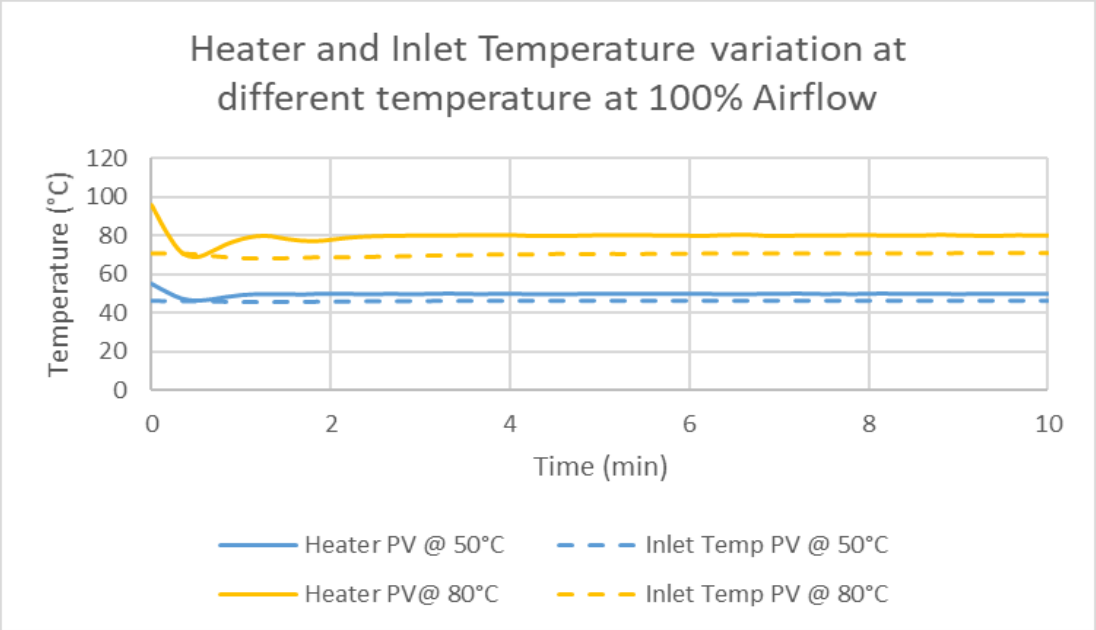

Figure 10-4. Heater and inlet temperature process value variation for different heater temperature set value

11 INSPECTION OF RESEARCH RESULTS

11.1 Determining the Equilibrium Moisture Content of Dry-polyacrylamide

The equilibrium moisture content does not get affected by the addition of cutting oil. In addition, from **Appendix A**, it is evident that the size of particle does not exhibit that much effect on the equilibrium moisture content. The size of the particle only helps in attaining the equilibrium moisture i.e. smaller the size of the particle earlier the equilibrium moisture achieved but the amount of moisture for the equilibrium remains same.

11.2 Effect of various Fluidized Bed Dryer operating parameters on drying of Polyacrylamide-gel

11.2.1 Residence Time

Residence time have a significant role in drying of the PAM-Gel. The residence time experimental data have been collected for 10, 15, 20, 40, 60, 80, 100 and 120 min. Although the heater temperature set point for each experiment was 80°C however, the actual inlet temperature for each experiment was 51.4°C, 60.3°C, 63.9°C, 66.8°C, 67.0°C, 68.0°C, 68.0°C, and 68.0°C respectively. After analyzing all the residence time data, it is evident that longer the residence time lower will be the evaporation rate for PAM-Gel as shown in **Figure 11-1**. However, while at the initial 2~3 minutes free moisture is removed followed by later 5~8 minutes the convective drying ends and diffusive drying starts.

In addition, it can also be seen that there is no significant change in between the moisture removed after residence time of 60 min and 80 min or higher. It is also important to mention that the feed particle size for different experiments carried out for residence time were different (refer to **Appendix E**).

The major particle size reduction from feed to product is seen at initial 10 min of residence time. However, for higher residence time than 40 min, there is no size reduction at all and size of the dried product remains unchanged (**Appendix E**).

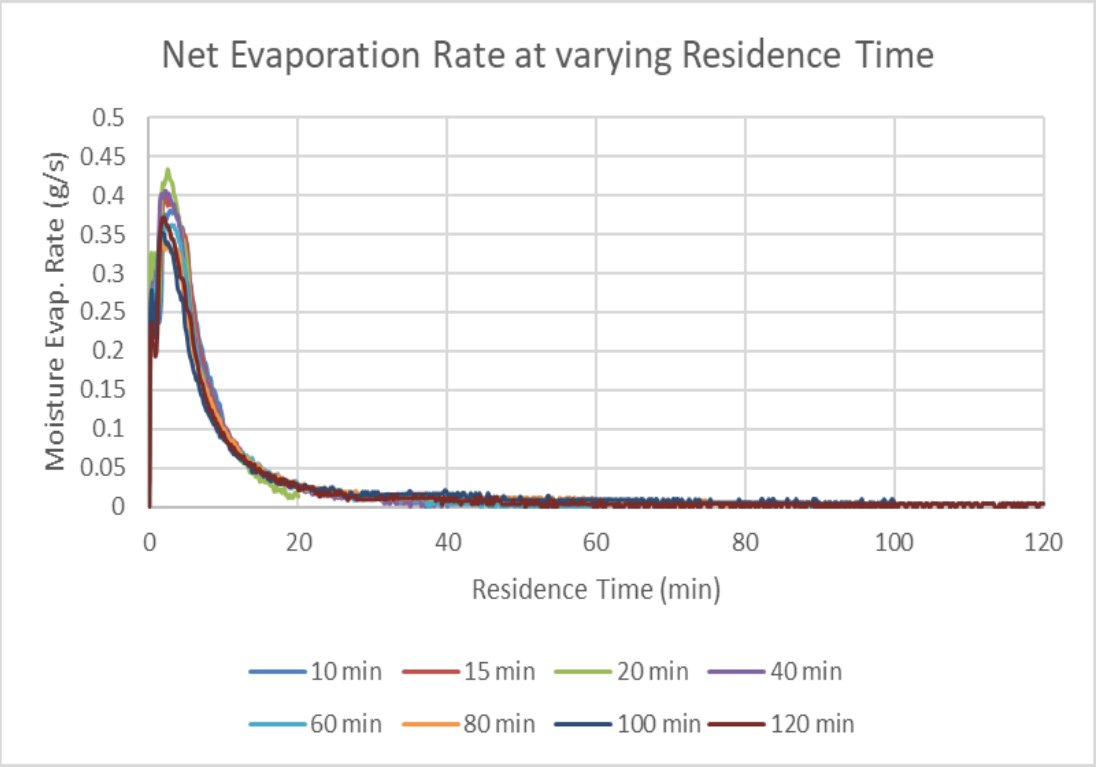

Figure 11-1. Net Evaporation Rate at varying Residence Time

11.2.2 Blower Airflow

The blower airflow experiment data have been collected for airflow rate of 0.0242, 0.0273, 0.0303 and 0.0333 m^3/s for 70%, 80%, 90% and 100% blower output setting respectively as shown in **Figure 11-2**. When the blower output was set to 60% i.e. 0.0208 m^3/s, then for bed load of 300 g and feed particle size 4.5 mm, there was no fluidization at all in the bed. During blower airflow experiments, residence time for all the experiments was 80 min. However, as it is clear from the **Figure 11-1**, that after 30 min., any important information cannot be retrieved from experimental data. Henceforth, the time scale in later figures are within scale from 0 to 30 min. The moisture removed from feed is not much affected by the blower airflow remaining stagnant to ~97% (approx.) irrespective of blower airflow setting.

Similar, experimental data for 3.0 mm particle size with above mentioned airflow is presented in **Appendix F**. It is also important to mention the actual inlet air temperature was 67.0°C to 68.5°C for the heater temperature set value of 80°C.

In addition, the particle size reduction remains the same as well. As the sampling size for the particle size distribution was notably small, the average diameter mentioned in

some cases may not be suffice to explain the entire size reduction phenomenon. Still, the total volume reduction of the bed was same as of in the previous residence time experiments when compared based on the bed height (Appendix F).

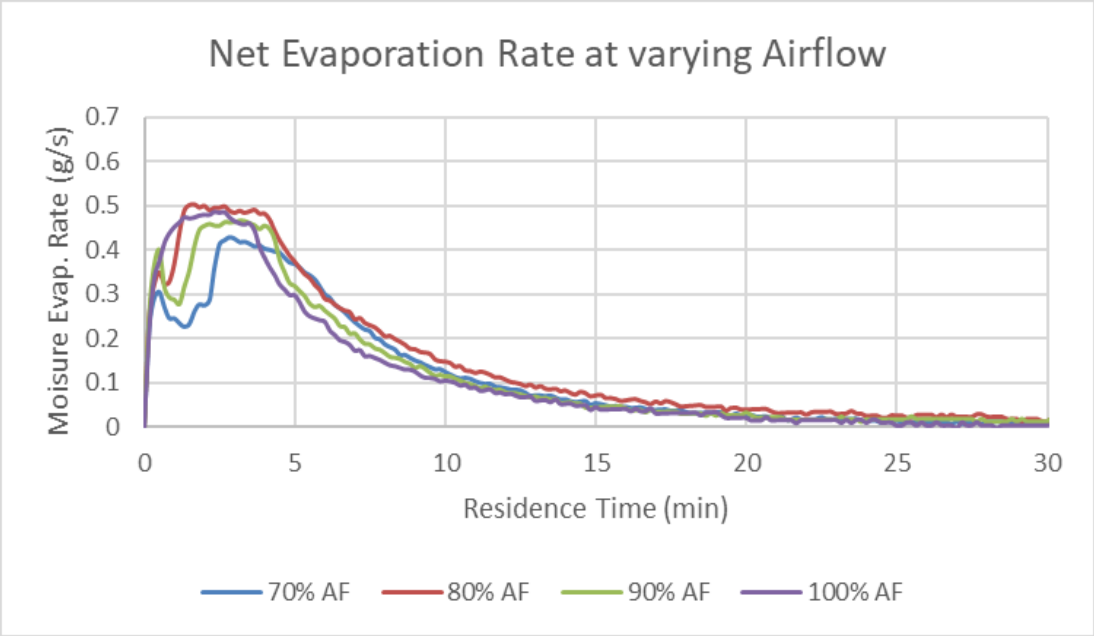

Figure 11-2. Net Evaporation Rate at varying Airflow for 4.5 mm Feed Particle Size

11.2.3 Feed Particle Size

The particle size data is carried out for 3 mm, 4.5 mm and 6 mm feed particle size. It is important to note that the 6 mm feed particles, bed was not showing any fluidization with blower airflow setting less than 0.0333 m^3/s (i.e. 100%). Hence, all the feed particle size experiments were performed at 100% blower airflow, actual air inlet temperature for heater set point 100°C varied from 82.5°C to 84.0°C and 80 min residence time as shown in Figure 11-3.

After analyzing the data, it was evident that smaller the feed particle size higher the net evaporation rate with higher amount of moisture removed from the feed. However, several other sets of experimental data was analyzed. Whilst, in Figure 11-4 and Figure 11-5, 3 mm and 4.5 mm feed particles were analyzed under different blower airflow set-point of 0.0242, 0.0273 and 0.0303 m^3/s (i.e. 70%, 80% and 90%) at between 67°C ~ 68°C actual inlet air temperature for 80°C heater set-point as shown respectively.

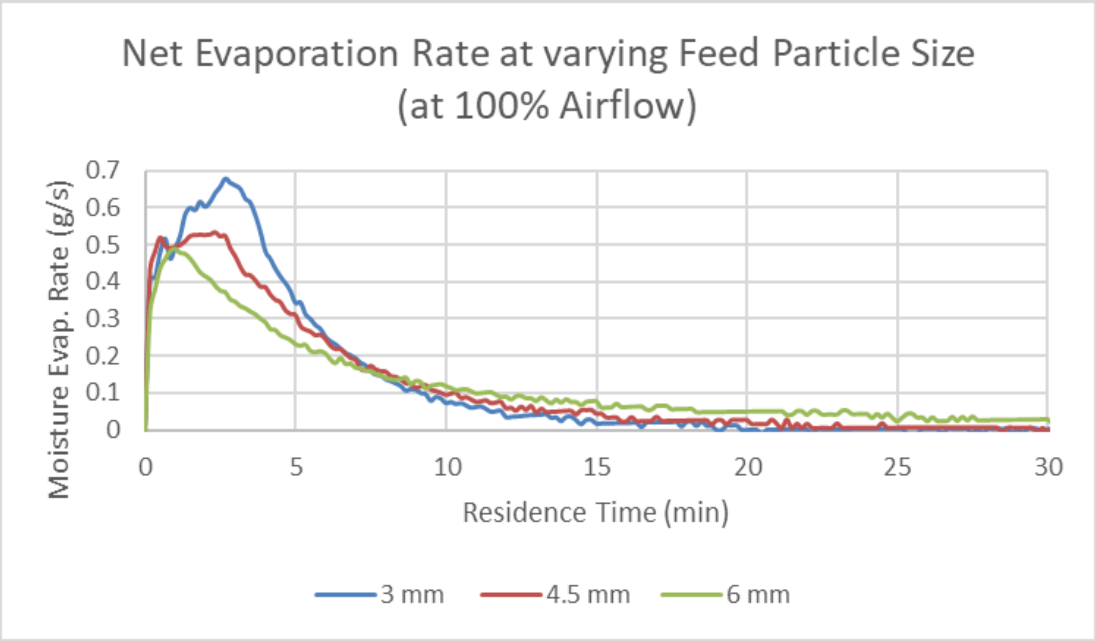

Figure 11-3. Net evaporation rate at varying Feed Particle Size at 100% Airflow

It can be deduced from the data analyzed that higher the blower airflow setting, higher was the moisture removed from the feed and higher the net evaporation rate. The particle size reduction was found higher with higher feed particle size. With 6 mm feed particle size at 0.0333 m^3/s (i.e. 100%) blower airflow setting, the bed volume reduction was found higher when compared with 3 mm feed particle size with the same operating conditions (**Appendix G**).

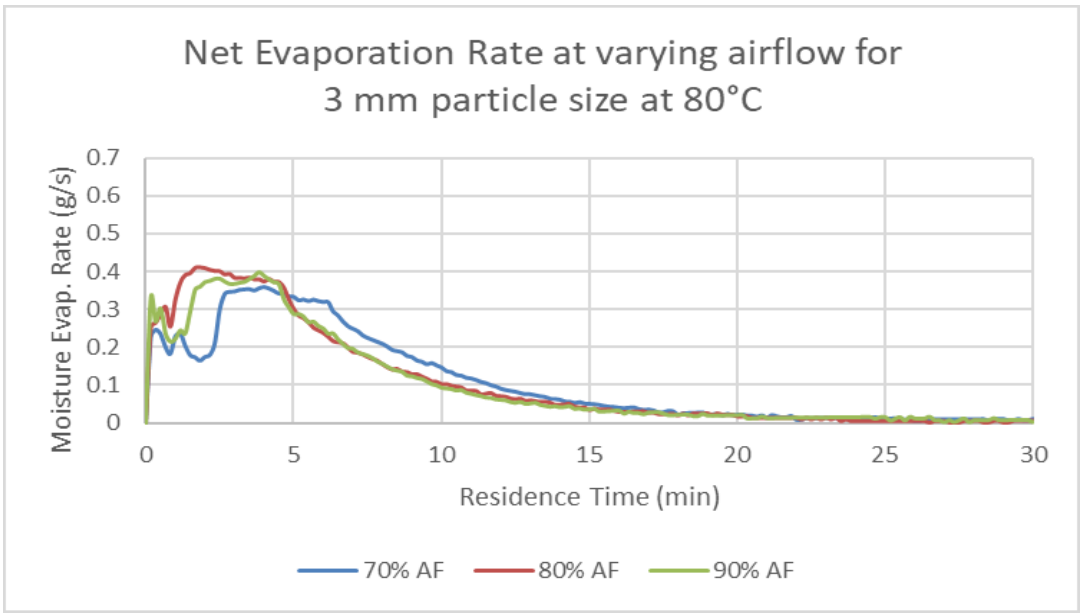

Figure 11-4. Net evaporation rate at 3 mm Feed Particle Size at varying Airflow

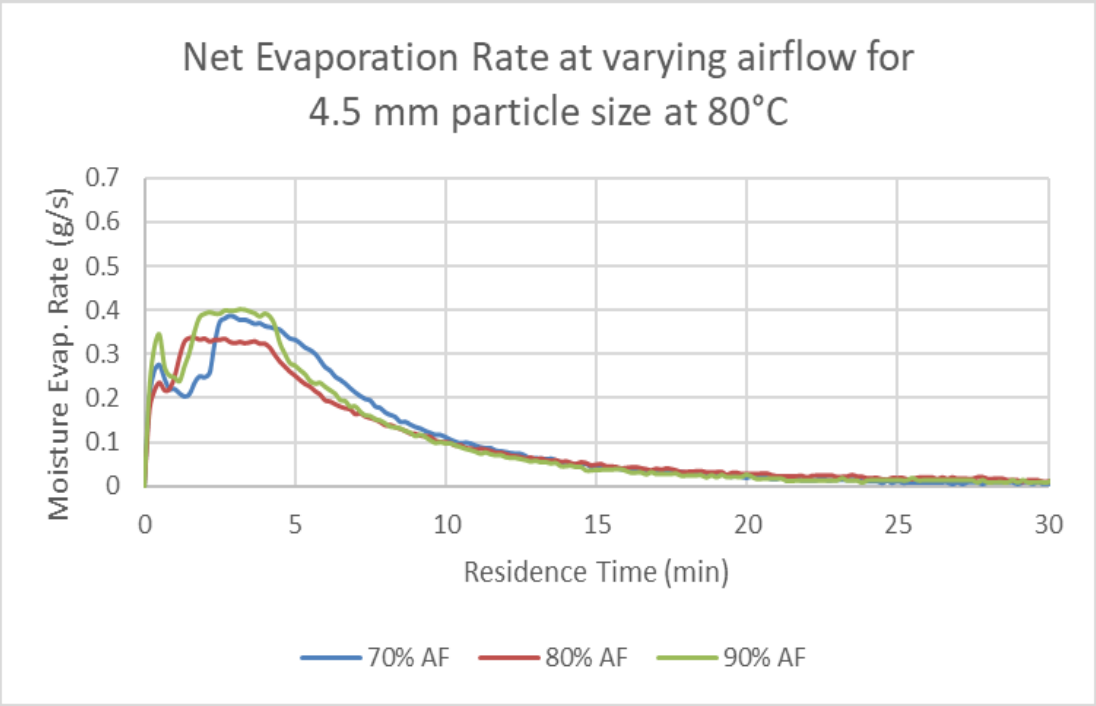

Figure 11-5. Net evaporation rate at 4.5 mm Feed Particle Size at varying Airflow

The total amount of moisture removal for smaller sized feed particle is higher when compared with larger particles. However, the drying rate is lower for the larger particles and vice versa for smaller particles.

11.2.4 Bed Loading

With varying bed load of 100, 200, 300, 400, 500 and 600 g, drying was carried out at 0.0273 m^3/s (i.e. 80% blower airflow set-point) with 67.5°C inlet temperature (at 80°C heater set-point) for 80 min of residence time with 4.5 mm feed particle size and experimental data was collected as shown in **Figure 11-6**. It is also important to mention that when 700 g of bed load was subjected to the same operating conditions, there was no fluidization is observed for the bed (refer to **Figure 11-7**). Even though the moisture content in the feed was almost the same for all the bed loads (viz. 68.5% ~ 69.0%). Moisture removed from the feed particle was in between 97~98% (approx.) However, bed load affects the fluidization regime of the bed, i.e. fixed, expanded, minimum fluidized or bubbling fluidized bed etc. While keeping the mentioned parameter bed load of 400 g have maximum moisture removed and complete fluidization was observed, when compared with other bed loads with same operating parameters. Bed load of 200 g and 100 g were under the turbulent to fast fluidization

regime (refer to Figure 11-8), hence leading to very short contact time between hot air and feed. Smaller bed loads consist less amount of moisture available to evaporate and hence, leading to lower net evaporation rate.

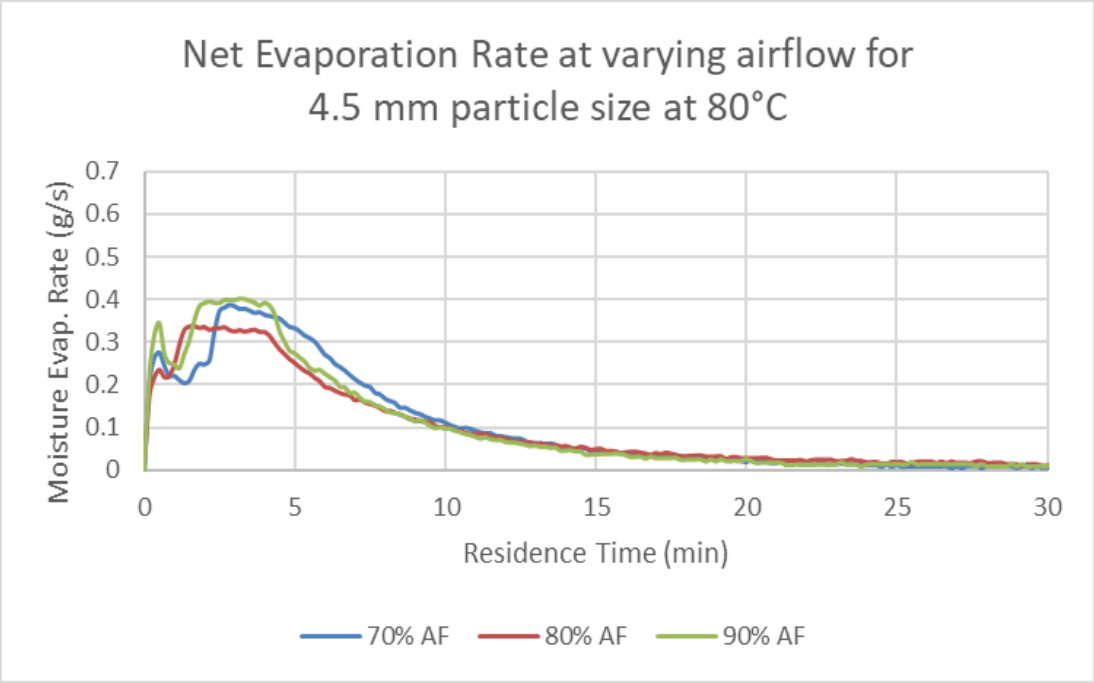

Figure 11-6. Net Evaporation Rate at varying Bed Load

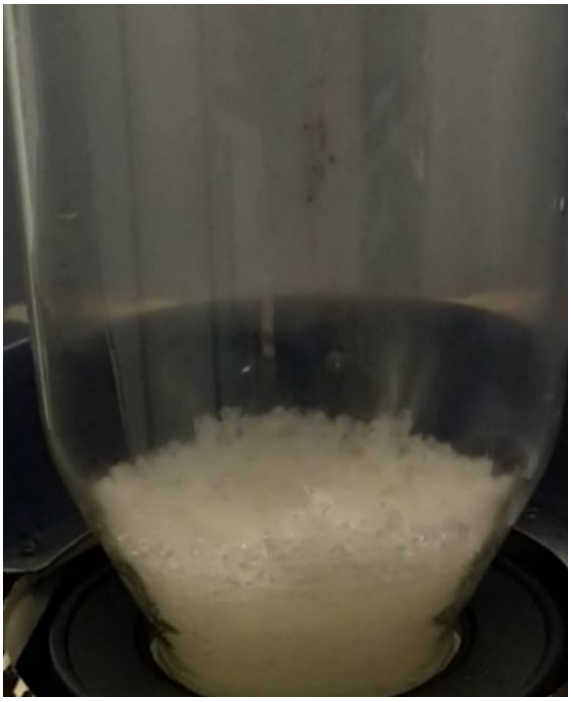

Figure 11-7. Fixed bed regime for Bed Load = 700 g with constant Airflow = 0.0273 m^3/s, Feed Particle Size = 4.5 mm and Residence Time = 80 min

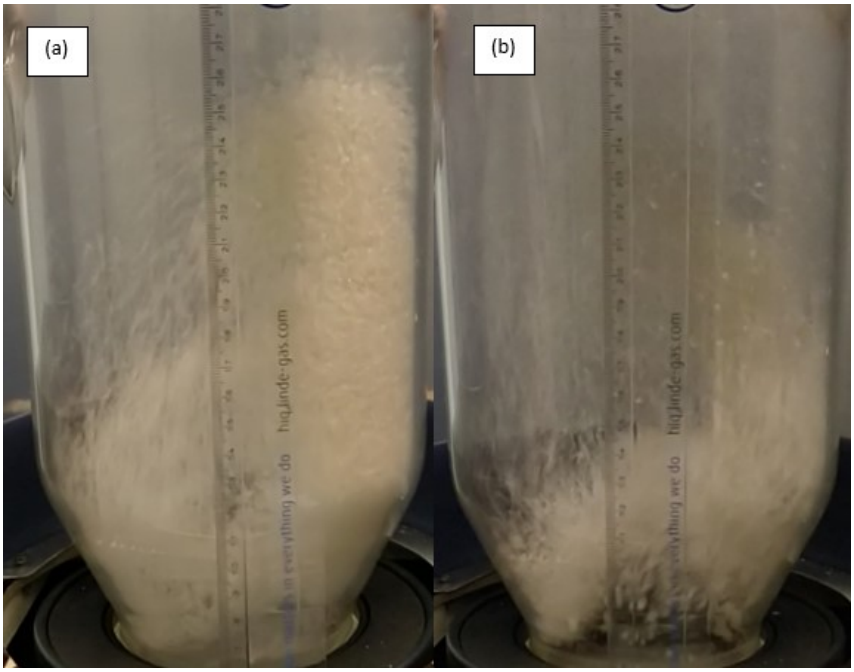

Figure 11-8. (a) Turbulent Bed regime for Bed Load = 200 g and (b) Fast fluidization bed regime for Bed Load =100 g, with constant Airflow = 0.0273 m³/s, Feed Particle Size = 4.5 mm and Residence Time = 80 min

In addition, overall volume reduction after drying was also found highest with bed load of 400 g, followed by bed load of 300 g. While, with higher bed loads i.e. 500 g and 600 g, neither overall volume is reduced that much nor the particle size when compared with the previous bed loads (**Appendix H**).

11.2.5 Heater Temperature

The inlet air temperature is directly dependent on the set heater temperature, and inlet air temperature have significant effect on the drying of the material as well. This was deduced from data analysis for the varying heater temperature with varying airflow rate and feed particle size. However, as mentioned earlier in section 10.3., that the actual inlet air temperature was lower than that of the heater set point and process value. As heater temperature was increased while keeping the airflow to 0.0333 m³/s (i.e. 100%) and particle size 6 mm with residence time 80 min, the moisture removed was evidently highest at 120°C followed by 100°C and 50°C respectively, with actual inlet temperature 83°C, 84°C and 45°C respectively, as shown in **Figure 11-9**. This variation in reading of the temperature was due to limitation of the H/T Probe.

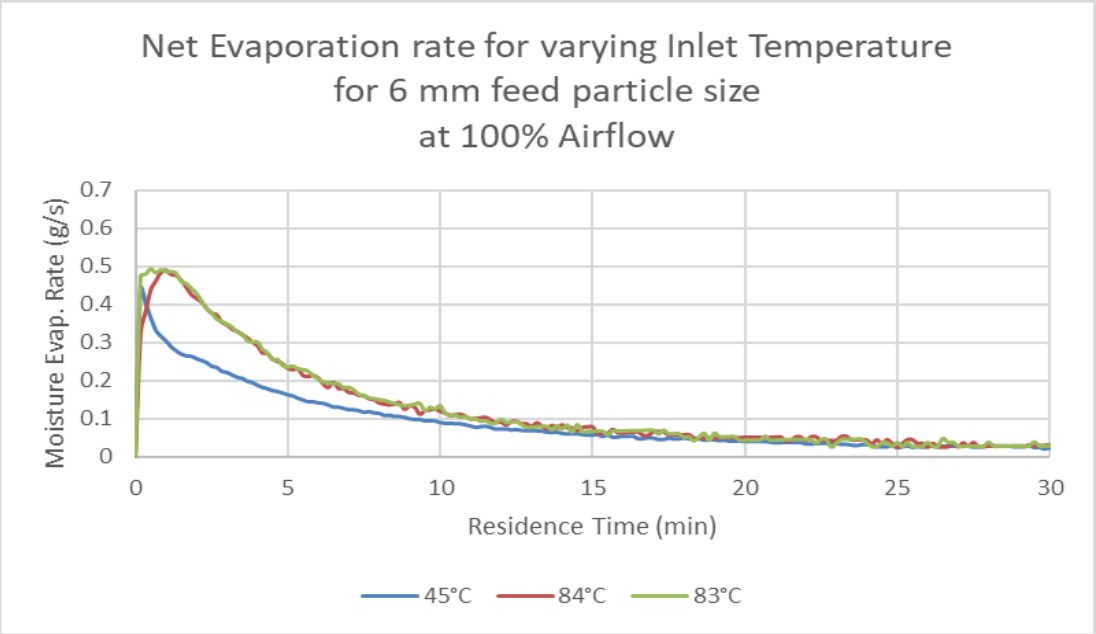

Figure 11-9. Net evaporation rate at varying Heater Temperature for 6.0 mm particle

For smaller feed particle size such as 4.5 mm and same airflow rate viz. 0.0333 m^3/s (i.e. 100%) for heater temperatures 50°C, 100°C and 120°C with actual inlet temperature 83°C, 84°C and 45°C respectively, the evaporation rate was higher with higher temperature as shown in Figure 11-10 and Figure 11-11.

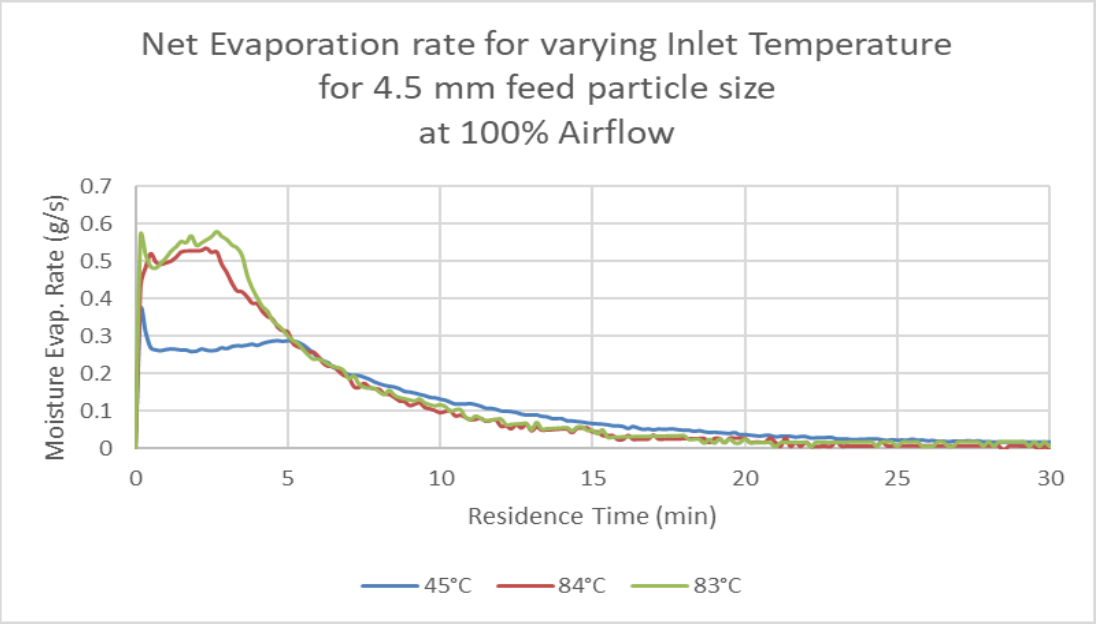

Figure 11-10. Net evaporation rate at varying Heater Temperature for 4.5 mm particle

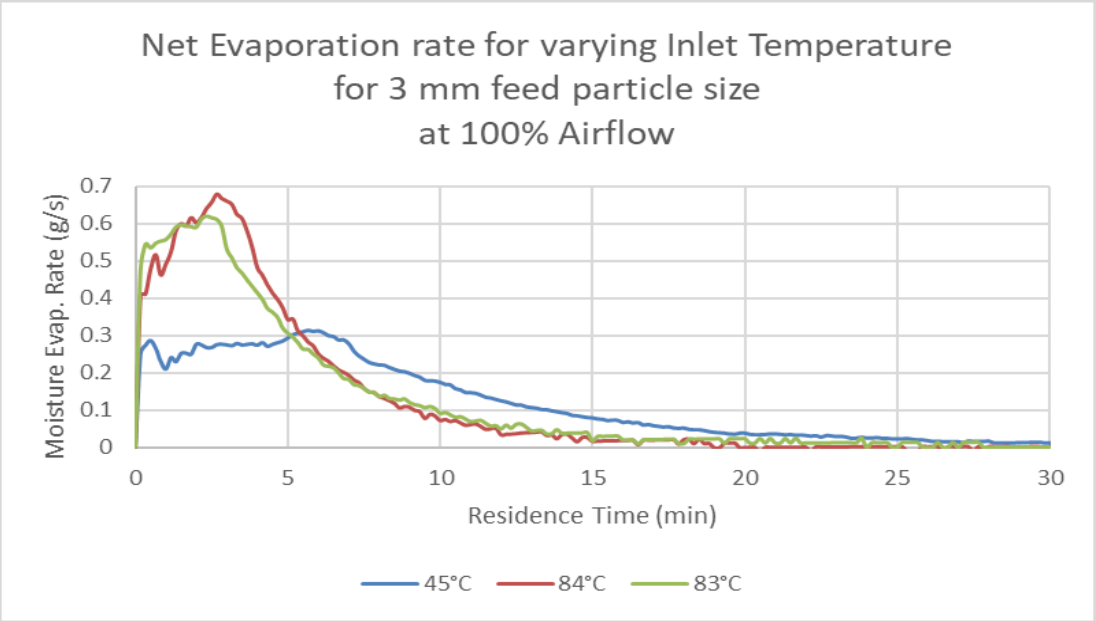

Figure 11-11. Net evaporation rate at varying Heater Temperature for 3.0 mm particle

Particle size reduction when analyzed based on the average particle diameter is also found to be increased with increase in the inlet temperature irrespective of feed particle size i.e. 3 mm, 4.5 mm and 6 mm (**Appendix I**).

12 CONCLUSION

The equilibrium moisture content of DPAM at different conditions in a closed environment is not majorly affected by addition of cutting oil or not. In addition, for all the particle sizes kept under observation in conditioning cabinet does not have any significant effect on the equilibrium moisture content of DPAM.

The effect of each operating parameter of fluid bed dryer over PAM-gel reflects varied affect. The residence time plays an important role up to a certain extent and afterwards the effect is almost negligible. When compared with the excess time period leading towards the overhead time and energy consumption with nearly no change in drying of PAM-gel as well as overall volume reduction of the bed. Airflow and bed load were observed to effect the fluidization of the bed while keeping other operating parameters as constant such as residence time and feed particle size. In contrast to other parameters, inlet temperature and feed particle size play significant role on the drying efficiency of the fluid bed dryer, with increase in inlet temperature, the drying rate also shows significant increase for a given bed load and vice versa for the feed particle size. In addition, particle size, bed volume for a given bed load, decreases as drying proceeds and both reduce until the equilibrium is reached. The volume reduction is up to 60%~62% for all the experiments carried out for residence time more than 40 min.

In conclusion, inlet temperature and feed particle size directly and majorly affect the drying process and act as a key operating parameters for the drying process. Residence time play a significant role up to a certain extent therefore must be taken into account carefully. However, airflow and bed load affect the fluidization conditions of the bed hence, airflow and bed load as operating parameters affect the drying process indirectly.

Further research work is required for better understanding of particle shrinkage and its dependency on various operating parameters of fluid bed dryer. Also, pores formation in the gel particles while drying and its effect of different operating parameters. In addition, some research is also suggested, in order to validate fluid bed drying process for gel particles of different ionic charges, molecular weight and charge density.

REFERENCES

[1] Huang, S.-Y., Lipp, D. W. and Farinato, R. S. 2001. Acrylamide Polymers. *Encyclopedia of Polymer Science and Technology*.

[2] H. Dautzenberg and co-workers, *Polyelectrolytes: Formation, Characterization and Application*, Hanser Publishers, New York, 1994, p. 272.

[3] R. S. Farinato, S.-Y. Huang, and P. Hawkins, in R. S. Farinato and P. L. Dubin, eds., *Colloid–Polymer Interactions: From Fundamentals to Practice*, John Wiley & Sons, Inc., New York, 1999, p. 3.

[4] S.-Y. Huang and D. W. Lipp, in J. C. Salamone, ed., *Polymeric Materials Encyclopedia*, Vol. 5, CRC Press, Inc., Boca Raton, Fla., 1996, p. 2427.

[5] H. I. Heitner, *Kirk-Othmer: Encyclopedia of Chemical Technology*, 4th ed., Vol. II, John Wiley & Sons, Inc., New York, 1994, p. 61.

[6] H. I. Heitner, T. Foster, and H. Panzer, in J. I. Kroschwitz, ed., *Encyclopedia of Polymer Science and Engineering*, 2nd ed., Vol. 9, Wiley-Interscience, New York, 1987, p. 824.

[7] H. Liu, Y. Bu, J.G. Sanjayan, A. Nazari, and Z. Shen, in *Construction and Building Materials,* Vol. 112, Elsevier, 2016, p. 253-260

[8] F. A. Bovey, *High Resolution NMR of Macromolecules*, Academic Press, New York, 1972, p. 147.

[9] W.-M. Kulicke, R. Kniewske, and J. Klein, eds., *Progress in Polymer Science*, Vol. 8, 379 (1982).

[10] O. G. Lewis, *Physical Constants of Linear Homopolymers*, Springer-Verlag, New York, 1968, p. 23

[11] I. Janigová and co-workers, Macromol. Chem. Phys. 195, 3609–3614 (1994).

[12] J. Brandrup and E. H. Immergut, eds., *Polymer Handbook*, 3rd ed., John Wiley & Sons, Inc., New York, 1989, p. VI–416.

[13] J. E. Lancaster and M. N. O'Connor, *J. Polym. Sci., Polym. Lett.* Ed. 20, 547 (1982)

[14] W.-M. Kulicke, R. Kniewske, and J. Klein*, Prog. Polym. Sci.* 8, 373–468 (1982).

[15] S. Sawant and H. Morawetz*, Macromolecules* 17, 2427 (1984).

[16] S. Sawant and H. Morawetz, J. Polym. Sci., Polym. Lett. Ed. 20, 385–388 (1982).

[17] S. J. Guerrero, P. B. Oldarino, and J. H. Zurimendi, J. Appl. Polym. Sci. 30, 962 (1985).

[18] W.-M. Kulicke, R. Kniewske, and J. Klein, Prog. Polym. Sci. 8, 383 (1982)

[19] J. Brandrup and E. H. Immergut, eds., Polymer Handbook, 3rd ed., John Wiley & Sons, Inc., New York, 1989, p. VII–383

[20] *SUPERFLOC 127 Flocculant, Material Safety Data*, Cytec Industries, West Paterson, N.J. 1996

[21] D. Hunkeler and J. H. Barajas, J. C. Salamone, ed., in *Polymeric Materials Encyclopedia*, Vol. 5, CRC Press, Inc., Boca Raton, Fla., 1996, p. 3330.

[22] J. Gregory, in C. A. Finch, ed., *Industrial Water Soluble Polymers*, The Royal Society of Chemistry, Cambridge, U.K., 1996, pp. 62–75

[23] J. K. Borchardt, in J. I. Kroschwitz, ed., *Encyclopedia of Polymer Science and Engineering*, 2nd ed., Vol. **10**, Wiley-Interscience, New York, 1987, p. 350

[24] J. M. W. Mackenzie, *Eng. Min. J.* 80–87 (Oct. 1980)

[25] J. P. MacDonald, P. L. Mattison, and J. M. W. MacKenzie, *J. S. Afr. Inst. Min. Metall.* **81**, 303 (1981)

[26] *Superfloc 16 Plus Flocculant*, Cytec Industries, West Patterson, N.J., 1997

[27] R. W. Adams and co-workers, *Mining Chemicals Handbook* (rev. ed.), Cytec Mining Technical Services, Cytec Industries Inc., Stamford, Conn., 1986

[28] Molnár K., Experimental Techniques in Drying, in *Handbook of Industrial Drying,* 3rd ed., CRC Press, Boca Raton, Fla., 2007, chap. 2, p. 33

[29] J.H. Perry, *Chemical Engineers' Handbook*, McGraw-Hill, New York, 1967

[30] A.V. Likov, *Theory of Drying*, Nehézipari Könyvkiadó, Budapest, 1952

[31] R.B. Keey, *Drying Principles and Practice*, Pergamon Press, Oxford, 1972

[32] R. Toei and S. Hayashi, *Memoirs Fac. Eng. Kyoto Univ.*, 25: 457 (1963)

[33] P. Toei and M. Okasaki, *Chem. Phys. J.*, 19: 464 (1970)

[34] A. Wexler, *Humidity and Moisture*, Reinhold, New York, 1965

[35] R.E. Treybal, *Mass Transfer Operations*, McGraw-Hill, New York, 1968

[36] S. Szentgyörgyi, *Period. Polytech. Mech. Eng.*, 24: 137 (1980)

[37] Gupta, C.K. and Sathiyamoorthy, D., *Fluid Bed Technology in Mineral Processing*, CRC Press, New York, 1999, chap. 1

[38] Mujumdar, A.S. and Devahasthin, S., Applications of fluidized bed drying, in *Handbook of Fluidization and Fluid Systems,* Yang, W.C., Ed., Marcel Dekker, New York, 2003, chap. 18.

[39] Law, C.L. and Mujumdar, A.S., Advantages and Limitation of FBDs, in *Handbook of Industrial Drying,* 4th ed., CRC Press, Boca Raton, Fla., 2014, chap. 8, p. 164

[40] Chen, J.C., Heat Transfer, in *Handbook of Fluidization and Fluid-Particle Systems,* Yang, W.C., Ed., Marcel Dekker, New York, 2003, chap. 10.

[41] Vreedenberg, H.A., Heat Transfer between a fluidized bed and a horizontal tube, *Chemical Engineering Science,* Vol. 9(1), 1958, p. 52-60.

[42] Ozkaynak, T.F., Chen, J.C., and Frankenfield, T.R., An experimental investigation of radiant heat transfer in high temperature fluidized bed, in *Fluidization IV*, Kunii, D. and Toei, R., Eds., Engineering Foundation, New York, 1983, p. 371-387

[43] Sarkits, V.B., *Heat transfer for Suspended Beds of Granular Materials to Heat Transfer Surfaces,* Leningrad Technology Institute, Lensoviet, 1959

[44] Baerg, A., Klassen, Y., and Gishler, P.E., Heat Transfer n fluidized solid beds, *Can. J. Res. Sect. F,* F28: 287, 1950

[45] Mersman, A., Zum Wärmetübergang in Wirbelschichten (heat transfer in fluidized bed), *Chem. Ing. Tech.,* 39:349-353, 1967

[46] Dow, W.M. and Jakob, M., Heat transfer between a vertical tube and fluidized bed air mixture, *Chem. Eng. Prog.,* 47:637, 1951

[47] Gaffney, B.J. and Drew, T.B., Mass transfer from packing of organic solvents in single phase flow through a column, *Ind. Eng. Chem.,* 42: 1120-1127, 1950

[48] Miller, C.O. and Logwinuk, A.K., Fluidization studies of particles, *Ind. Eng. Chem.,* 43: 1220-1226, 1951

[49] Wicke, E. and Hedden, F., Stromungsformen and Warmeubertragung in von luft aufgewirbelten schuttgutschichten (Flow forms and heat transfer in air agitated bulk solids), *Chem. Ing. Tech.,* 24(2): 82, 1952

[50] Traber, P.G., Pomaventsev, V.M., Mukhenov, I.P., and Sarkis, V.B., Heat transfer from a suspended layer of catalyst to the heat transfer surfaces, *Zh. Prilkl. Khim.,* 35: 2386, 1962

[51] Baskakov, A.P., High speed non-oxidative heating and heat treatment in a fluidized bed, *Metallurgia,* Moscow, 1968

[52] Vreedenberg, H.A., Heat transfer between fluidized beds and vertically inserted tubes, *J. Appl. Chem.,* 2: 26, 1952

[53] Wender, L. and Cooper, G.T., Heat transfer between fluidized bed and boundary surfaces: correlation data, *AIChE J.,* 4(1): 15-23, 1958

[54] Botterill, J.S.M., Teoman, Y., and Yuregir, K.R., Temperature effect on the heat transfer behavior of gas fluidized beds, *AIChE Symp. Ser.,* 77(208): 308, 1984

[55] Xavier, A.M. and Davidson, J.F., Convective heat transfer in fluidized beds, in *Fluidization,* 2nd ed., Davidson, J.F., Clift, R., and Harrison, D., Eds., Academic Press, London, 1985, chap. 13

[56] Gelperin, N.I., and Einstein, V.G., Heat transfer in fluidized beds, in *Fluidization*, Davidson, J.F. and Harrison, D., Eds., Academic Press, New York, 1971, chap. 10

[57] Zahed, H.A., and Epstein, N., Batch and continuous spouted drying of cereal grains: the thermal equilibrium model, *Can. J. Chem. Eng.,* 70: 945-953, 1992

[58] Martinez-Vera, C., Vizcarra-Mendoza, M., Galan-Domingo, O., and Ruiz-Martinez, R., Experimental validation of mathematical model for the batch drying of corn grains, *Drying Technology,* 13(1-2): 333-350, 1995

[59] Crank, J., *The Mathematics of Diffusion,* 2nd ed., Clarendon Press, Oxford, 1975, chap. 6

[60] Rossello, C., Canellas, J., Simal, S. and Berna, A., Simple mathematical model to predict the drying rate of potatoes, *J. Agric. Food Chem.,* 40(12): 2374-2378, 1992

[61] Senadeera, W., Bhandari, B. R., Young, G., and Wijesinghe, B. Influence of shapes of selected vegetable materials on drying kinetics during fluidized bed drying, *J. Food Eng.,* 58: 277-283, 2003

[62] Lewis, W.K., The rate of drying of solid materials, *J. Ind. Eng.,* 13(5): 427-432, 1921

[63] Henderson, S.M. and Pabis, S., Grain Drying Theory I: temperature effect on drying coefficient, *J. Agric. Eng. Res.,* 6: 169-174, 1961

[64] Sherwoods, W.C.H., Drying of solids, *J. Food Eng. Chem.,* 21(1): 12-16, 1929

[65] Lopez, A., Iguaz, A., Esnoz, A., and Virseda, P., Thin layer drying behaviour of vegetable wastes from wholesale market, *Drying Technol.,* 18(4-5): 995-1006, 2000

[66] Page, G., Factors Influencing the Maximum Rate of Air Drying Shelled Corn in Thin Layers, M.Sc. Thesis, Purdue University, West Lafayette, 1949

[67] Sharma, A.D., Kunre, O.R., and Tolley, H.D., Rough rice drying as a two compartment model, *Trans. ASAE,* 27: 195-200, 1982

[68] Toomey, R.D., and Johnstone, H.F., Gaseous fluidization of solid particles, *Chem. Eng. Prog.*, 48:220-226, 1952

[69] Alaathar, I., Hartage, E., Heinrich, S., and Werther, J., Modeling and flowsheet simulation of continuous fluidized bed dryers, *Powder Technology*, 238: 132-141, 2013

[70] K. Hilligardt, J. Werther, Local bubble gas-holdup and expansion of gas/solid fluidized beds, *German Chemical Engineering*, 9: 215–221, 1986

[71] Zahed, A.H., Zhu, J.X., and Grace, J.R., Modelling and simulation of batch and continuous fluidized bed dryers, Drying Technology, 13(1-2): 1-28, 1995

[72] C. L. Law, and A. S. Mujumdar, Fluidized Bed Dryers, in *Handbook of Industrial Drying,* 3rd ed., CRC Press, Boca Raton, Fla., 2007, chap. 8, p. 173-201

[73] Vanecek, V., Picka, J., and Drbohlav, R., Some basic information on the drying of granulated NPK fertilizers, *Int. Chem. Eng.,* 17: 2271-2291, 1964

[74] Reay, D., Fluidized Bed Drying, in *Gas Fluidization Technology,* Geldart, D., Ed., John Wiley and Sons, New York, 1985, Chap. 10

[75] Reay, D., and Baker, C.G.J., Drying, in *Fluidization*, 2nd ed., Davidson, J.F., Clift, R., and Harrison, D., Eds., Academic Press, London, 1985, Chap. 16

[76] Reay, D., and Allen, R.W.K., Predicting the performance of a continuous well-mixed fluidized bed dryer from batch tests, in *Proceedings of the Third International Drying Symposium,* Ashworth, J.G., Ed., Birmingham, England, Vol. 2, 1982, pp. 130-140

[77] Baker C.G.J., Predicting the energy consumption of continuous well-mixed fluidized bed dryers from kinetic data, *Drying Technology,* 17 (7-8): 2327-2349, 1999

[78] Baker C.G.J., The design and performance of continuous well-mixed fluidized bed dryers – an analytical approach, *Drying Technology,* 18 (10): 2327-2349, 2000

[79] Lee, D.H., and Kim, S.D., Drying characteristics of starch in an inert medium fluidized bed, *Chem. Eng. Tech.,* 16: 263-269, 1993

[80] Ed Randel, Jim Schak, and Ananta Islam, 2013, Fluid-bed dryers: Static versus vibrating, in *GEA Process Engineering,* CRC Publishing, [ONLINE] Available at: http://www.gea.com. [Accessed 25 October 2018].

[81] Z. Pakowski, and A. S. Mujumdar, Basic Process Calculations and Simulation in Drying, in *Handbook of Industrial Drying,* 3rd ed., CRC Press, Boca Raton, Fla., 2007, chap. 3, p. 53-80

[82] W. Wagner and A. Pruß, The IAPWS Formulation 1995 for the Thermodynamic Properties of Ordinary Water Substance for General and Scientific Use, in *Journal of Physical and Chemical Reference Data*, June 2002, Volume 31, Issue 2, pp. 387-535

APPENDIX – A

Equilibrium Moisture Content of Dry Polyacrylamide at varying Relative Humidity and Temperature

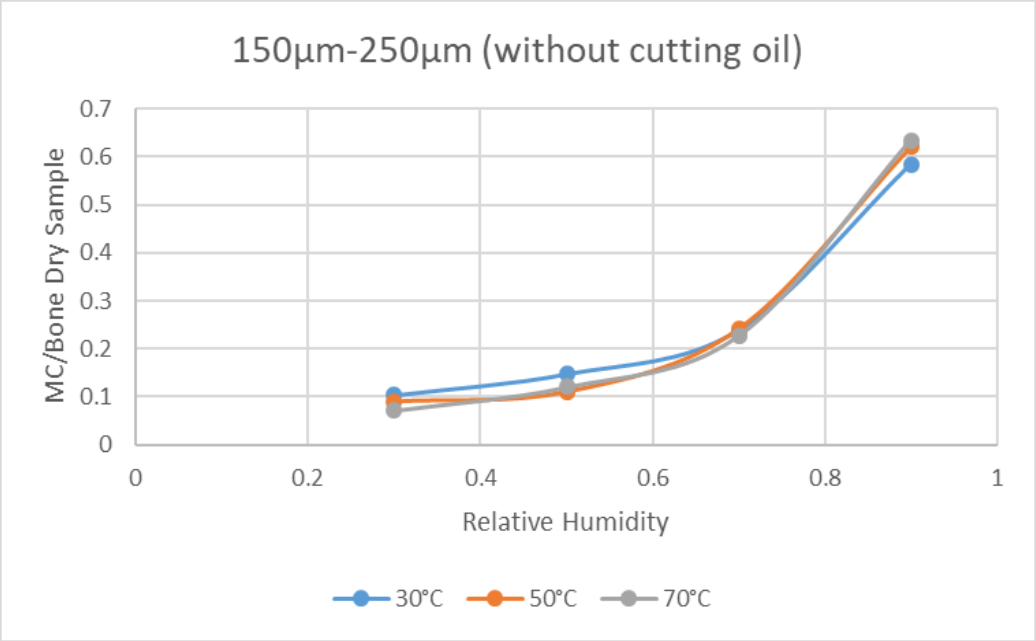

Figure A-1. Equilibrium Moisture Content for particle size 150µm – 250µm without cutting oil

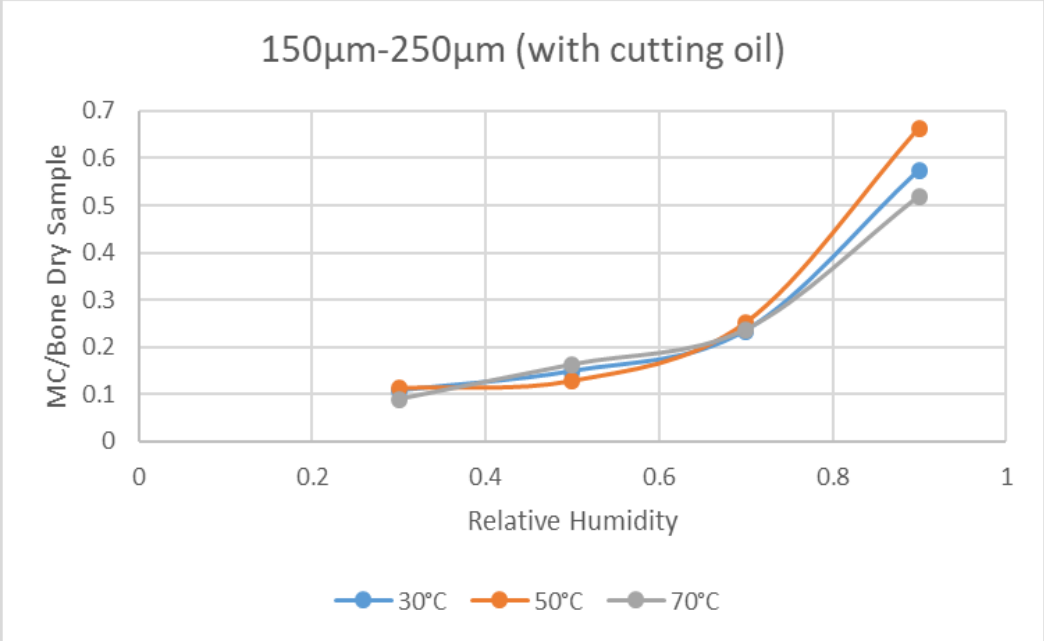

Figure A-2. Equilibrium Moisture Content for particle size 150µm – 250µm without cutting oil

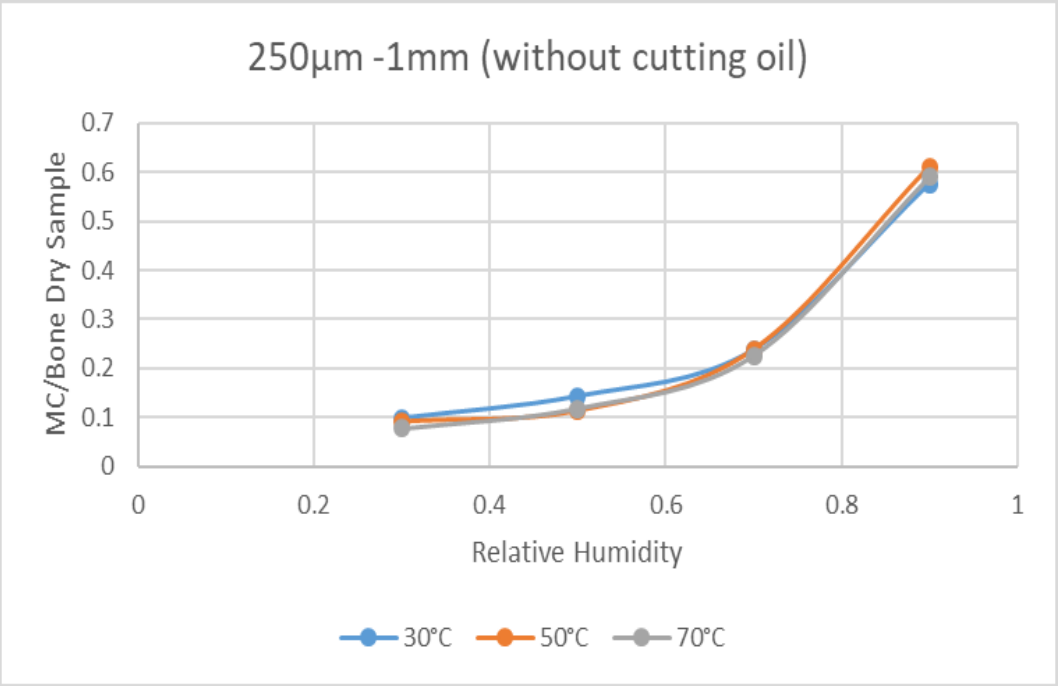

Figure A-3. Equilibrium Moisture Content for particle size 250µm – 1mm without cutting oil

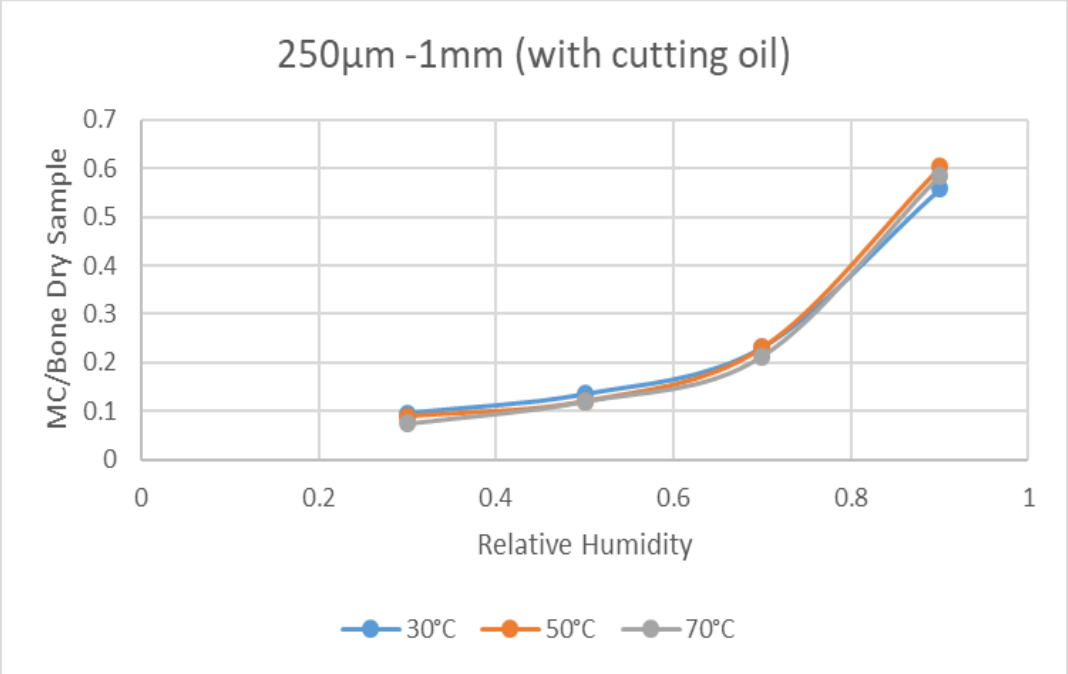

Figure A-4. Equilibrium Moisture Content for particle size 250µm – 1mm with cutting oil

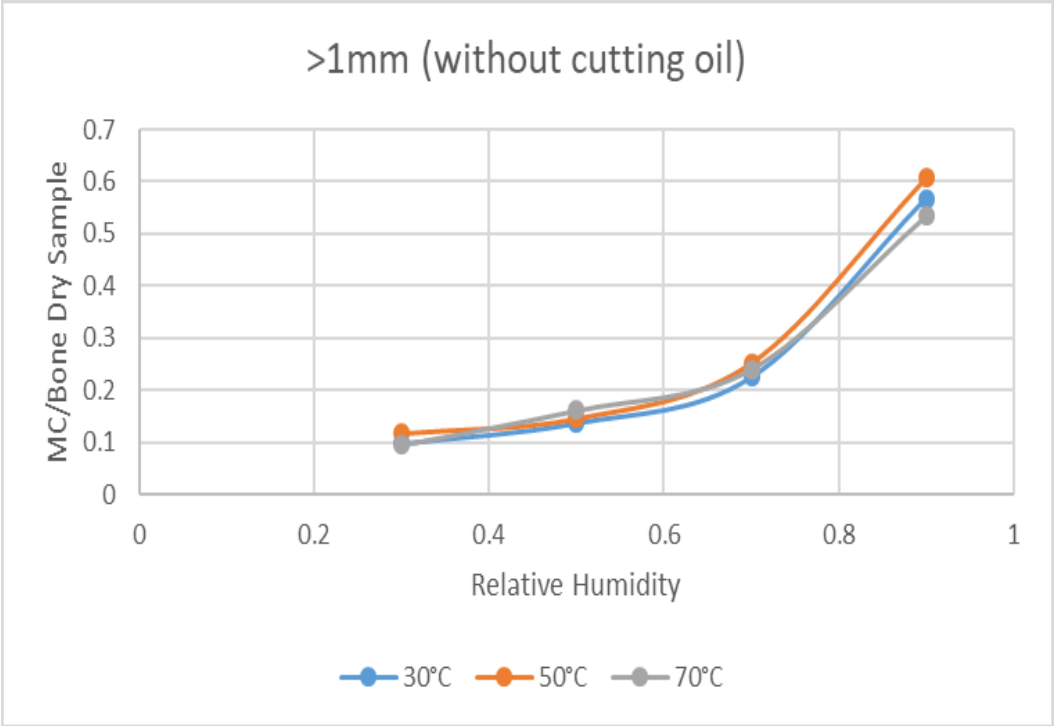

Figure A-5. Equilibrium Moisture Content for particle size >1mm without cutting oil

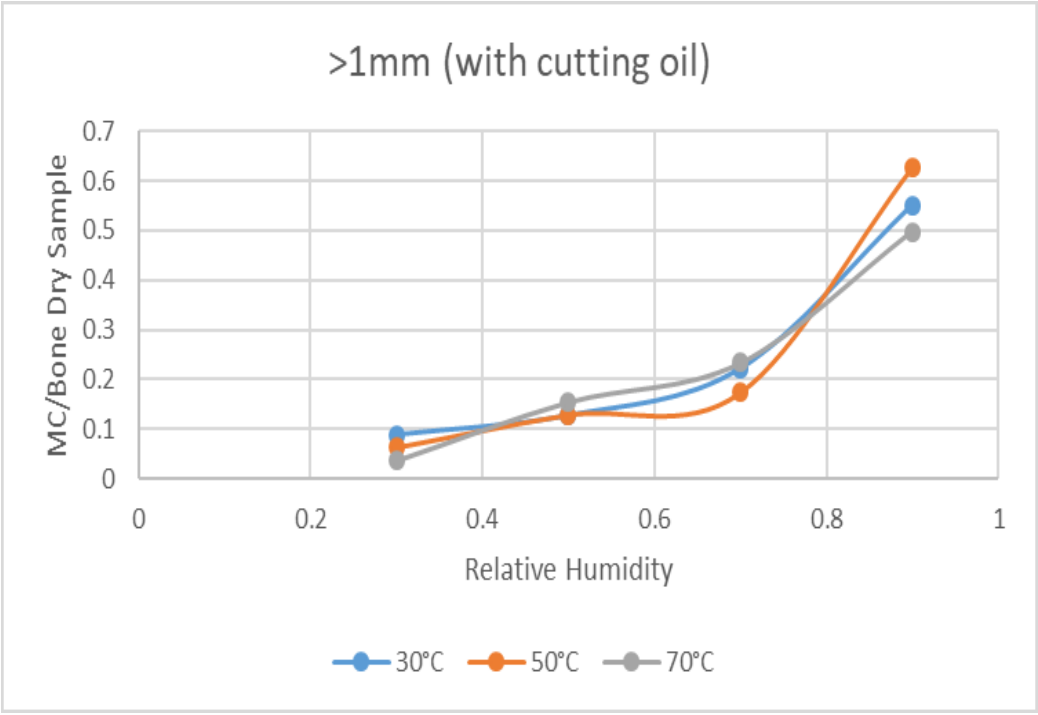

Figure A-6. Equilibrium Moisture Content for particle size >1mm with cutting oil

APPENDIX – B

Moisture content deviation in Xsolid and Xgas at varying operating conditions

Table B-1. Moisture content deviation in X_{solid} and X_{gas} at varying Residence Time

RESIDENCE TIME			
Dryer Operating Parameters (Constant)			
Airflow		**Feed Particle Size**	**Bed Load**
%	**m³/s**	**mm**	**g**
80	0.0273	4.5	300

Dryer Operating Parameter (Variable)						
Residence Time	**Inlet Temperature**		**Cumulative Moisture Content**		**Deviation (g)**	**Deviation (%)**
min	**Set value (°C)**	**Actual (°C)**	**X_{solid} (g)**	**X_{gas} (g)**		
5	80	32.7	99.83	104.29	4.46	4.28
10	80	51.4	159.00	200.61	41.61	20.74
15	80	60.3	178.31	205.45	27.14	13.21
20	80	63.9	182.32	181.41	-0.91	-0.50
40	80	66.8	197.33	225.51	28.18	12.50
60	80	67.0	200.06	251.53	51.47	20.46
80	80	68.5	200.63	298.37	97.74	32.76
100	80	67.5	200.86	260.24	59.38	22.82
120	80	67.5	201.78	245.91	44.13	17.95
				Average	**39.24**	**16.02**

Table B-2. Moisture content deviation in X_{solid} and X_{gas} at varying Airflow for Feed Particle Size 4.5 mm

AIRFLOW		
Dryer Operating Parameters (Constant)		
Residence Time	**Feed Particle Size**	**Bed Load**
min	**mm**	**g**
80	4.5	300

Dryer Operating Parameter (Variable)							
Airflow		**Inlet Temperature**		**Cumulative Moisture Content**		**Deviation (g)**	**Deviation (%)**
%	**m³/s**	**Set value (°C)**	**Actual (°C)**	**X_{solid} (g)**	**X_{gas} (g)**		
70	0.0242	80	67.2	201.29	223.32	22.03	9.86
80	0.0273	80	68.5	200.63	298.37	97.74	32.76
90	0.0303	80	68.0	201.54	234.49	32.95	14.05
100	0.0333	80	68.5	201.13	229.81	28.68	12.48
					Average	**45.35**	**17.29**

Table B-3. Moisture content deviation in X_{solid} and X_{gas} at varying Airflow for Feed Particle Size 3.0 mm

AIRFLOW		
Dryer Operating Parameters (Constant)		
Residence Time	**Feed Particle Size**	**Bed Load**
min	**mm**	**g**
80	3.0	300

Dryer Operating Parameter (Variable)							
Airflow		**Inlet Temperature**		**Cumulative Moisture Content**		**Deviation (g)**	**Deviation (%)**
%	**m³/s**	**Set value (°C)**	**Actual (°C)**	**X_{solid} (g)**	**X_{gas} (g)**		
70	0.0242	80	66.8	199.55	249.20	49.65	19.92
80	0.0273	80	67.8	201.74	245.12	43.38	17.70
90	0.0303	80	68.2	199.47	256.36	56.89	22.19
100	0.0333	80	69.0	198.85	244.18	45.33	18.56
					Average	**48.81**	**19.59**

Table B-4. Moisture content deviation in X_{solid} and X_{gas} at varying Feed Particle Size 3.0 mm

FEED PARTICLE SIZE			
Dryer Operating Parameters (Constant)			
Residence Time	**Airflow**		**Bed Load**
min	**%**	**m³/s**	**g**
80	100	0.0333	300

Dryer Operating Parameter (Variable)						
Particle Size	**Inlet Temperature**		**Cumulative Moisture Content**		**Deviation (g)**	**Deviation (%)**
mm	**Set value (°C)**	**Actual (°C)**	**X_{solid} (g)**	**X_{gas} (g)**		
3.0	50	44.7	197.58	223.73	26.15	11.69
3.0	100	83.8	204.61	232.09	27.48	11.84
3.0	120	82.5	199.17	217.90	18.73	8.60
				Average	**24.12**	**10.71**

Table B-5. Moisture content deviation in X_{solid} and X_{gas} at varying Feed Particle Size 4.5 mm

FEED PARTICLE SIZE			
Dryer Operating Parameters (Constant)			
Residence Time	**Airflow**		**Bed Load**
min	**%**	**m³/s**	**g**
80	100	0.0333	300

Dryer Operating Parameter (Variable)						
Particle Size	**Inlet Temperature**		**Cumulative Moisture Content**		**Deviation (g)**	**Deviation (%)**
mm	**Set value (°C)**	**Actual (°C)**	**X_{solid} (g)**	**X_{gas} (g)**		
4.5	50	44.7	195.88	205.46	9.58	4.66
4.5	100	83.4	194.03	238.41	44.38	18.61
4.5	120	82.7	198.94	252.89	53.95	21.33
				Average	**35.97**	**14.87**

Table B-6. Moisture content deviation in X_{solid} and X_{gas} at varying Feed Particle Size 6.0 mm

FEED PARTICLE SIZE						
Dryer Operating Parameters (Constant)						
Residence Time	**Airflow**		**Bed Load**			
min	**%**	**m³/s**	**g**			
80	100	0.0333	300			
Dryer Operating Parameter (Variable)						
Particle Size	**Inlet Temperature**		**Cumulative Moisture Content**		**Deviation (g)**	**Deviation (%)**
mm	**Set value (°C)**	**Actual (°C)**	**X_{solid} (g)**	**X_{gas} (g)**		
6.0	50	44.5	176.68	189.17	12.49	6.60
6.0	100	82.4	191.85	258.40	66.55	25.75
6.0	120	81.0	195.25	293.60	98.35	33.50
				Average	**59.13**	**21.95**

Table B-7. Moisture content deviation in X_{solid} and X_{gas} at varying Bed Load

BED LOAD						
Dryer Operating Parameters (Constant)						
Residence Time	**Airflow**		**Feed Particle Size**			
min	**%**	**m³/s**	**mm**			
80	80	0.0273	4.5			
Dryer Operating Parameter (Variable)						
Bed Load	**Inlet Temperature**		**Cumulative Moisture Content**		**Deviation (g)**	**Deviation (%)**
g	**Set value (°C)**	**Actual (°C)**	**X_{solid} (g)**	**X_{gas} (g)**		
100	80	67.9	66.99	76.62	9.63	12.57
200	80	67.5	133.92	130.13	-3.79	-2.91
300	80	68.5	200.86	298.37	97.51	32.68
400	80	67.5	268.50	322.88	54.38	16.84
500	80	67.0	332.63	405.39	72.76	17.95
600	80	65.4	400.97	461.70	60.73	13.15
				Average	**48.54**	**15.05**

Table B-8. Moisture content deviation in X_{solid} and X_{gas} at varying Inlet Temperature for Feed Particle Size = 3.0 mm

INLET TEMPERATURE		
Dryer Operating Parameters (Constant)		
Residence Time	**Feed Particle Size**	**Bed Load**
min	**mm**	**g**
80	3.0	300

Dryer Operating Parameters (Variable)							
Inlet Temperature		**Airflow**		**Cumulative Moisture Content**		**Deviation (g)**	**Deviation (%)**
Set value (°C)	**Actual (°C)**	**%**	**m³/s**	**X_{solid} (g)**	**X_{gas} (g)**		
120	95.6	65	0.0225	206.76	235.26	28.50	12.11
115	92.1	70	0.0242	205.94	238.33	32.39	13.59
100	82.0	80	0.0273	206.38	259.59	53.21	20.50
80	67.8	80	0.0273	201.74	245.12	43.38	17.70
50	44.0	80	0.0273	200.22	226.57	26.35	11.63
120	82.5	100	0.0333	199.70	217.90	18.20	8.35
100	83.8	100	0.0333	204.61	232.09	27.48	11.84
50	44.7	100	0.0333	197.58	223.73	26.15	11.69
					Average	**31.96**	**13.43**

Table B-9. Moisture content deviation in X_{solid} and X_{gas} at varying Inlet Temperature for Feed Particle Size = 4.5 mm

INLET TEMPERATURE		
Dryer Operating Parameters (Constant)		
Residence Time	**Feed Particle Size**	**Bed Load**
min	**mm**	**g**
80	4.5	300

Dryer Operating Parameters (Variable)							
Inlet Temperature		**Airflow**		**Cumulative Moisture Content**		**Deviation (g)**	**Deviation (%)**
Set value (°C)	**Actual (°C)**	**%**	**m³/s**	**X_{solid} (g)**	**X_{gas} (g)**		
115	89.5	70	0.0242	203.54	257.54	54.00	20.97
100	81.9	80	0.0273	202.19	313.95	111.76	35.60
80	68.5	80	0.0273	200.86	298.37	97.51	32.68
50	44.3	80	0.0273	195.73	252.40	56.67	22.45
120	82.7	100	0.0333	198.94	252.89	53.95	21.33
100	83.4	100	0.0333	194.03	238.41	44.38	18.61
50	44.7	100	0.0333	195.88	205.46	9.58	4.66
					Average	**61.12**	**22.33**

Table B-10. Moisture content deviation in X_{solid} and X_{gas} at varying Inlet Temperature for Feed Particle Size = 6.0 mm

INLET TEMPERATURE		
Dryer Operating Parameters (Constant)		
Residence Time	**Feed Particle Size**	**Bed Load**
min	**mm**	**g**
80	6.0	300

Dryer Operating Parameters (Variable)							
Inlet Temperature		**Airflow**		**Cumulative Moisture Content**		**Deviation (g)**	**Deviation (%)**
Set value (°C)	**Actual (°C)**	**%**	**m³/s**	**X_{solid} (g)**	**X_{gas} (g)**		
120	81.0	100	0.0333	195.25	293.60	98.35	33.50
100	82.4	100	0.0333	191.85	258.4	66.55	25.75
50	44.5	100	0.0333	176.68	189.17	12.49	6.60
					Average	**59.13**	**21.95**

APPENDIX – C

Moisture removed for varying operating conditions

Table C-1. Moisture removed at varying Residence Time

RESIDENCE TIME			
Dryer Operating Parameters (Constant)			
Airflow		Feed Particle Size	Bed Load
%	m^3/s	mm	g
80	0.0273	4.5	300

Dryer Operating Parameter (Variable)			Moisture Content in		Moisture Removed (g)	Moisture Removed (%)	Volume Reduction (%)
Residence Time (min)	Inlet Temperature						
	Set value (°C)	Actual (°C)	Initial Feed (g)	Final Product (g)			
10	80	51.4	208.15	48.89	159.26	76.51	53.09
15	80	60.3	204.52	25.01	179.51	87.77	59.84
20	80	63.9	204.53	24.19	180.34	88.17	60.11
40	80	66.8	206.98	12.29	194.69	94.06	64.90
60	80	67.0	207.28	7.08	200.20	96.58	66.73
80	80	68.5	206.03	6.39	199.64	96.90	66.55
100	80	67.5	203.41	6.21	197.20	96.95	65.73
120	80	67.5	207.03	5.46	201.57	97.36	67.19

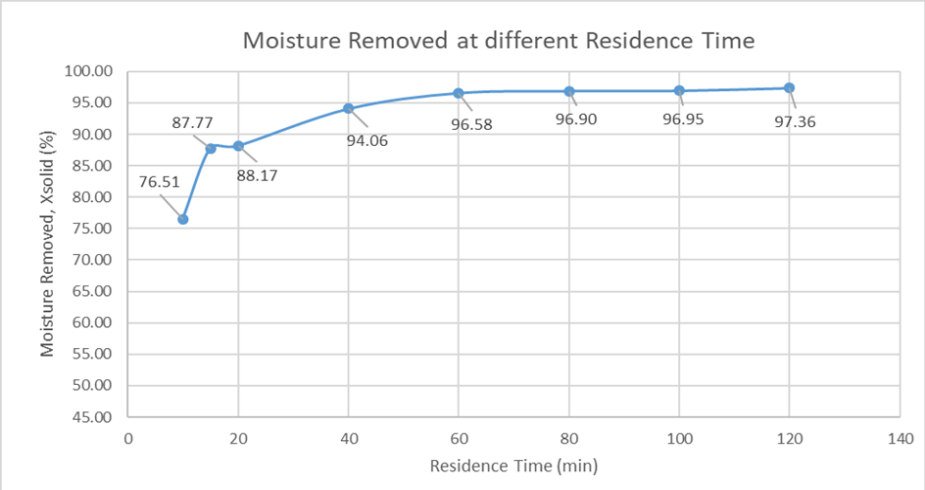

Figure C-1. Moisture removed at different Residence Time

Table C-2. Moisture removed at varying Airflow for Feed Particle Size = 4.5 mm

AIRFLOW		
Dryer Operating Parameters (Constant)		
Residence Time	Feed Particle Size	Bed Load
min	mm	g
80	4.5	300

Dryer Operating Parameter (Variable)				Moisture Content in		Moisture Removed (g)	Moisture Removed (%)	Volume Reduction (%)
Airflow		Inlet Temperature						
%	m³/s	Set value (°C)	Actual (°C)	Initial Feed (g)	Final Product (g)			
70	0.0242	80	67.2	206.98	6.35	200.63	96.93	66.88
80	0.0273	80	68.5	206.08	6.39	199.69	96.90	66.56
90	0.0303	80	68.0	207.15	5.92	201.23	97.14	67.08
100	0.0333	80	68.5	206.60	6.63	199.97	96.79	66.66

Table C-3. Moisture removed at varying Airflow for Feed Particle Size = 3.0 mm

AIRFLOW		
Dryer Operating Parameters (Constant)		
Residence Time	Feed Particle Size	Bed Load
min	mm	g
80	3.0	300

Dryer Operating Parameter (Variable)				Moisture Content in		Moisture Removed (g)	Moisture Removed (%)	Volume Reduction (%)
Airflow		Inlet Temperature						
%	m³/s	Set value (°C)	Actual (°C)	Initial Feed (g)	Final Product (g)			
70	0.0242	80	66.8	203.81	5.85	197.96	97.13	65.99
80	0.0273	80	67.8	207.96	5.45	202.51	97.38	67.50
90	0.0303	80	68.2	204.09	5.37	198.72	97.37	66.24
100	0.0333	80	69.0	205.13	5.50	199.63	97.32	66.54

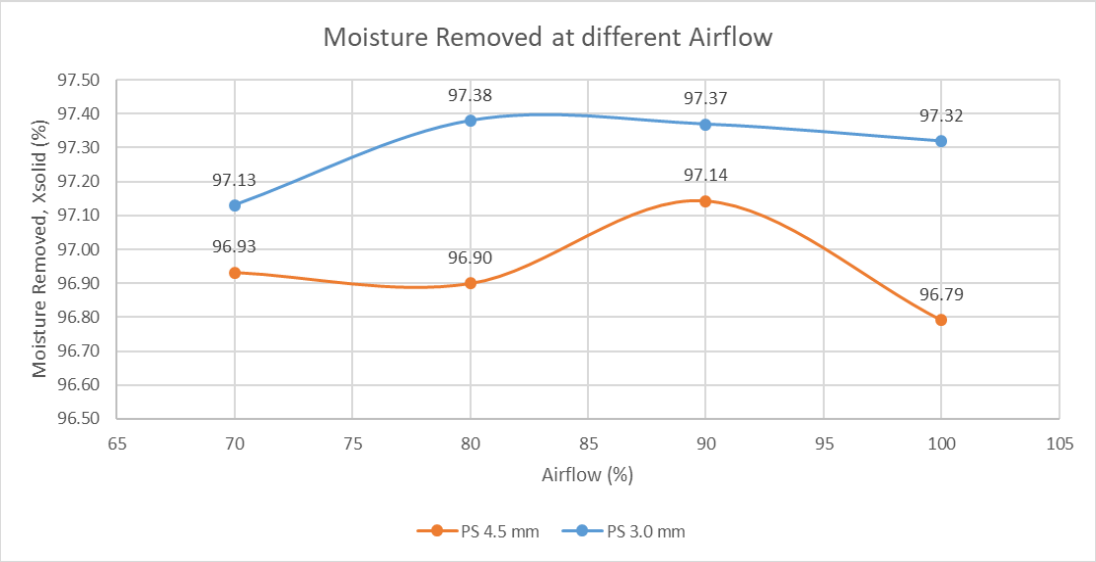

Figure C-2. Moisture removed at different Airflow

Table C-4. Moisture removed at varying Feed Particle Size = 3.0 mm

FEED PARTICLE SIZE						
Dryer Operating Parameters (Constant)						
Residence Time	Airflow		Bed Load			
min	%	m³/s	g			
80	100	0.0333	300			
Dryer Operating Parameter (Variable)			Moisture Content in		Moisture Removed (g)	Moisture Removed (%)
Particle Size	Inlet Temperature					
mm	Set value (°C)	Actual (°C)	Initial Feed (g)	Final Product (g)		
3.0	50	44.7	205.26	9.30	195.96	95.47
3.0	100	83.8	204.99	5.17	199.82	97.48
3.0	120	82.5	200.95	4.15	196.80	97.93

Table C-5. Moisture removed at varying Feed Particle Size = 4.5 mm

FEED PARTICLE SIZE						
Dryer Operating Parameters (Constant)						
Residence Time	Airflow		Bed Load			
min	%	m³/s	g			
80	100	0.0333	300			
Dryer Operating Parameter (Variable)			Moisture Content in		Moisture Removed (g)	Moisture Removed (%)
Particle Size	Inlet Temperature					
mm	Set value (°C)	Actual (°C)	Initial Feed (g)	Final Product (g)		
4.5	50	44.7	205.12	12.01	193.11	94.14
4.5	100	83.4	197.16	4.63	192.53	97.65
4.5	120	82.7	200.80	4.81	195.99	97.60

Table C-6. Moisture removed at varying Feed Particle Size = 6.0 mm

FEED PARTICLE SIZE						
Dryer Operating Parameters (Constant)						
Residence Time	Airflow		Bed Load			
min	%	m³/s	g			
80	100	0.0333	300			
Dryer Operating Parameter (Variable)			Moisture Content in		Moisture Removed (g)	Moisture Removed (%)
Particle Size	Inlet Temperature					
mm	Set value (°C)	Actual (°C)	Initial Feed (g)	Final Product (g)		
6.0	50	44.5	203.52	18.59	184.93	90.87
6.0	100	82.4	201.72	10.51	191.21	94.79
6.0	120	81.0	203.31	10.77	192.54	94.70

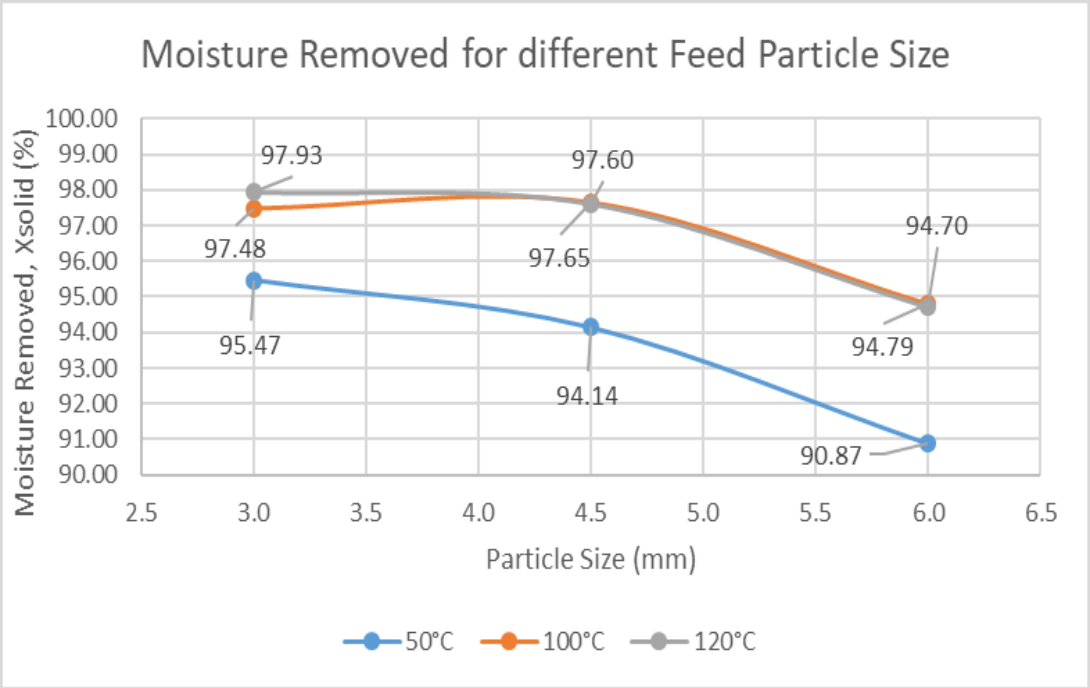

Figure C-3. Moisture removed for different Feed Particle Size

Table C-7. Moisture removed at varying Bed Load

BED LOAD			
Dryer Operating Parameters (Constant)			
Residence Time	Airflow		Feed Particle Size
min	%	m³/s	mm
80	80	0.0273	4.5

Dryer Operating Parameter (Variable)			Moisture Content in		Moisture Removed (g)	Moisture Removed (%)
Bed Load (g)	Inlet Temperature					
	Set value (°C)	Actual (°C)	Initial Feed (g)	Final Product (g)		
100	80	67.9	68.88	2.40	66.48	96.52
200	80	67.5	137.79	4.62	133.17	96.65
300	80	68.5	206.03	6.39	199.64	96.90
400	80	67.5	273.78	8.69	265.09	96.83
500	80	67.0	342.91	11.62	331.29	96.61
600	80	65.4	416.90	14.53	402.37	96.51

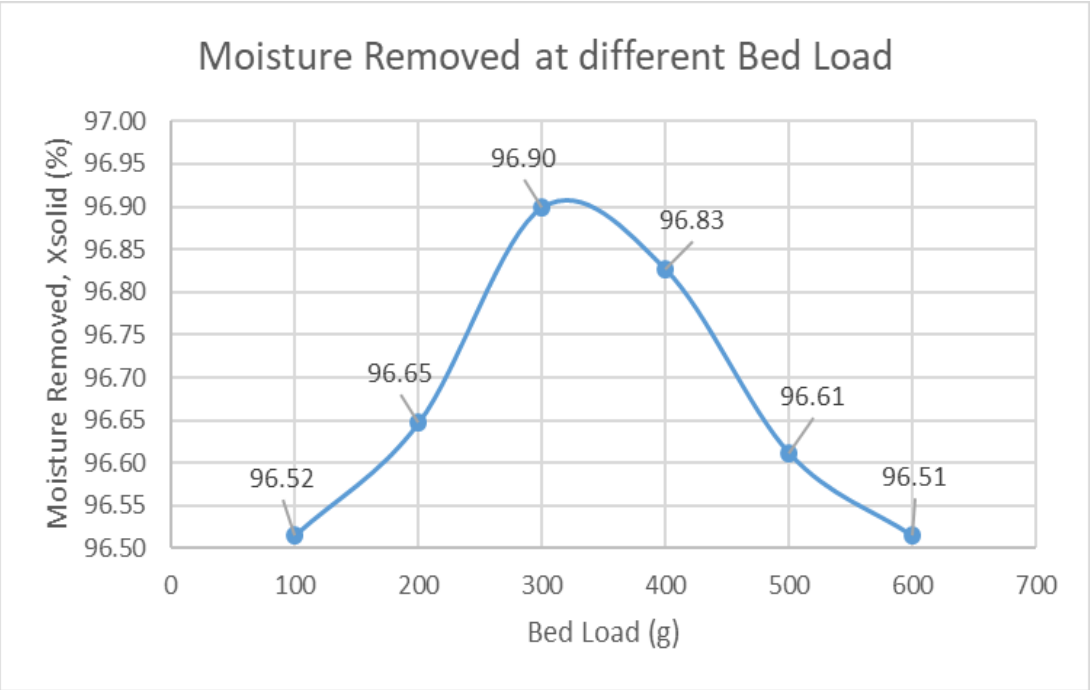

Figure C-4. Moisture removed at different Bed Load

Table C-8. Moisture removed at varying Inlet Temperature for Feed Particle Size = 4.5 mm

INLET TEMPERATURE		
Dryer Operating Parameters (Constant)		
Residence Time	Feed Particle Size	Bed Load
min	mm	g
80	4.5	300

Dryer Operating Parameter (Variable)				Moisture Content in		Moisture Removed (g)	Moisture Removed (%)
Inlet Temperature		Airflow					
Set value (°C)	Actual (°C)	%	m³/s	Initial Feed (g)	Final Product (g)		
115	89.5	70	0.0242	205.24	3.78	201.46	98.16
100	81.9	80	0.0273	205.00	4.38	200.62	97.86
80	68.5	80	0.0273	206.03	6.39	199.64	96.90
50	44.3	80	0.0273	204.65	11.55	193.10	94.36
120	82.7	100	0.0333	200.80	4.81	195.99	97.60
100	83.4	100	0.0333	197.16	4.63	192.53	97.65
50	44.7	100	0.0333	205.12	12.01	193.11	94.14

Table C-9. Moisture removed at varying Inlet Temperature for Feed Particle Size = 3.0 mm

INLET TEMPERATURE		
Dryer Operating Parameters (Constant)		
Residence Time	Feed Particle Size	Bed Load
min	mm	g
80	3.0	300

Dryer Operating Parameter (Variable)				Moisture Content in		Moisture Removed (g)	Moisture Removed (%)
Inlet Temperature		Airflow					
Set value (°C)	Actual (°C)	%	m³/s	Initial Feed (g)	Final Product (g)		
120	95.6	65	0.0225	208.17	2.70	205.47	98.70
115	92.1	70	0.0242	207.40	2.96	204.44	98.57
100	82.0	80	0.0273	207.65	3.76	203.89	98.19
80	67.8	80	0.0273	207.96	5.45	202.51	97.38
50	44.0	80	0.0273	208.00	8.58	199.42	95.88
120	82.5	100	0.0333	200.95	4.15	196.80	97.93
100	83.8	100	0.0333	204.99	5.17	199.82	97.48
50	44.7	100	0.0333	205.26	9.30	195.96	95.47

Table C-10. Moisture removed at varying Inlet Temperature for Feed Particle Size = 6.0 mm

INLET TEMPERATURE		
Dryer Operating Parameters (Constant)		
Residence Time	Feed Particle Size	Bed Load
min	mm	g
80	6.0	300

Dryer Operating Parameter (Variable)				Moisture Content in		Moisture Removed (g)	Moisture Removed (%)
Inlet Temperature		Airflow					
Set value (°C)	Actual (°C)	%	m³/s	Initial Feed (g)	Final Product (g)		
120	81.0	100	0.0333	203.31	10.77	192.54	94.70
100	82.4	100	0.0333	201.72	10.51	191.21	94.79
50	44.5	100	0.0333	203.52	18.59	184.93	90.87

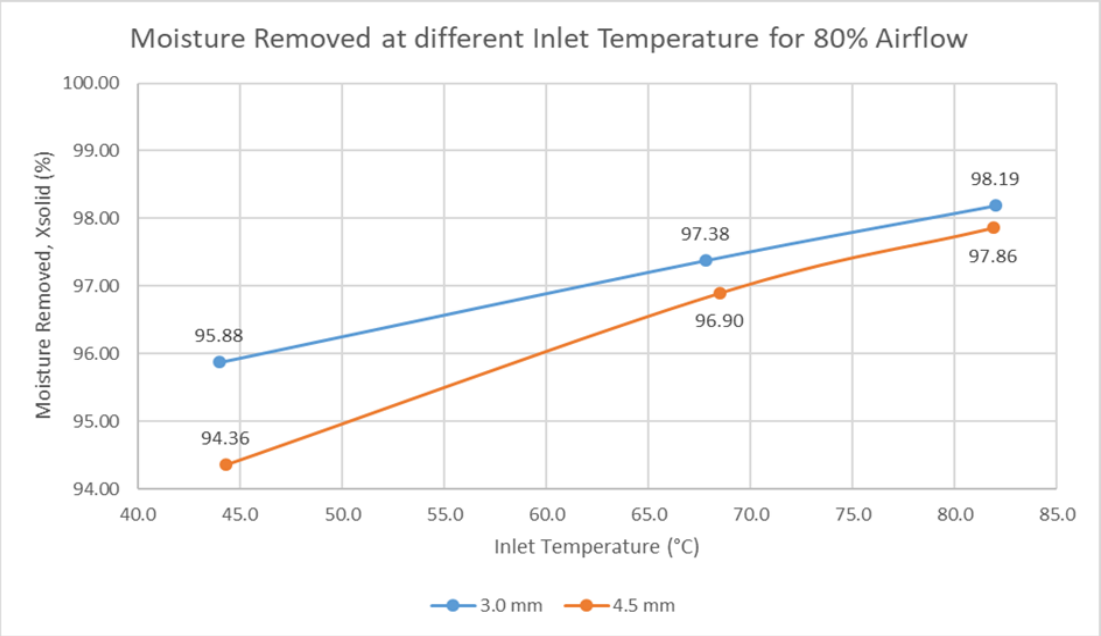

Figure C-5. Moisture removed at different Inlet Temperature for 80% Airflow

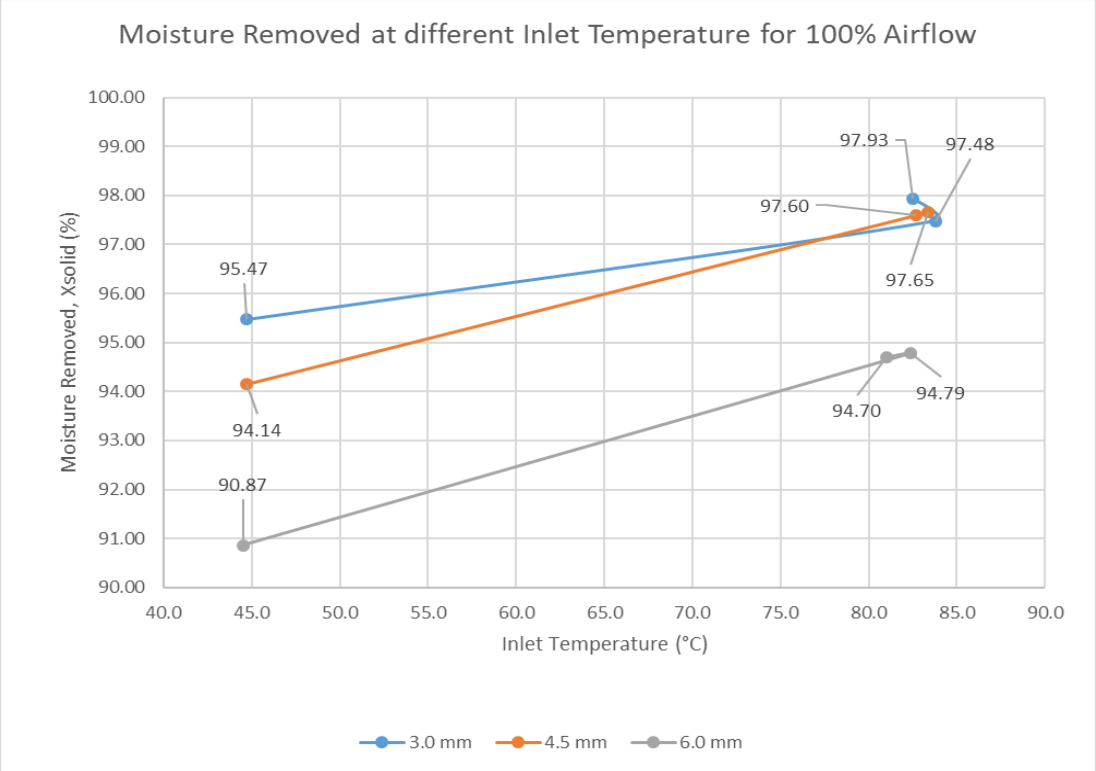

Figure C-6. Moisture removed at different Inlet Temperature for 100% Airflow

APPENDIX – D

Deviation in Actual Inlet Temperature and Process Value for specified Heater Set Value

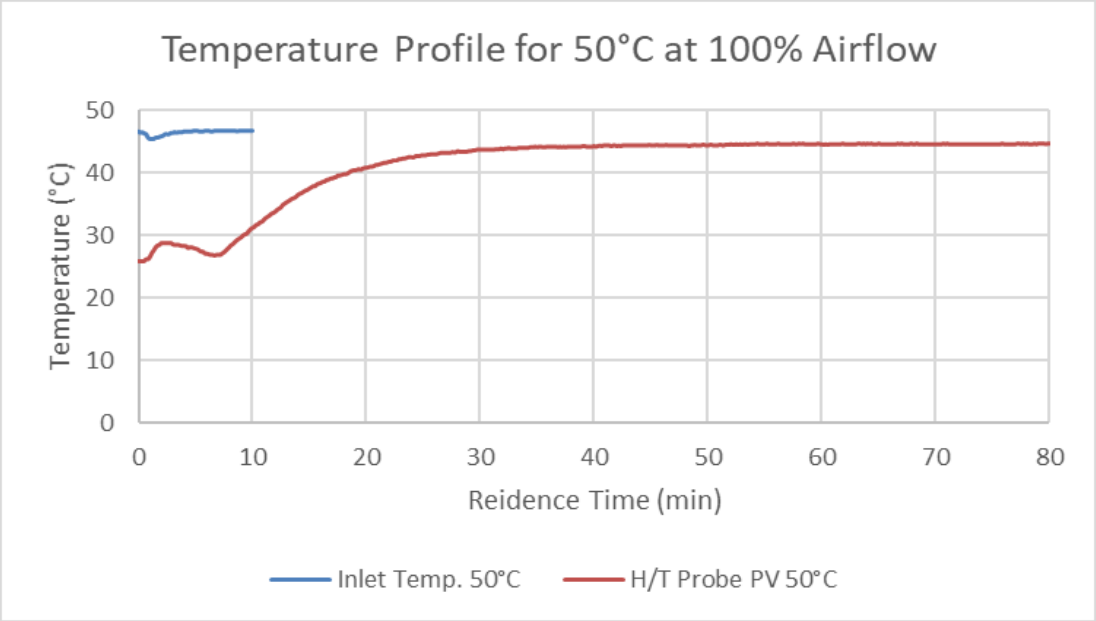

Figure D-1. Temperature Profile for 50°C at 100% Airflow

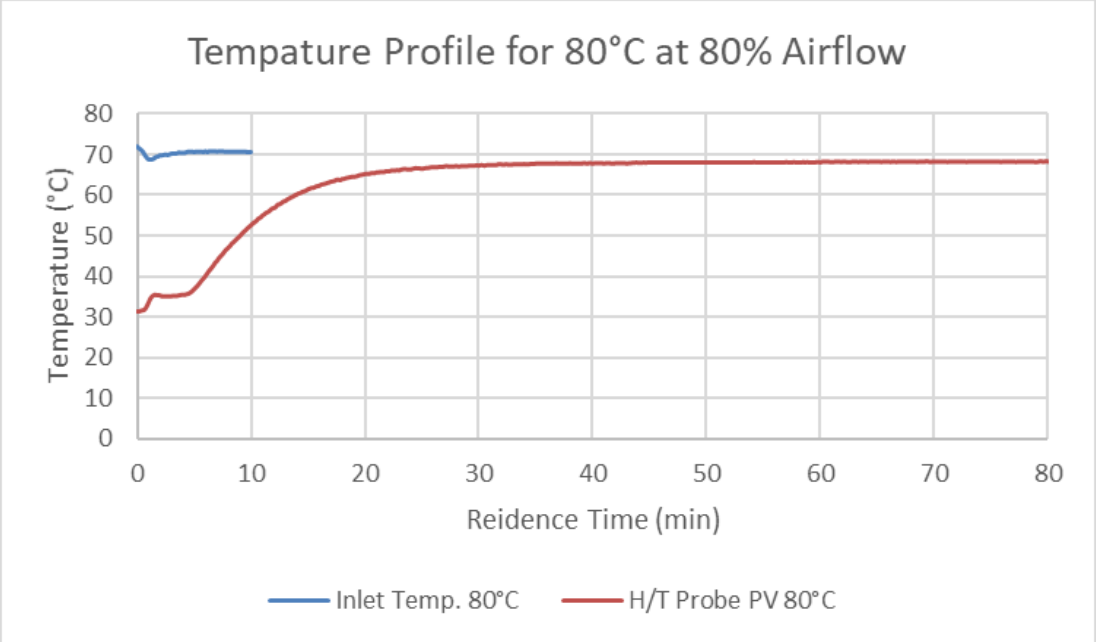

Figure D-2. Temperature Profile for 80°C at 80% Airflow

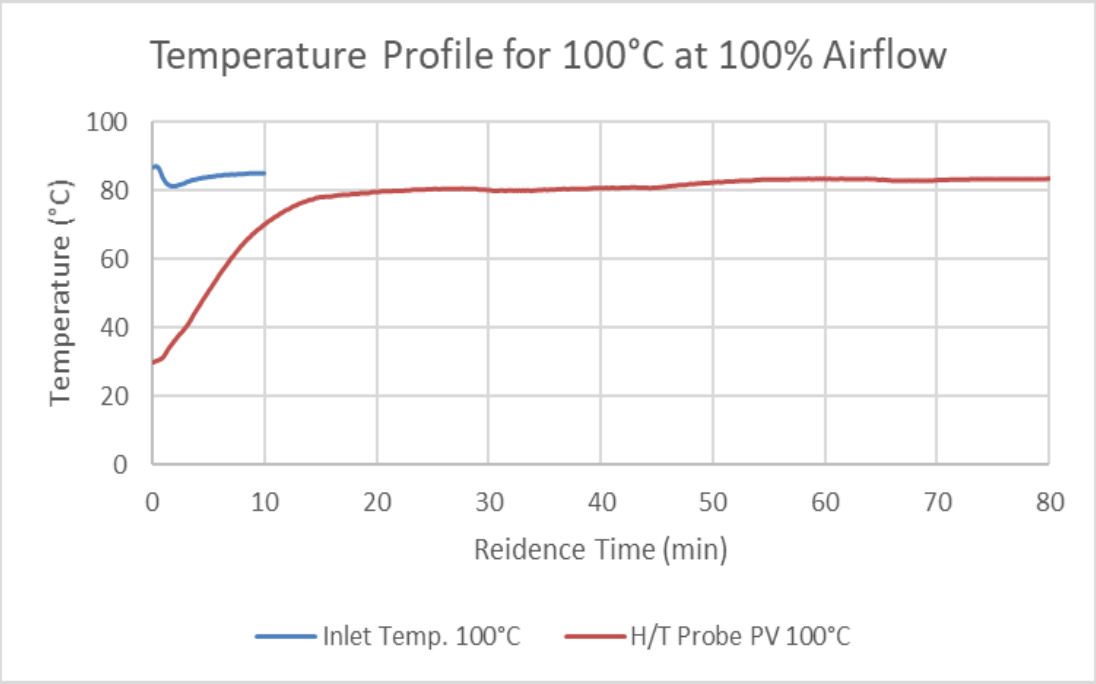

Figure D-3. Temperature Profile for 100°C at 100% Airflow

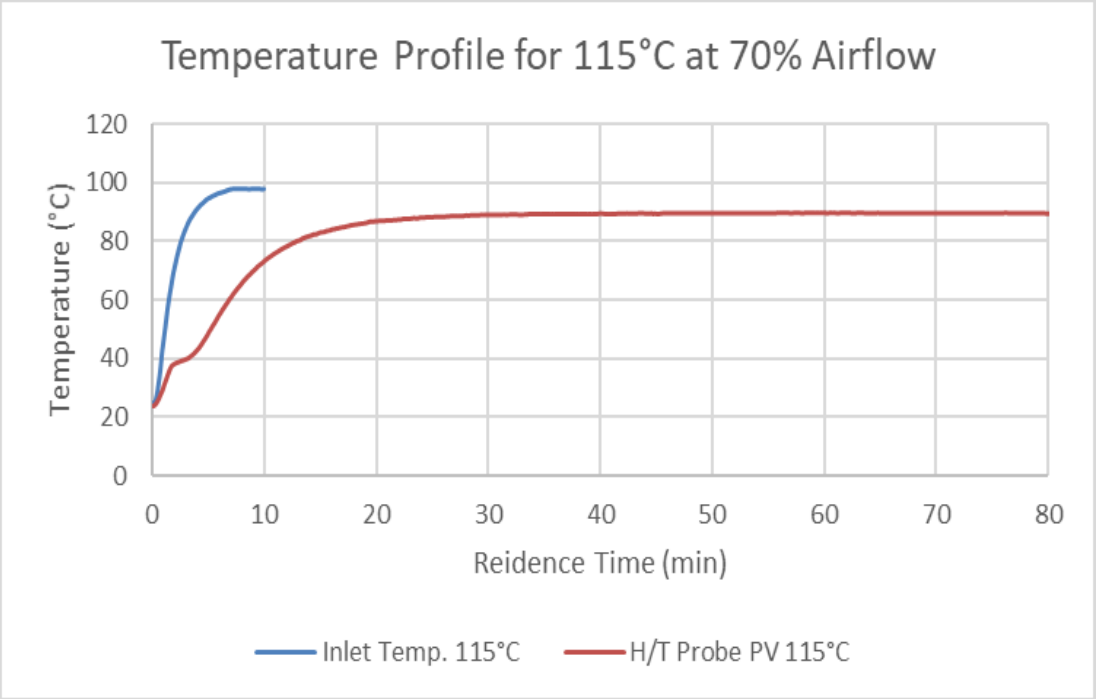

Figure D-4. Temperature Profile for 115°C at 70% Airflow

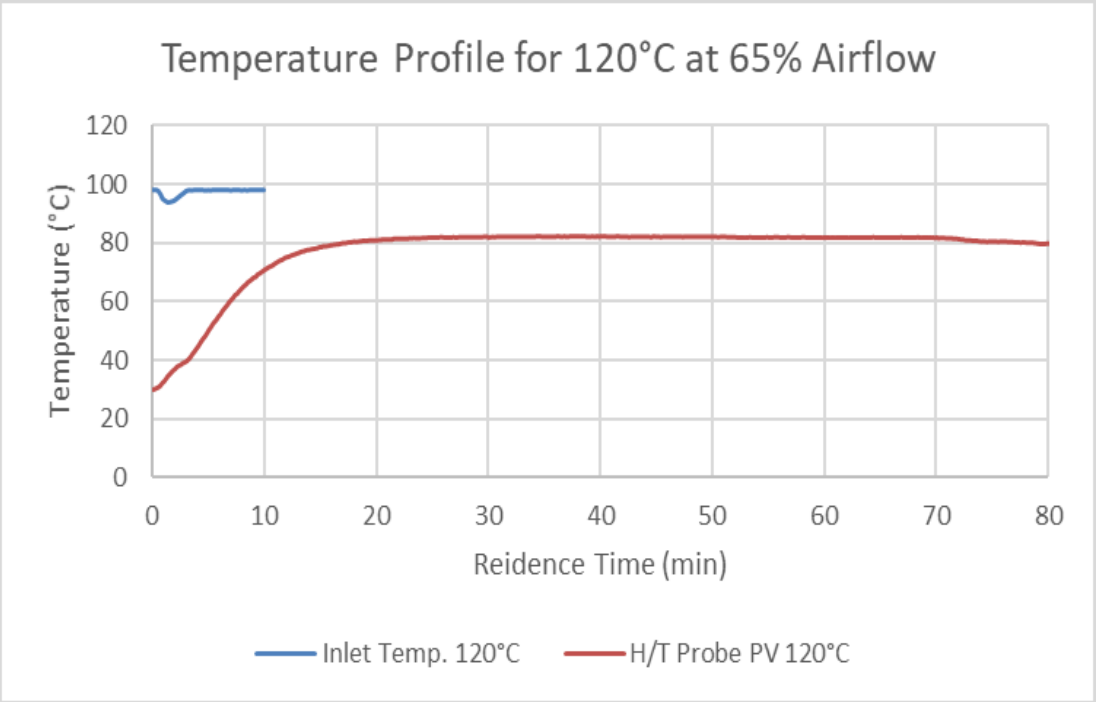

Figure D-5. Temperature Profile for 120°C at 65% Airflow

APPENDIX – E

Net Evaporation Rate and Particle Size Distribution for before and after drying at varying Residence Time

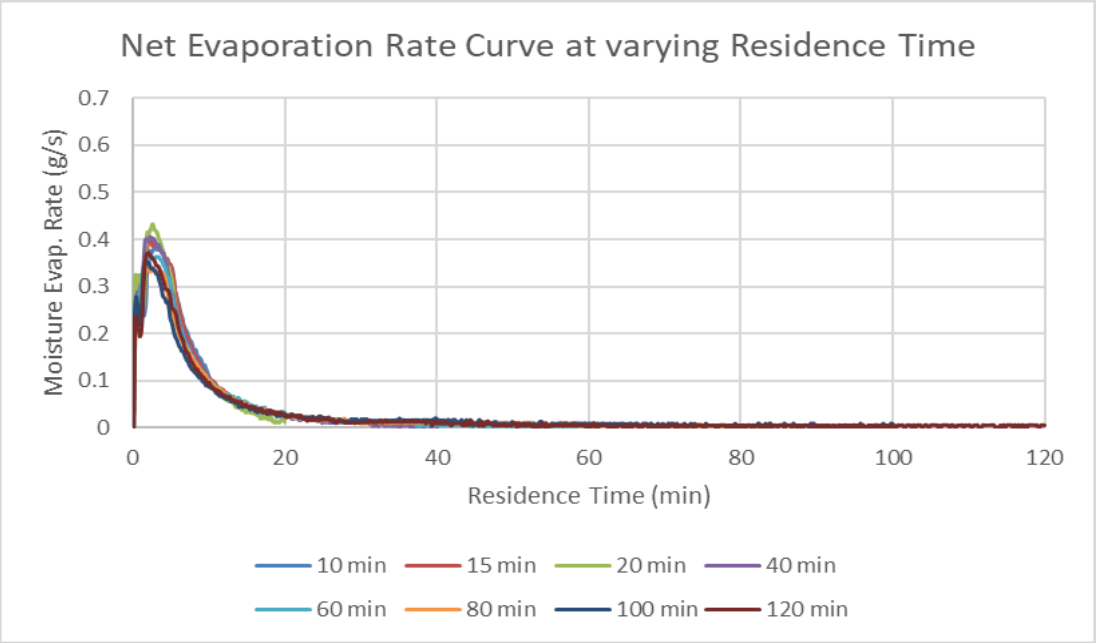

Figure E-1. Net Evaporation Rate Curve at varying Residence Time

PARTICLE SIZE DISTRIBUTION AT VARYING RESIDENCE TIME

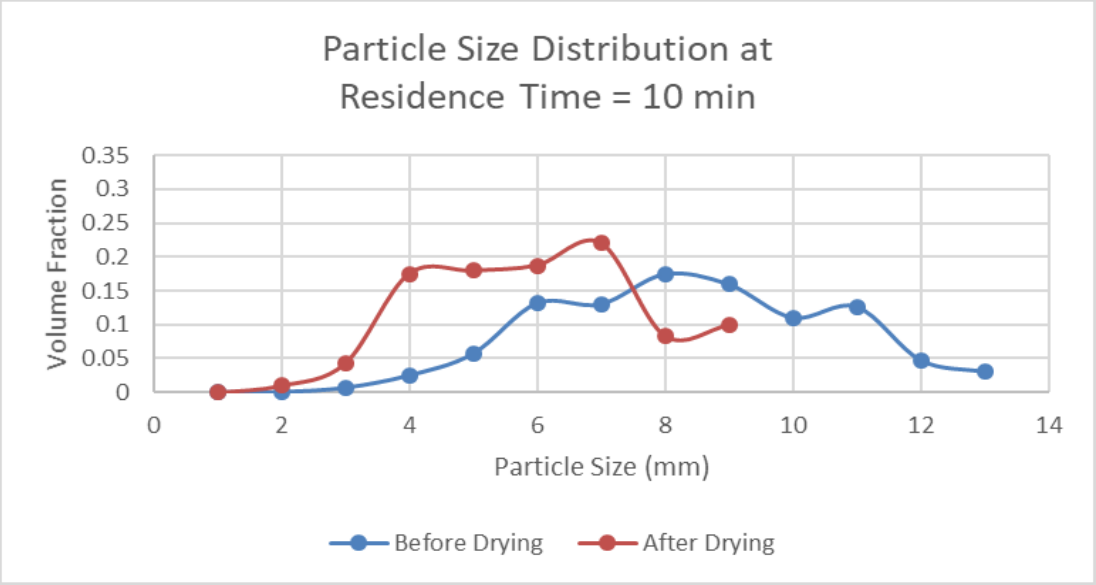

Figure E-2. Particle Size Distribution at Residence Time = 10 min

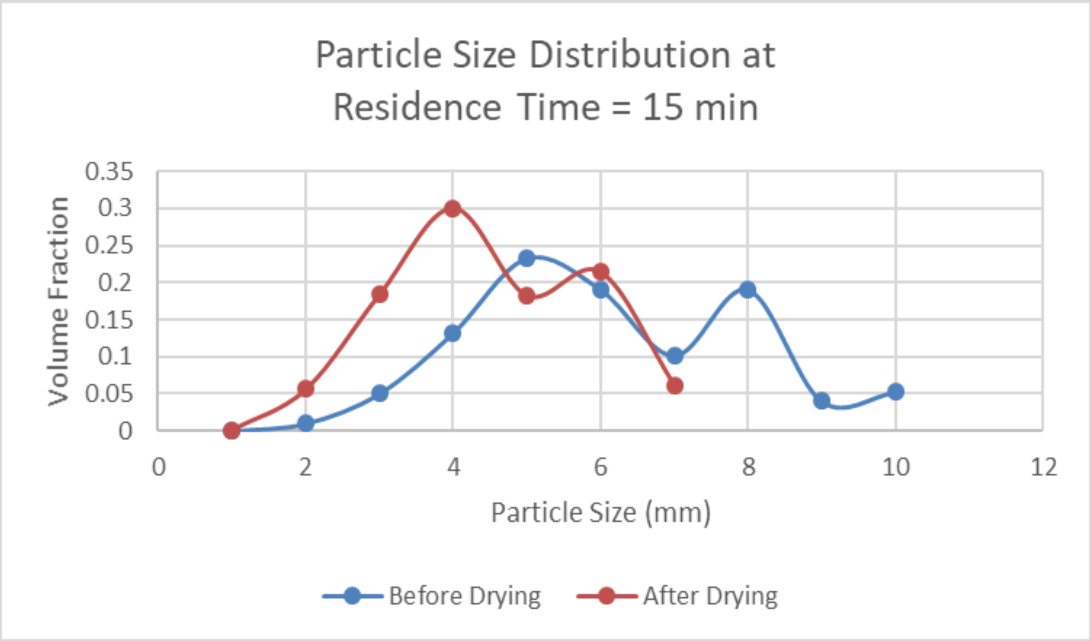

Figure E-3. Particle Size Distribution at Residence Time = 15 min

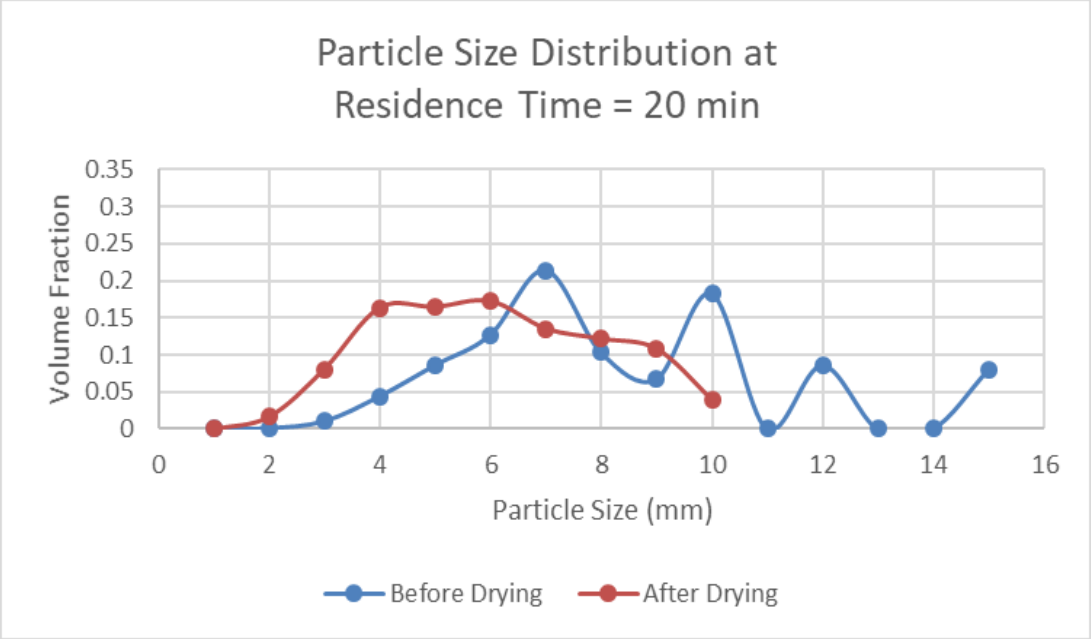

Figure E-4. Particle Size Distribution at Residence Time = 20 min

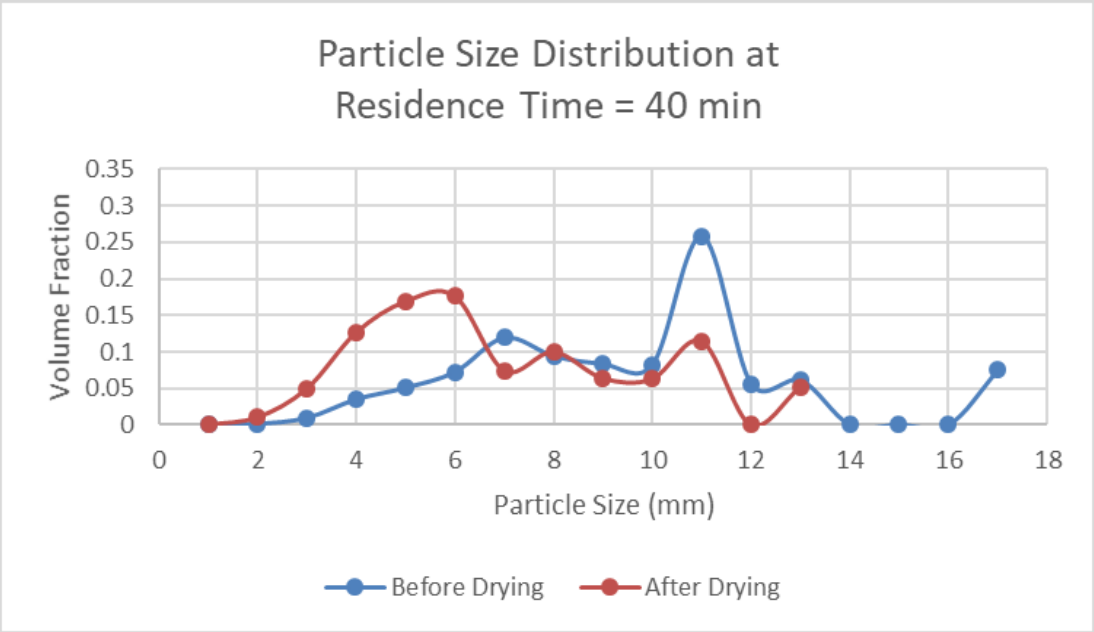

Figure E-5. Particle Size Distribution at Residence Time = 40 min

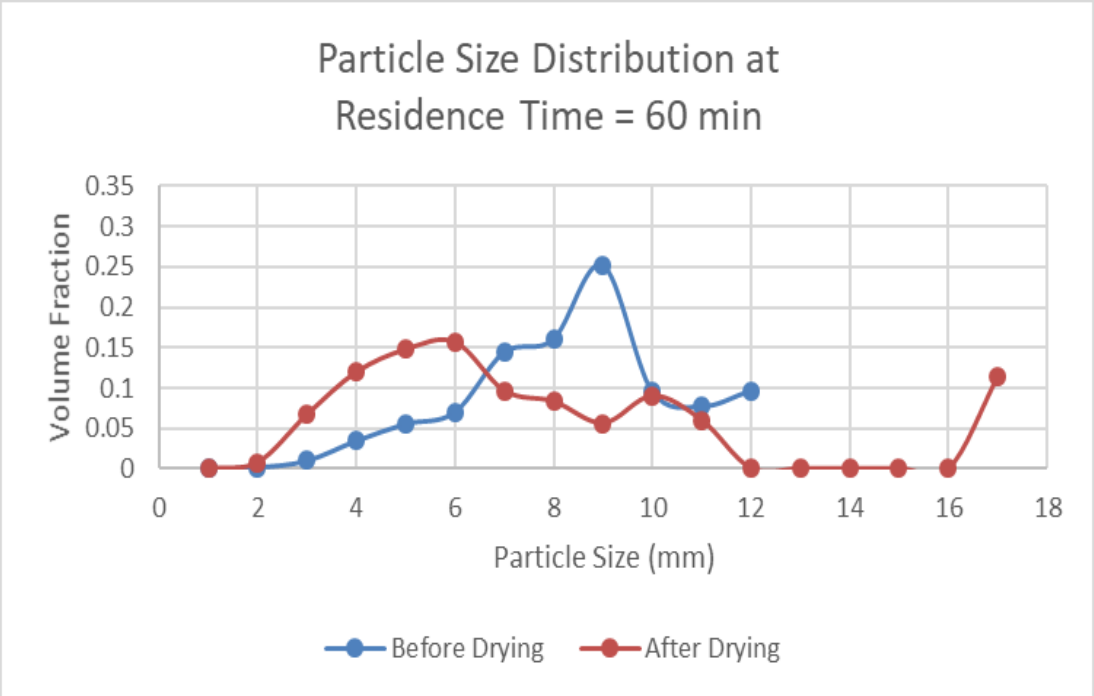

Figure E-6. Particle Size Distribution at Residence Time = 60 min

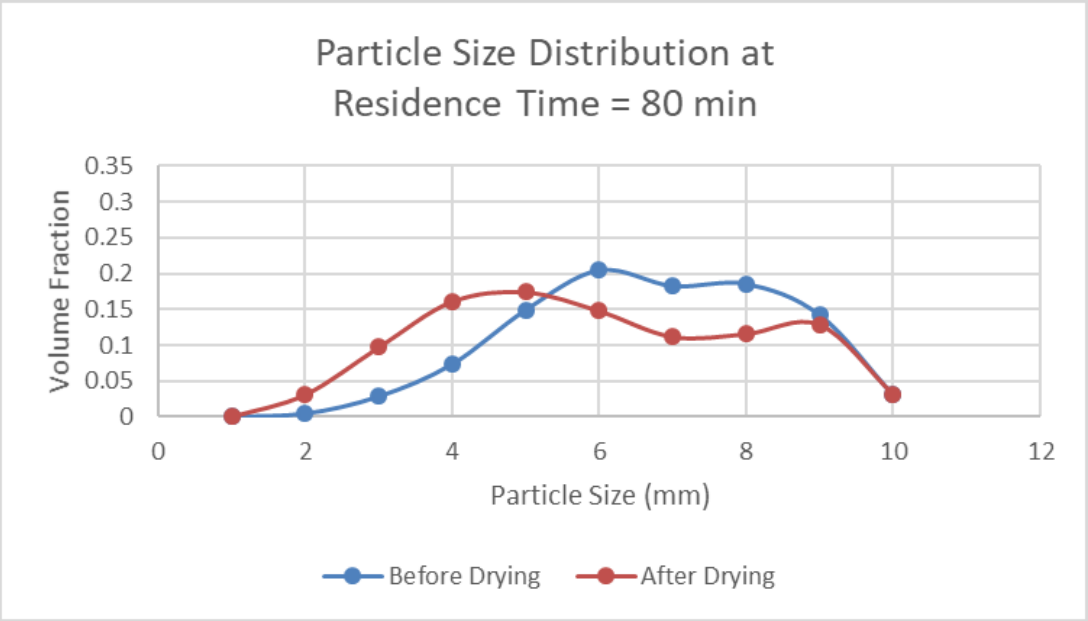

Figure E-7. Particle Size Distribution at Residence Time = 80 min

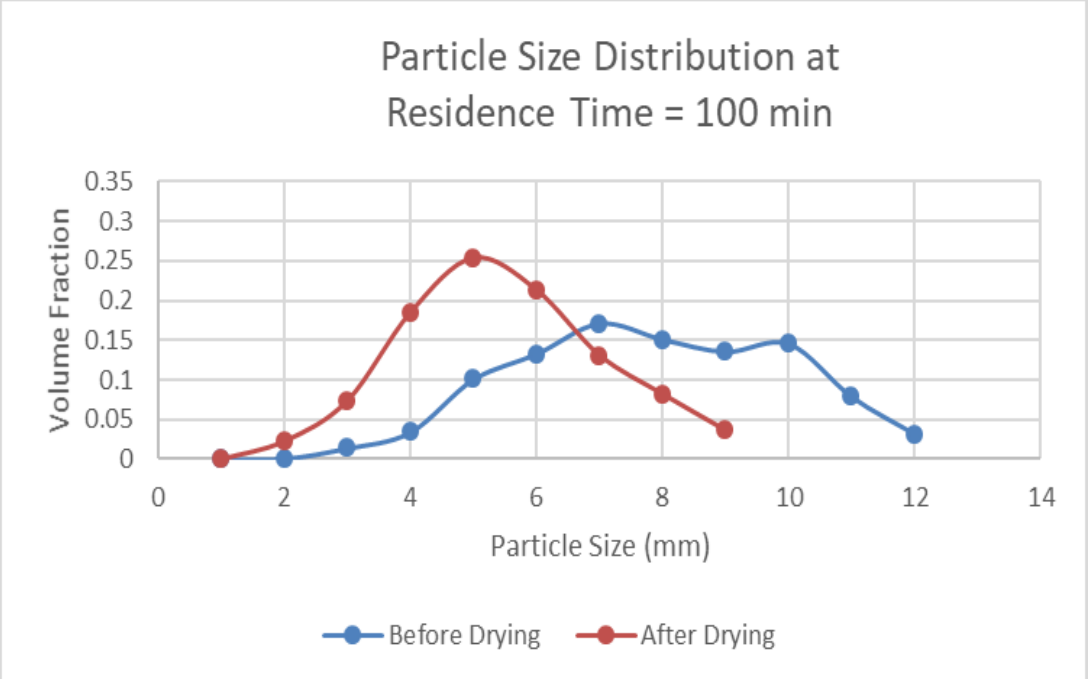

Figure E-8. Particle Size Distribution at Residence Time = 100 min

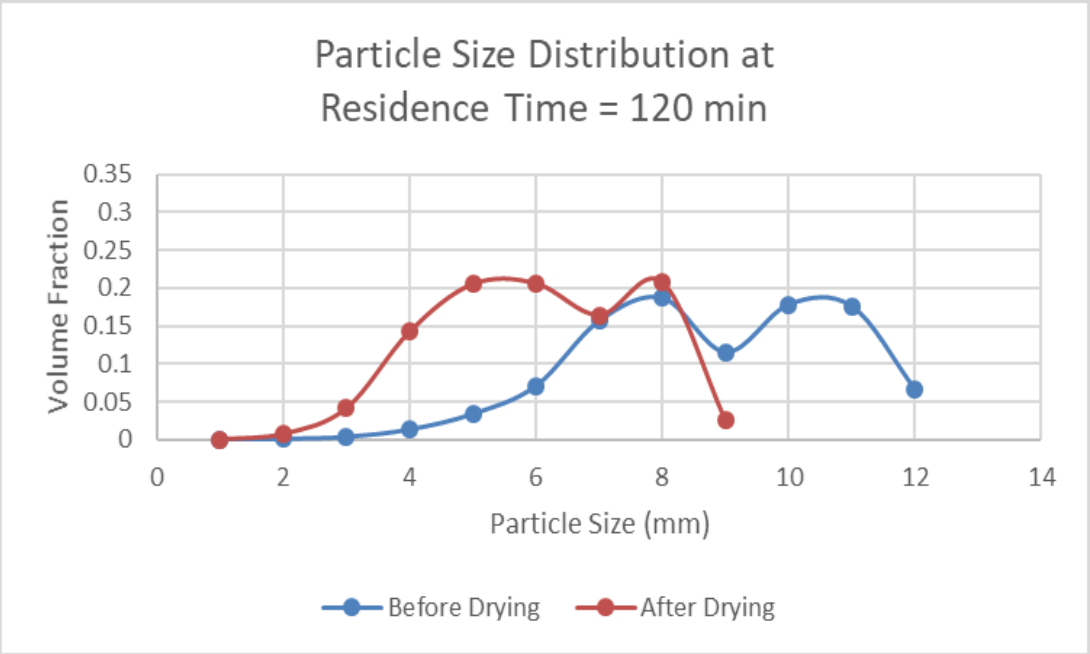

Figure E-9. Particle Size Distribution at Residence Time = 120 min

APPENDIX – F

Net Evaporation Rate and Particle Size Distribution for before and after drying at varying Airflow

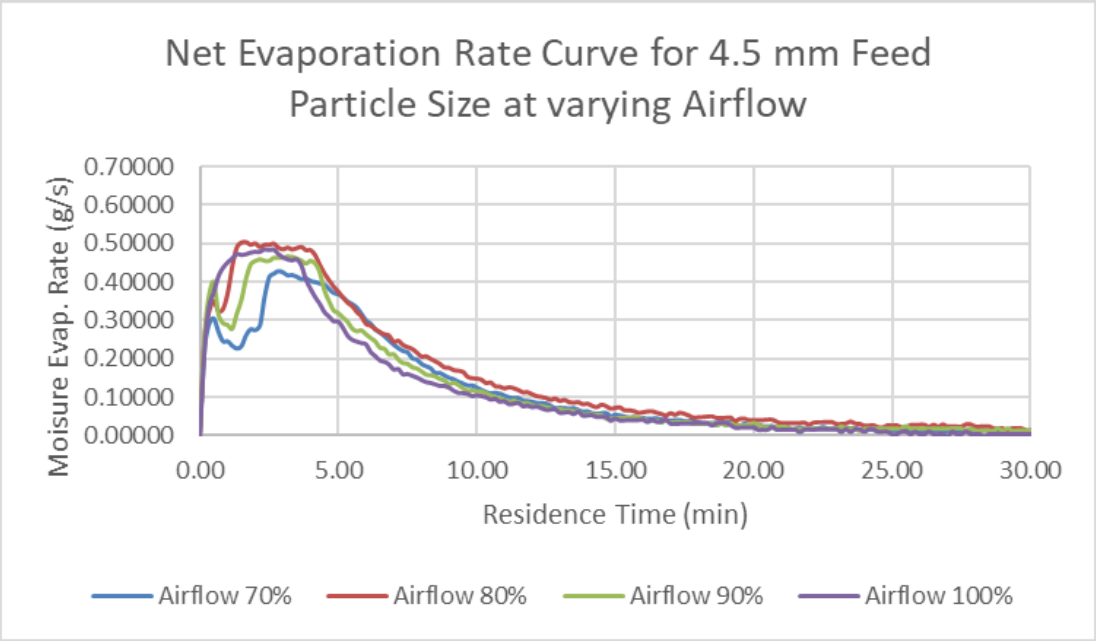

Figure F-1. Net Evaporation Rate Curve at varying Airflow for Feed Particle Size = 4.5 mm

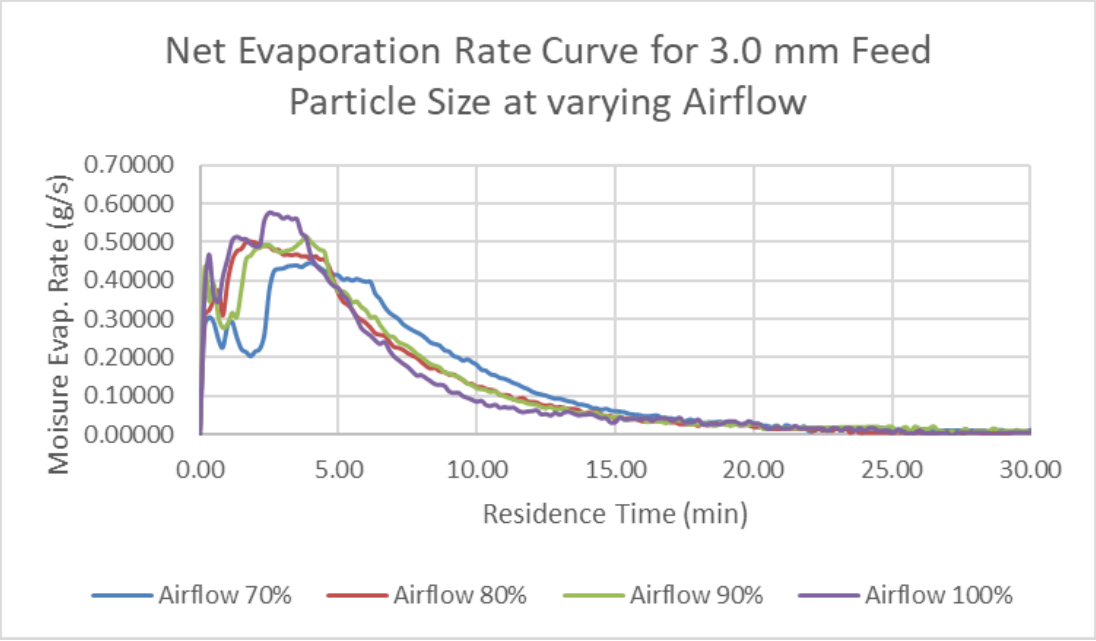

Figure F-2. Net Evaporation Rate Curve at varying Airflow for Feed Particle Size = 3.0 mm

PARTICLE SIZE DISTRIBUTION AT VARYING AIRFLOW

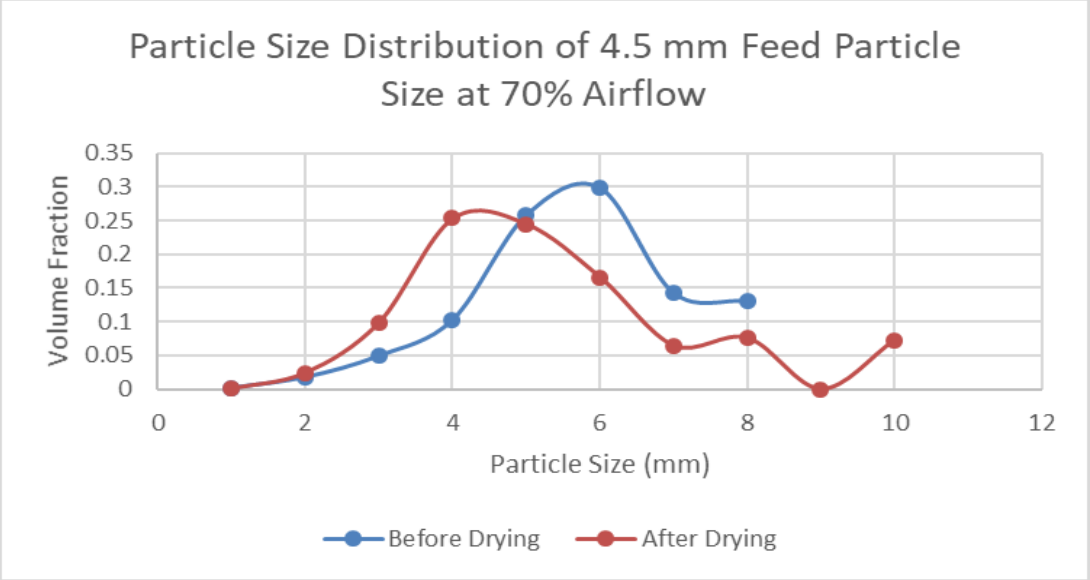

Figure F-3. Particle Size Distribution at 70% Airflow for Feed Particle Size = 4.5 mm

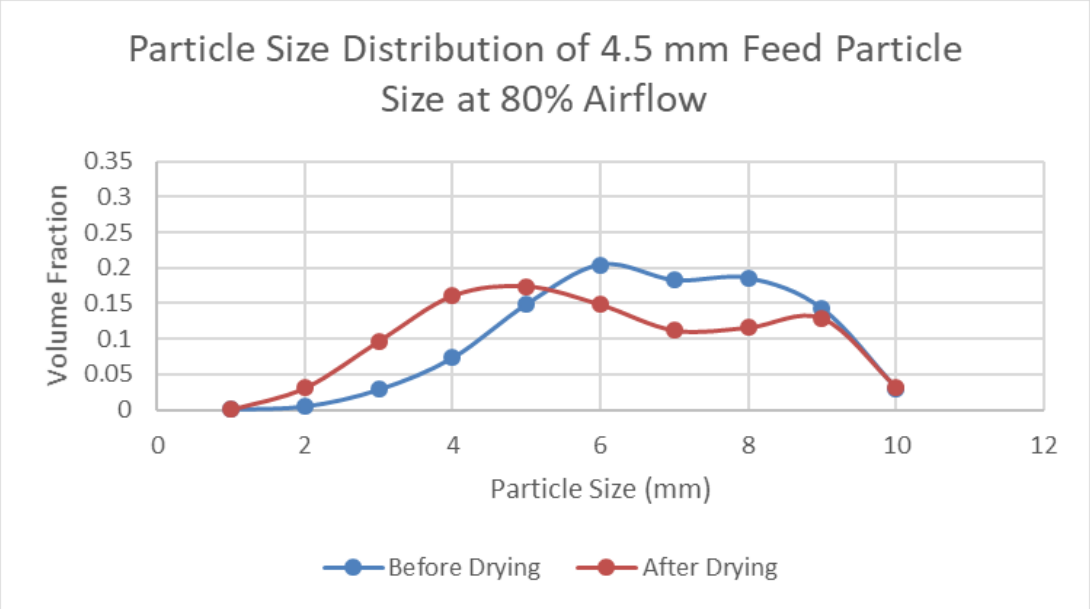

Figure F-4. Particle Size Distribution at 80% Airflow for Feed Particle Size = 4.5 mm

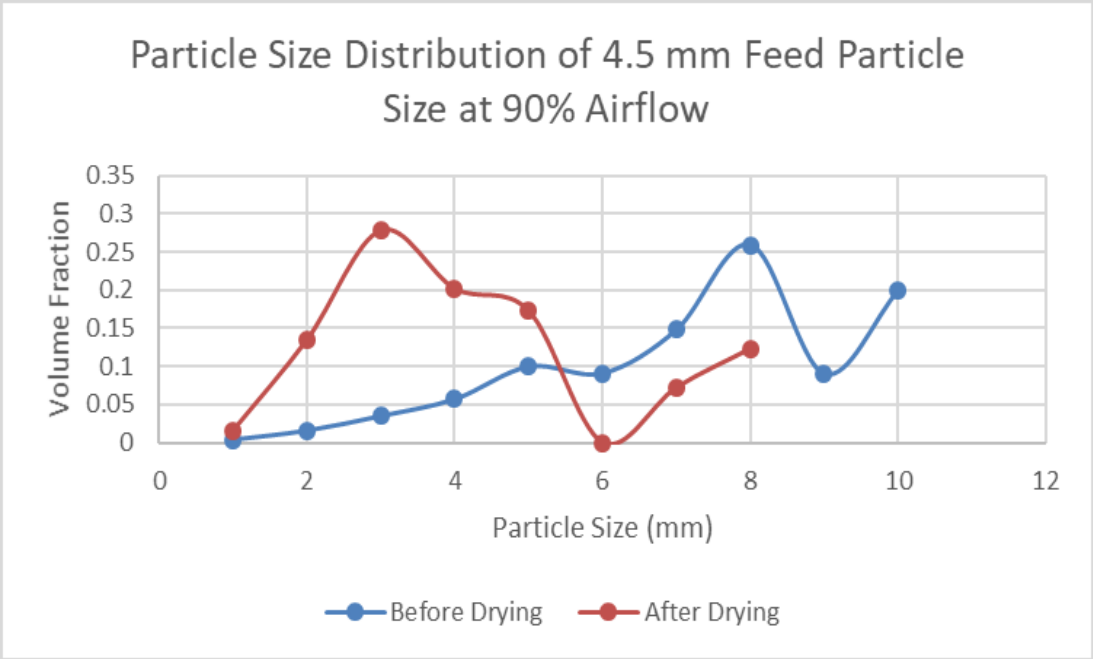

Figure F-5. Particle Size Distribution at 90% Airflow for Feed Particle Size = 4.5 mm

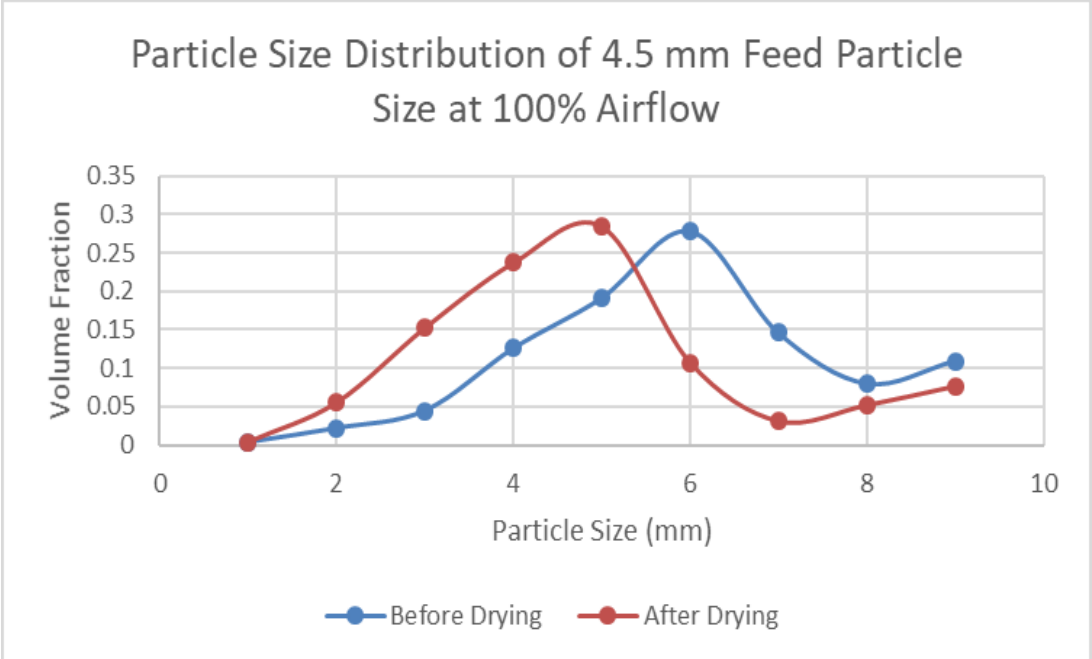

Figure F-6. Particle Size Distribution at 100% Airflow for Feed Particle Size = 4.5 mm

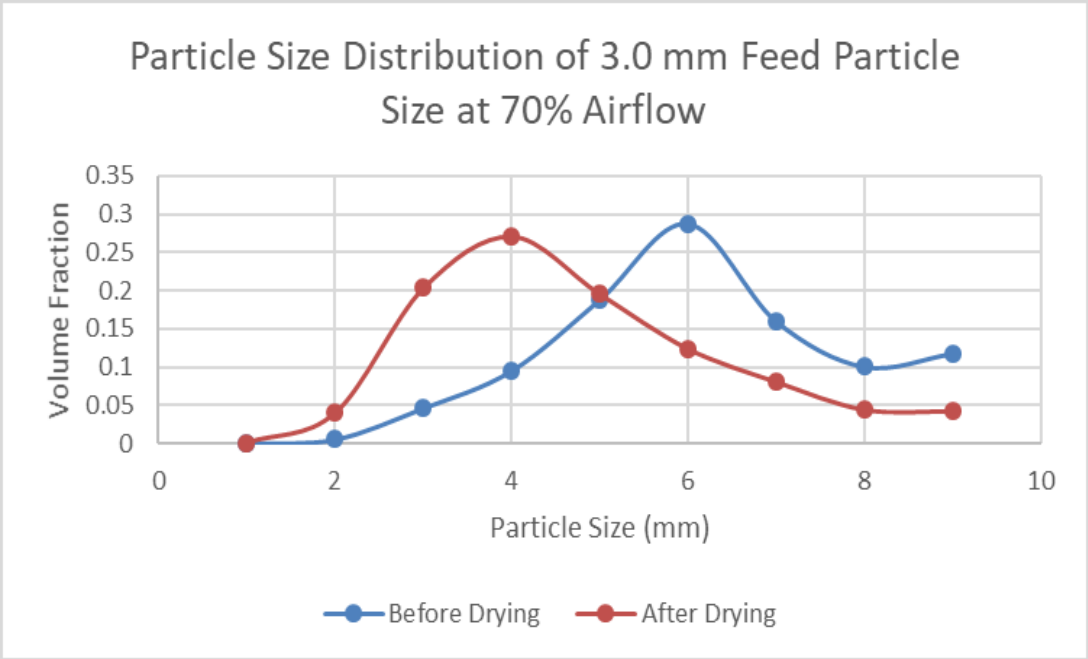

Figure F-7. Particle Size Distribution at 70% Airflow for Feed Particle Size = 3.0 mm

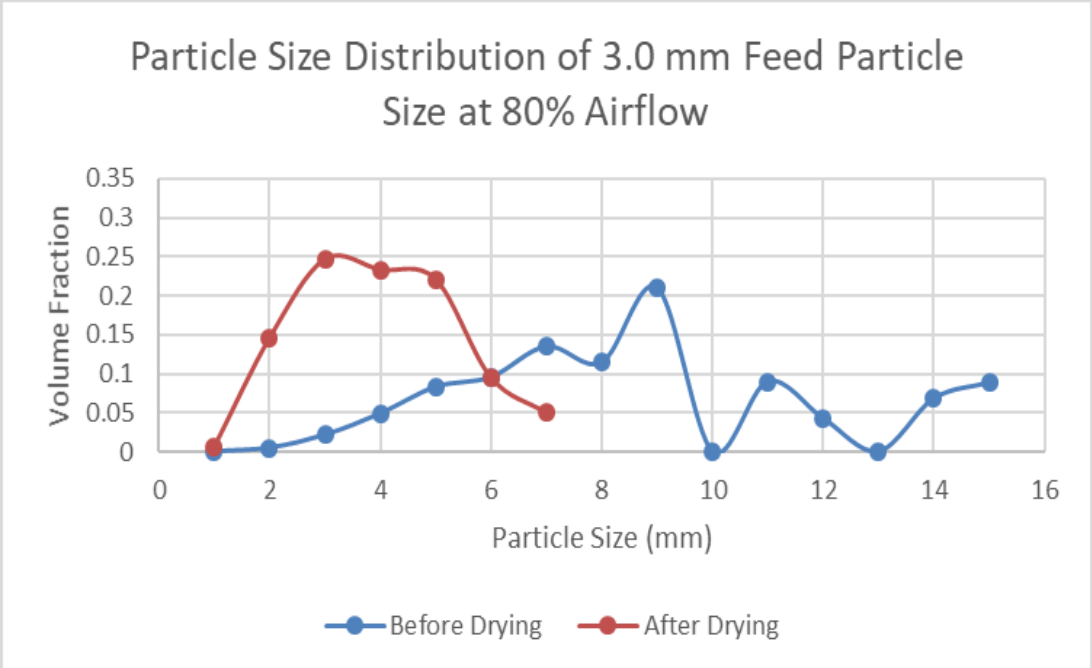

Figure F-8. Particle Size Distribution at 80% Airflow for Feed Particle Size = 3.0 mm

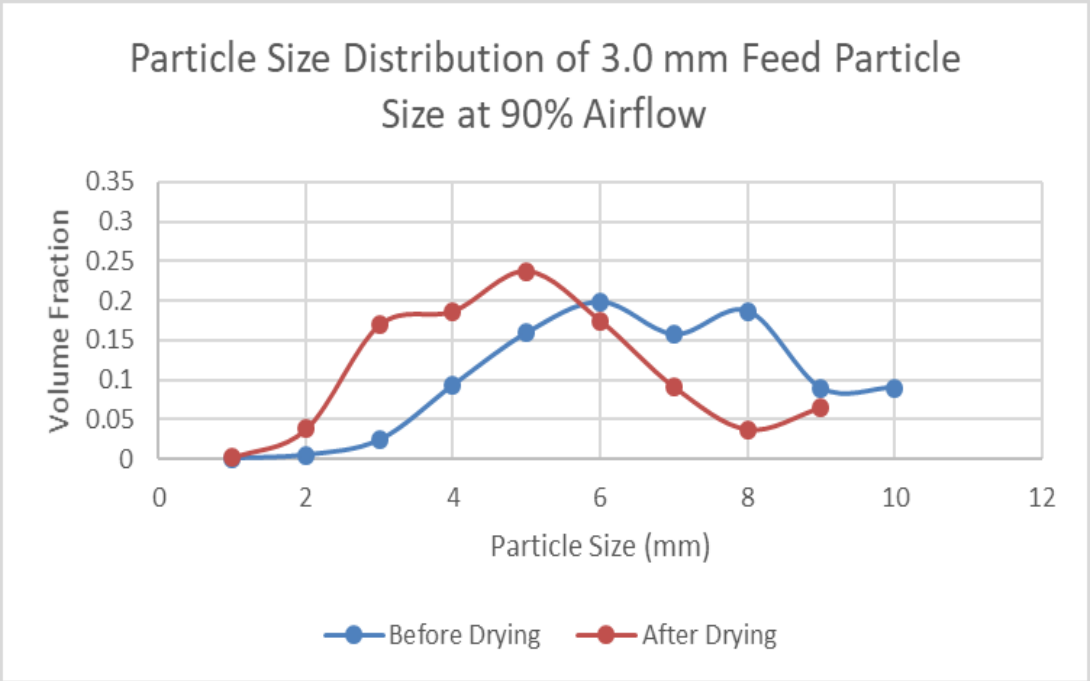

Figure F-9. Particle Size Distribution at 90% Airflow for Feed Particle Size = 3.0 mm

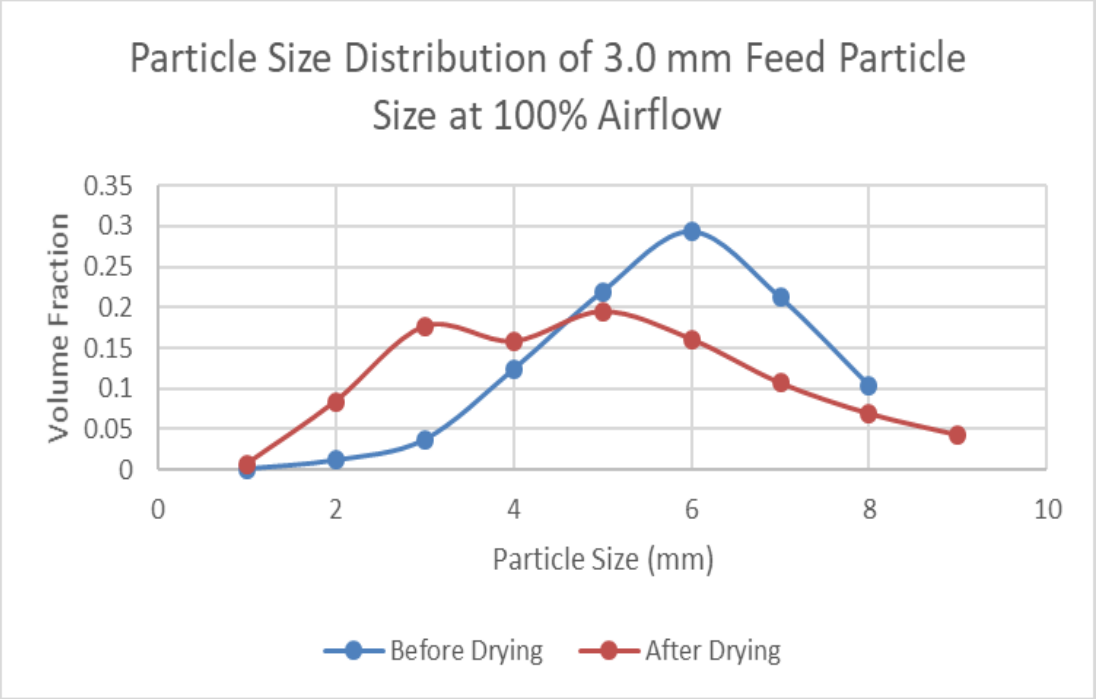

Figure F-10. Particle Size Distribution at 90% Airflow for Feed Particle Size = 3.0 mm

APPENDIX – G

Net Evaporation Rate and Particle Size Distribution for before and after drying at varying Feed Particle Size

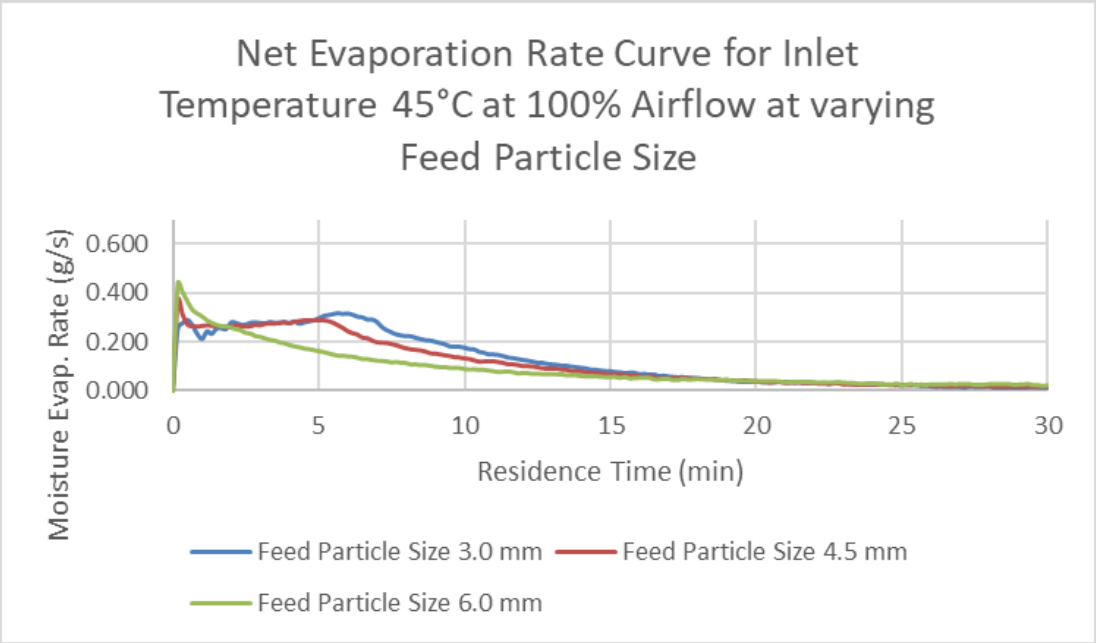

Figure G-1. Net Evaporation Rate Curve at varying Feed Particle Size for Inlet Temperature = 45°C at 100% Airflow

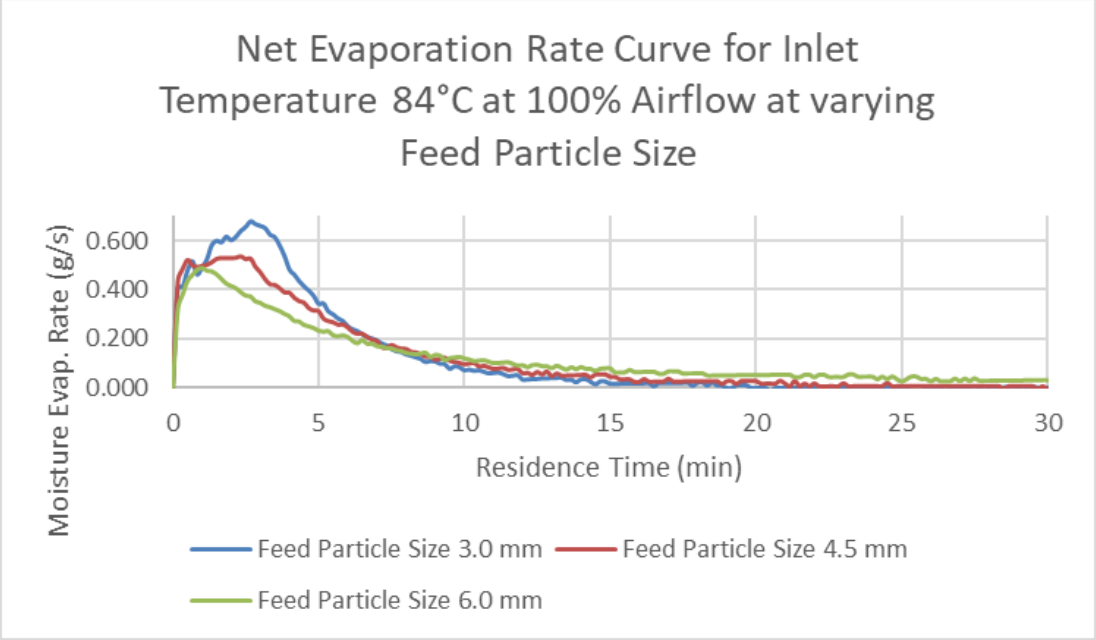

Figure G-2. Net Evaporation Rate Curve at varying Feed Particle Size for Inlet Temperature = 84°C at 100% Airflow

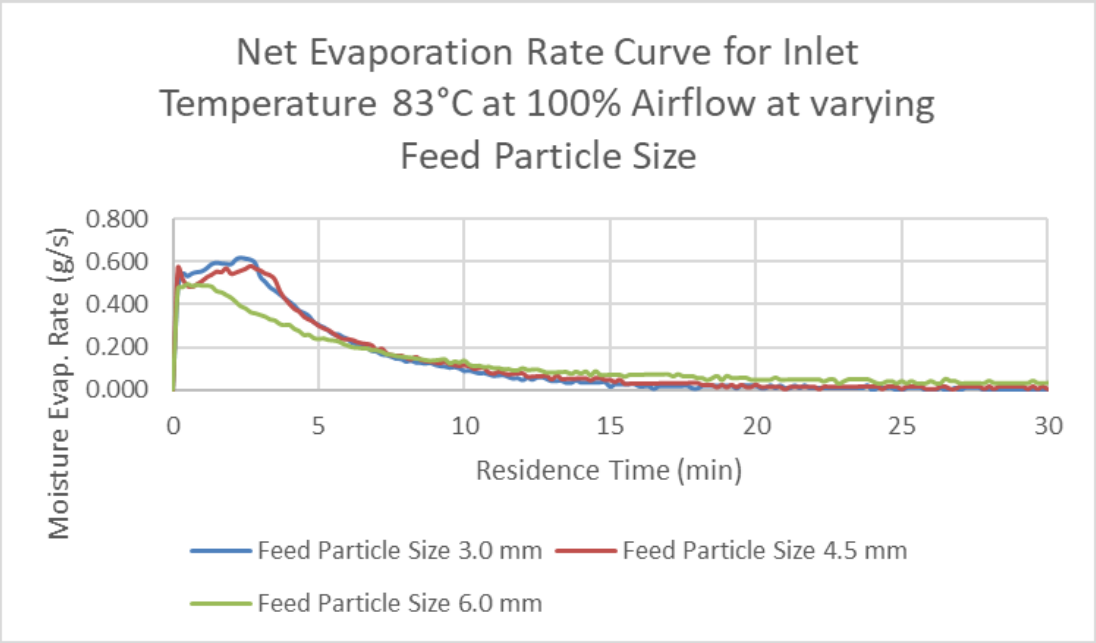

Figure G-3. Net Evaporation Rate Curve at varying Feed Particle Size for Inlet Temperature = 83°C at 100% Airflow

PARTICLE SIZE DISTRIBUTION AT VARYING FEED PARTICLE SIZE

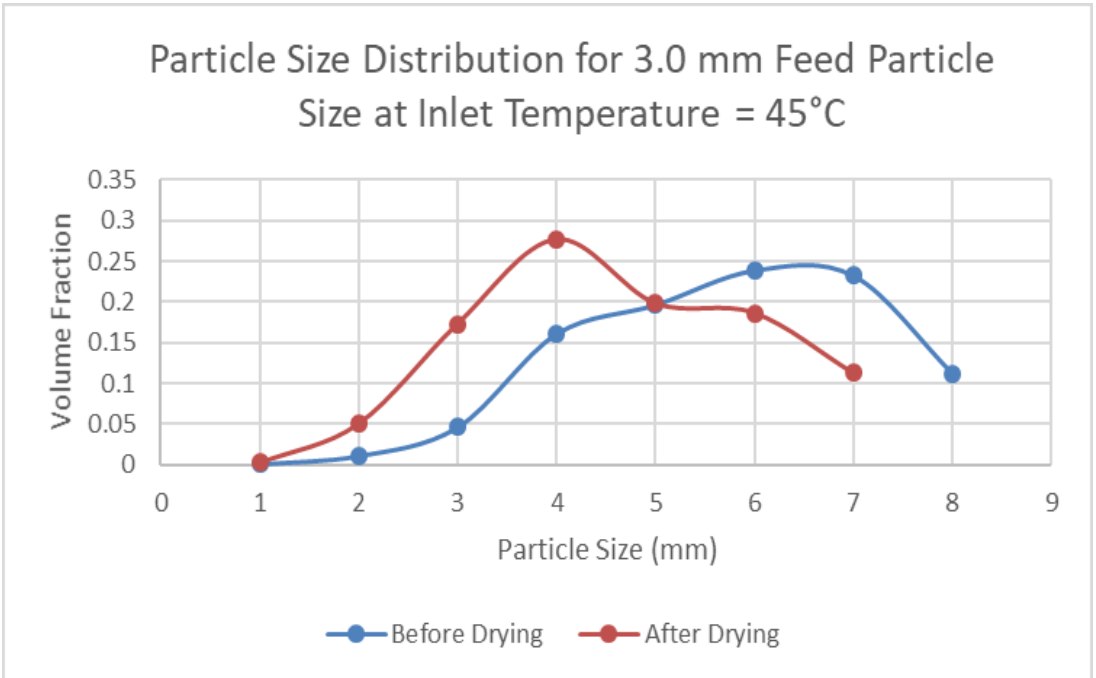

Figure G-4. Particle Size Distribution for Feed Particle Size = 3.0 mm at Inlet Temperature = 45°C

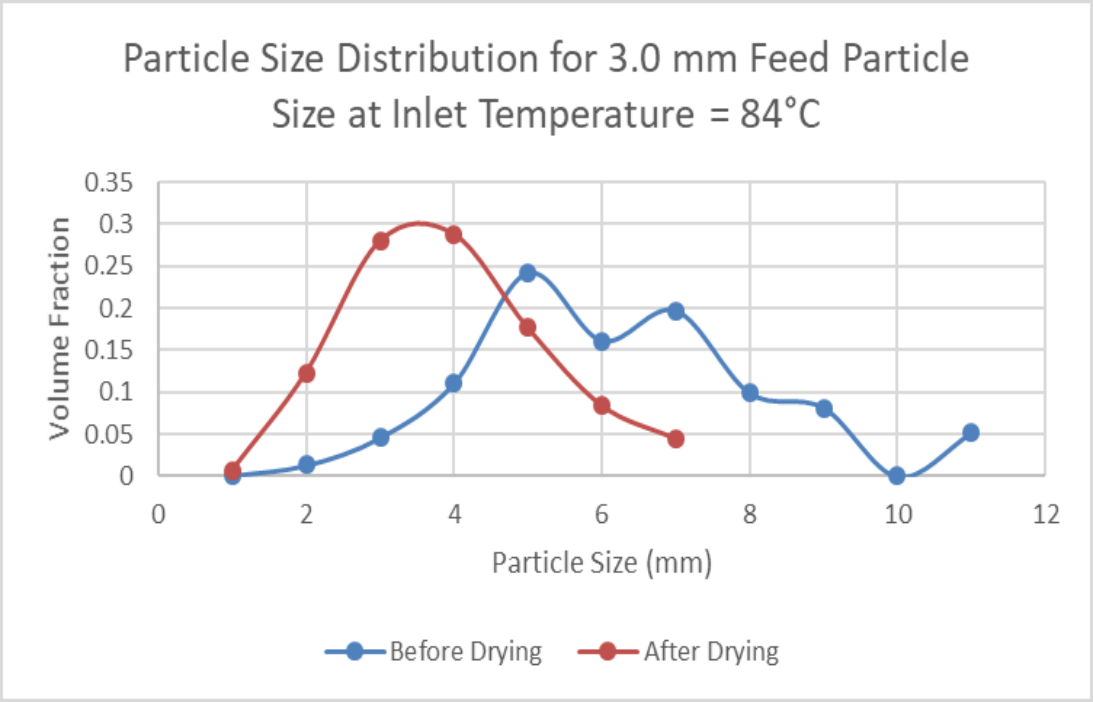

Figure G-5. Particle Size Distribution for Feed Particle Size = 3.0 mm at Inlet Temperature = 84°C

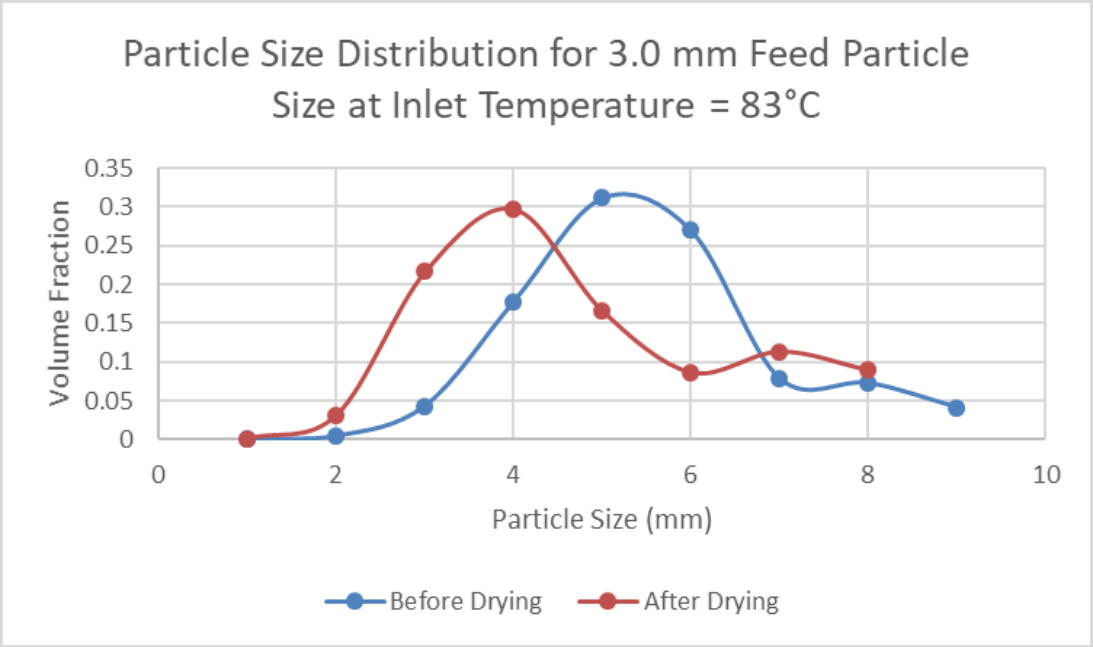

Figure G-6. Particle Size Distribution for Feed Particle Size = 3.0 mm at Inlet Temperature = 83°C

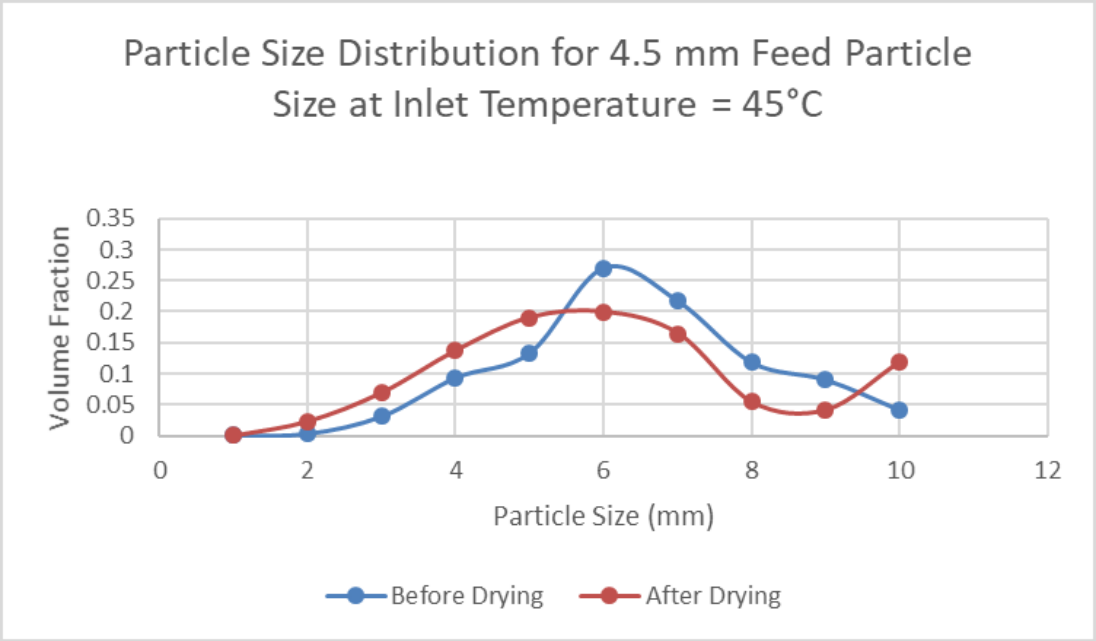

Figure G-7. Particle Size Distribution for Feed Particle Size = 4.5 mm at Inlet Temperature = 45°C

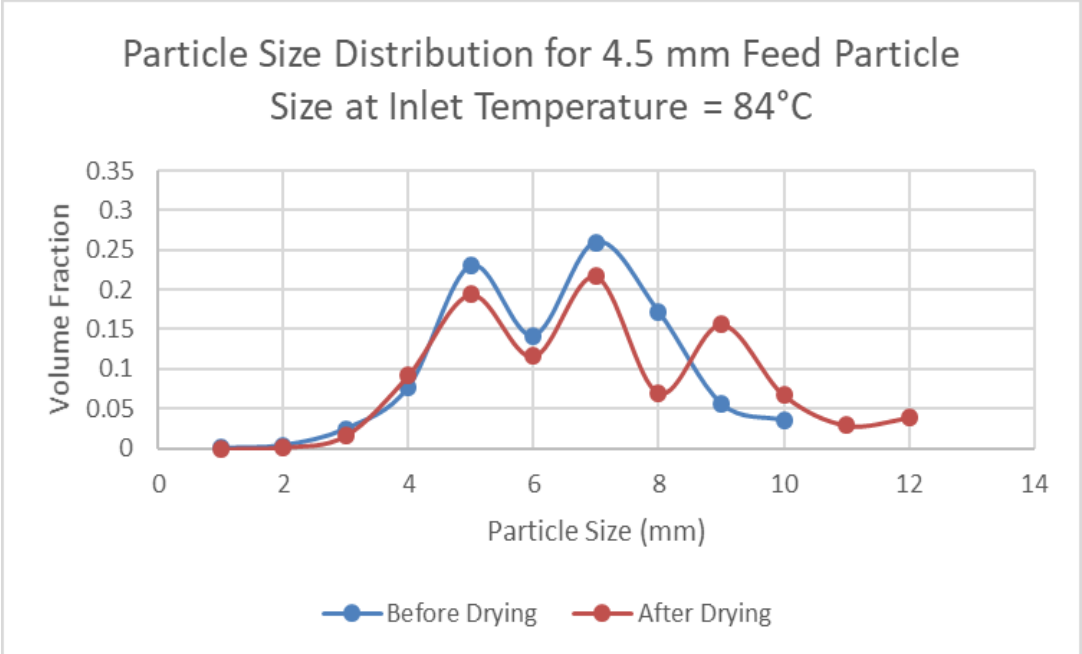

Figure G-8. Particle Size Distribution for Feed Particle Size = 4.5 mm at Inlet Temperature = 84°C

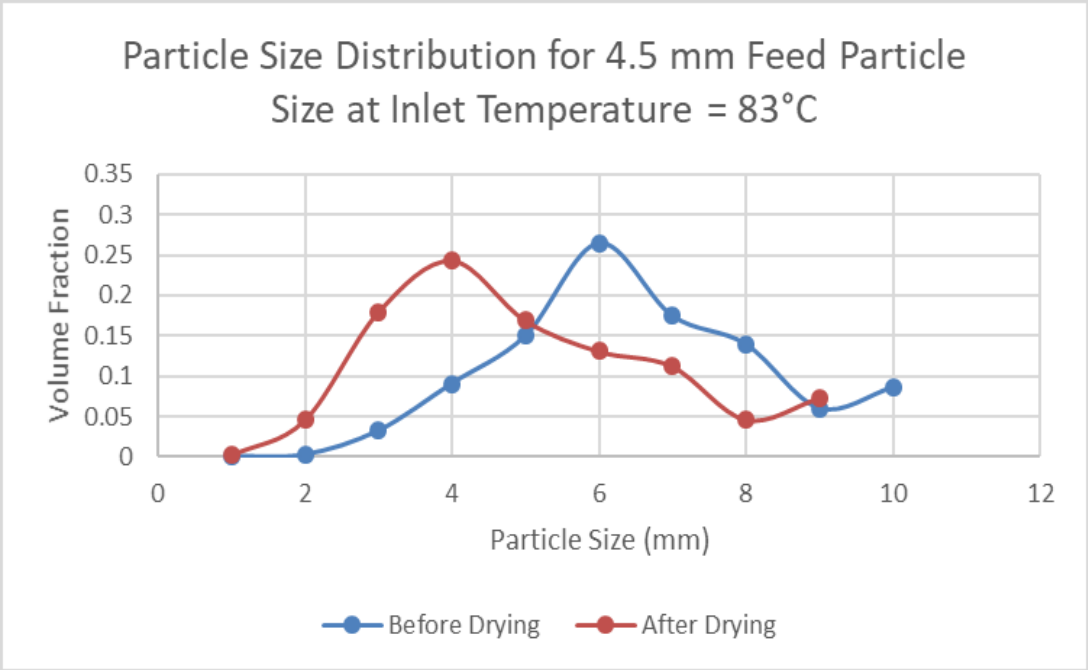

Figure G-9. Particle Size Distribution for Feed Particle Size = 4.5 mm at Inlet Temperature = 83°C

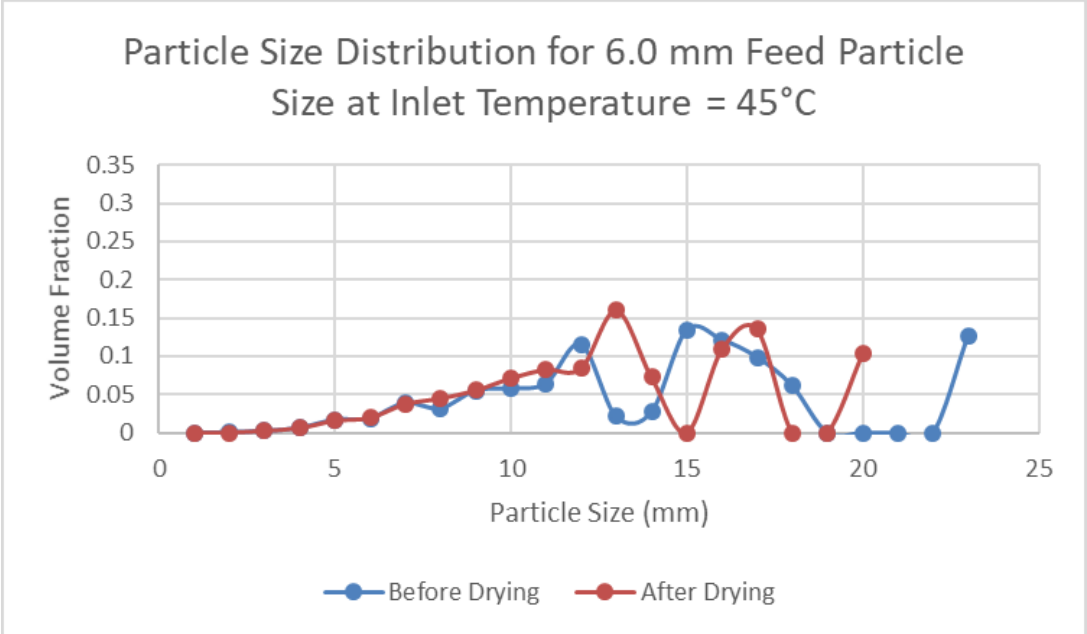

Figure G-10. Particle Size Distribution for Feed Particle Size = 6.0 mm at Inlet Temperature = 45°C

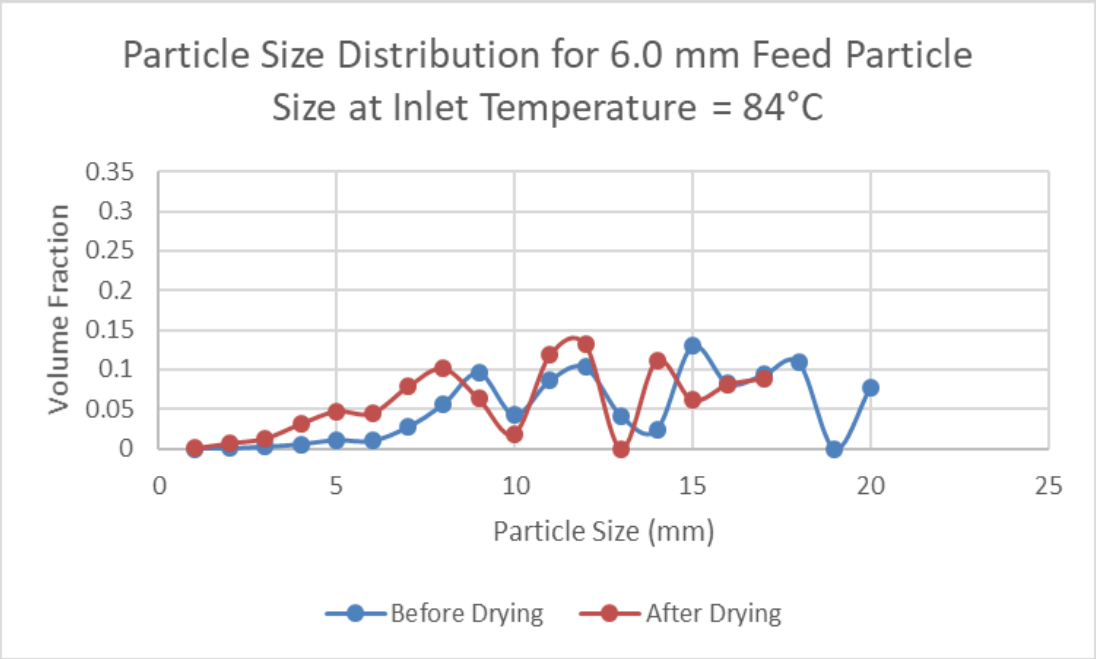

Figure G-11. Particle Size Distribution for Feed Particle Size = 6.0 mm at Inlet Temperature = 84°C

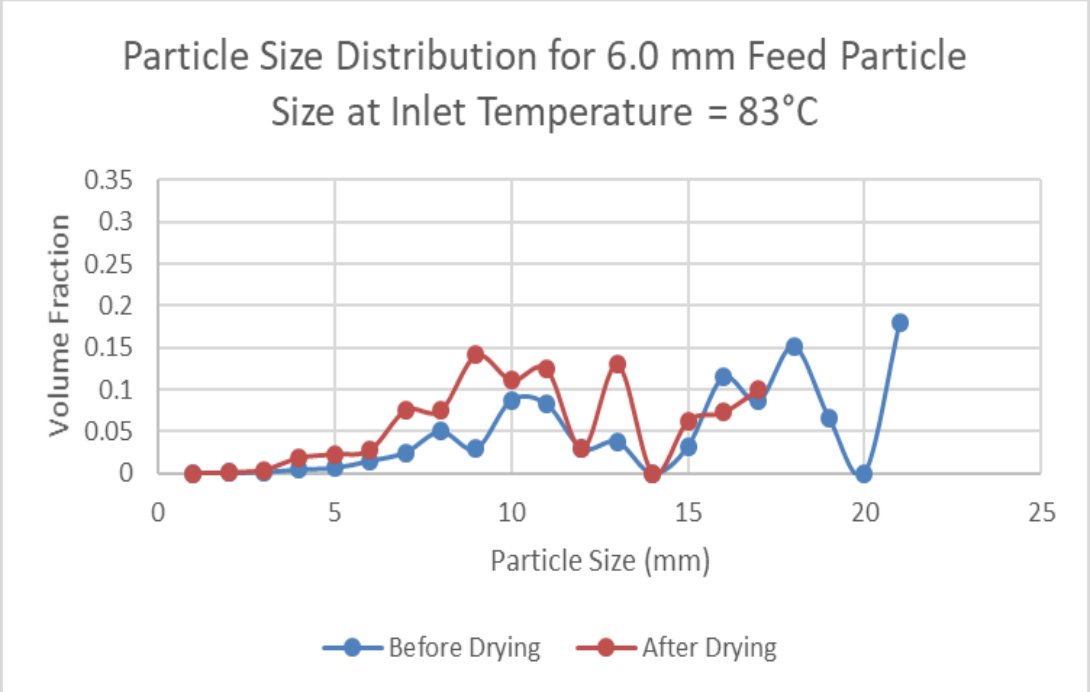

Figure G-12. Particle Size Distribution for Feed Particle Size = 6.0 mm at Inlet Temperature = 83°C

APPENDIX – H

Net Evaporation Rate and Particle Size Distribution for before and after drying at varying Bed Load

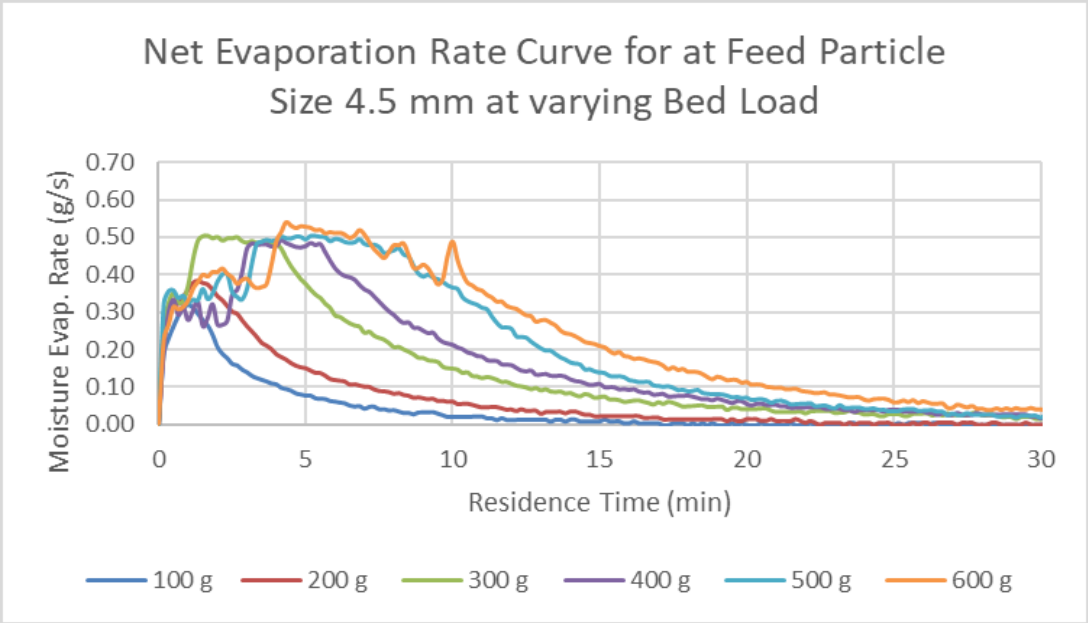

Figure H-1. Net Evaporation Rate Curve at varying Bed Load

PARTICLE SIZE DISTRIBUTION AT VARYING BED LOAD

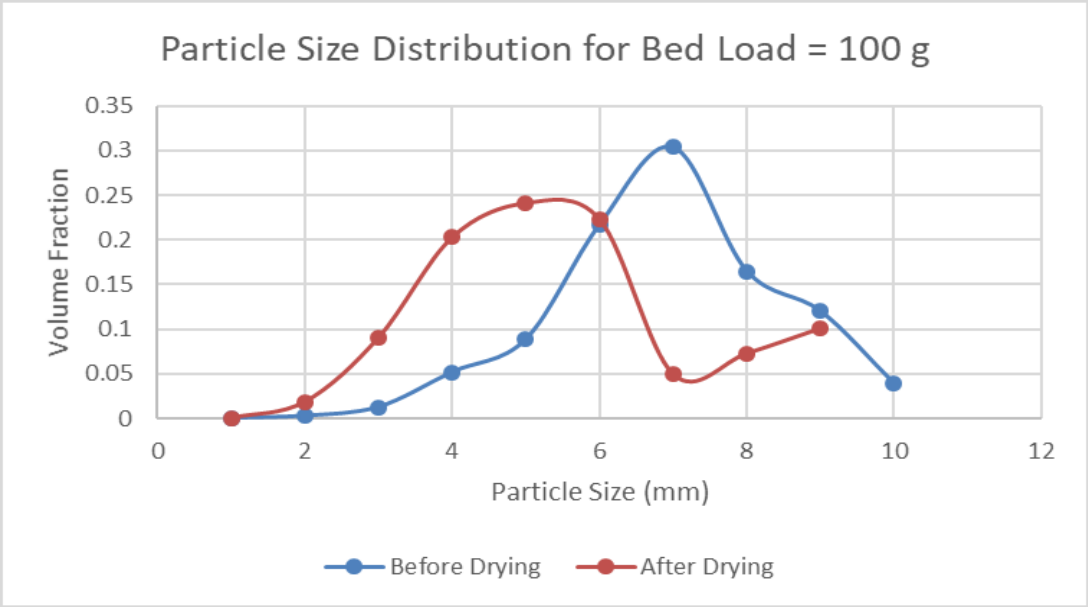

Figure H-2. Particle Size Distribution at Bed Load = 100 g

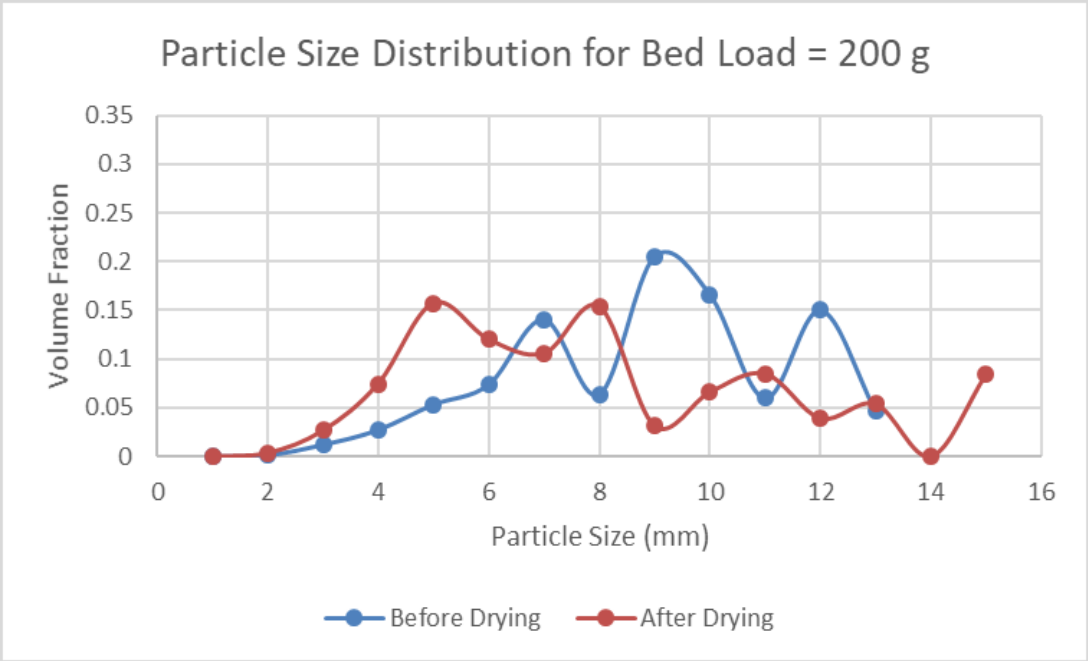

Figure H-3. Particle Size Distribution at Bed Load = 200 g

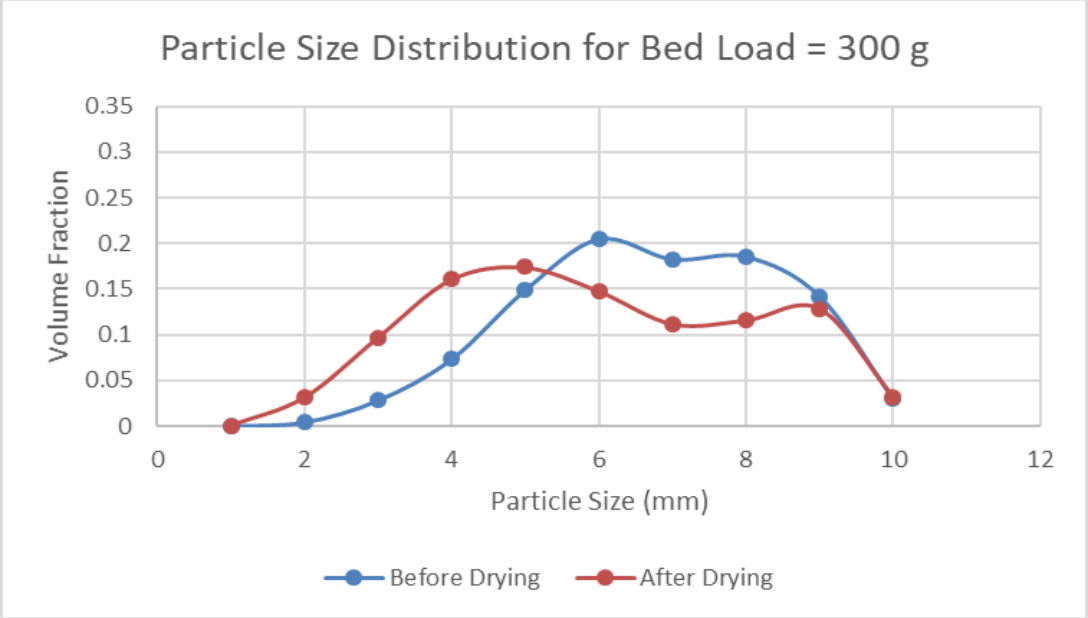

Figure H-4. Particle Size Distribution at Bed Load = 300 g

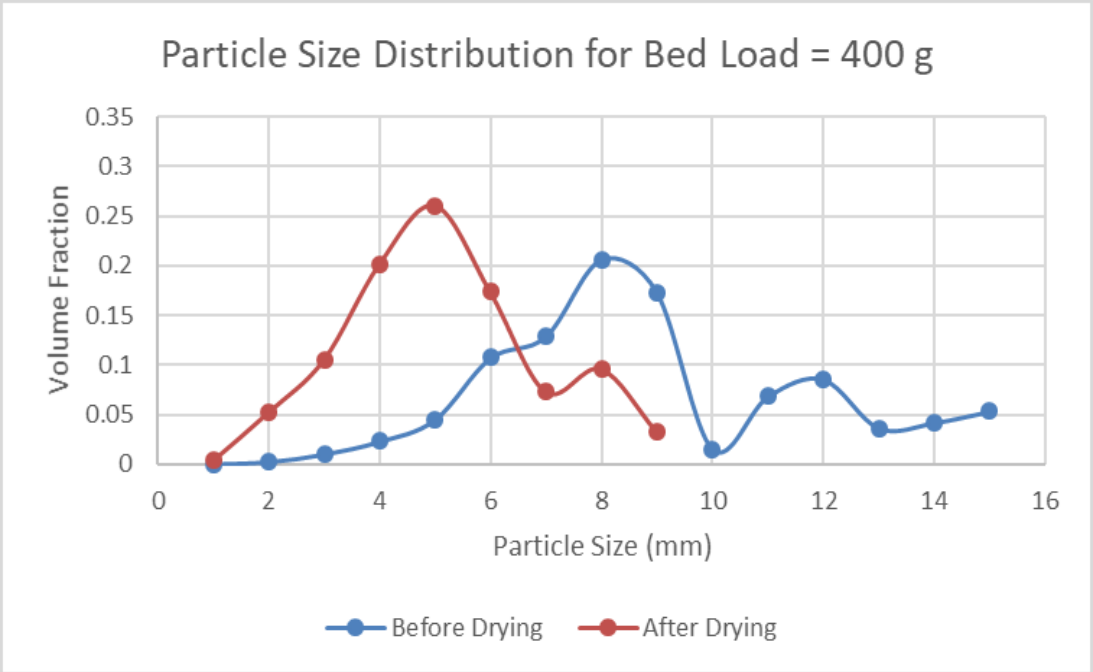

Figure H-5. Particle Size Distribution at Bed Load = 400 g

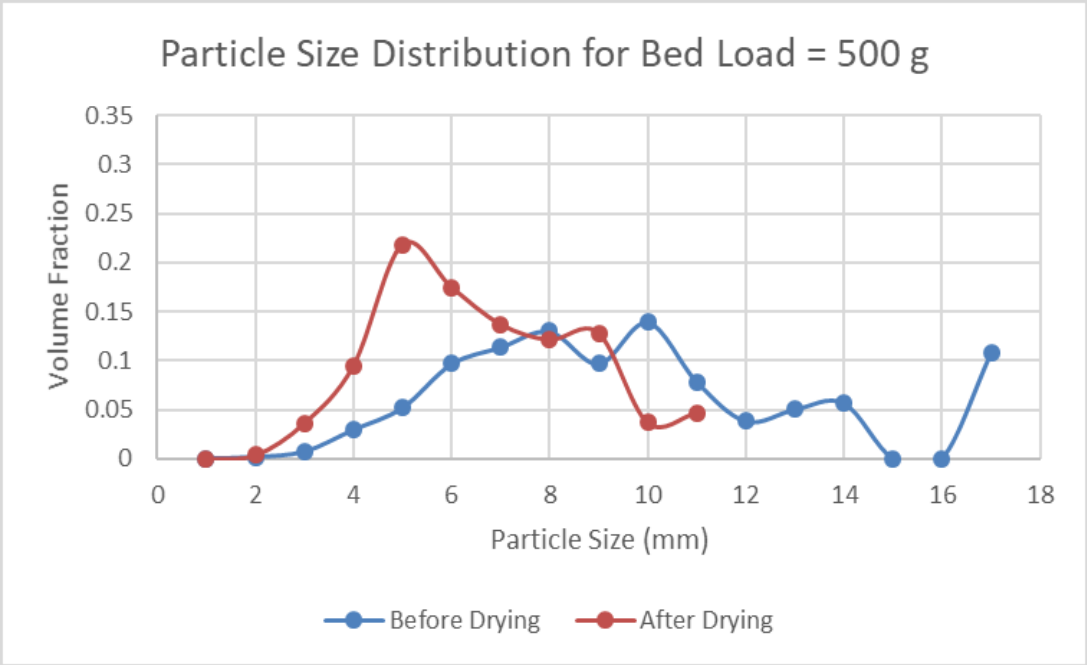

Figure H-6. Particle Size Distribution at Bed Load = 500 g

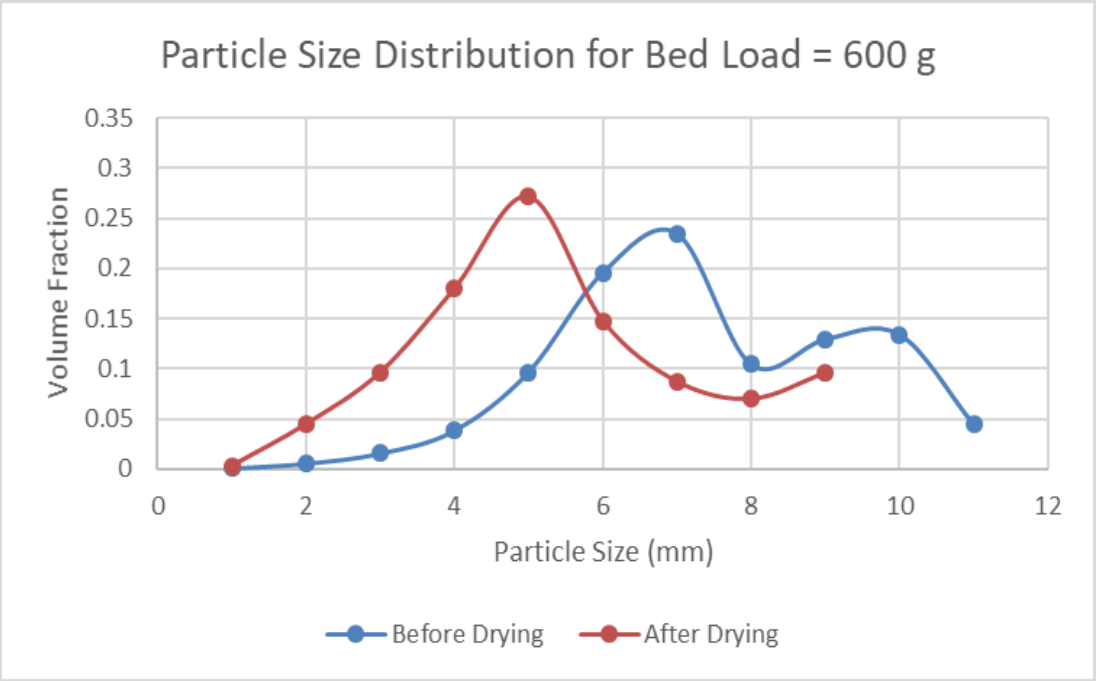

Figure H-7. Particle Size Distribution at Bed Load = 600 g

APPENDIX – I

Net Evaporation Rate and Particle Size Distribution for before and after drying at varying Inlet Temperature

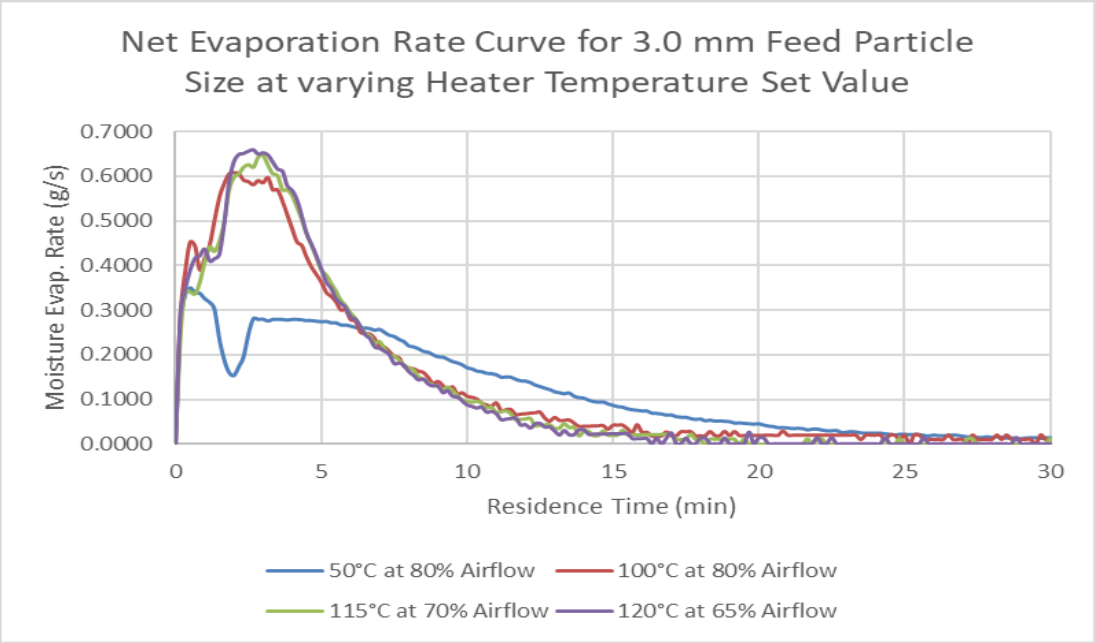

Figure I-1. Net Evaporation Rate Curve for 3.0 mm Feed Particle Size at varying Heater Temperature Set Value

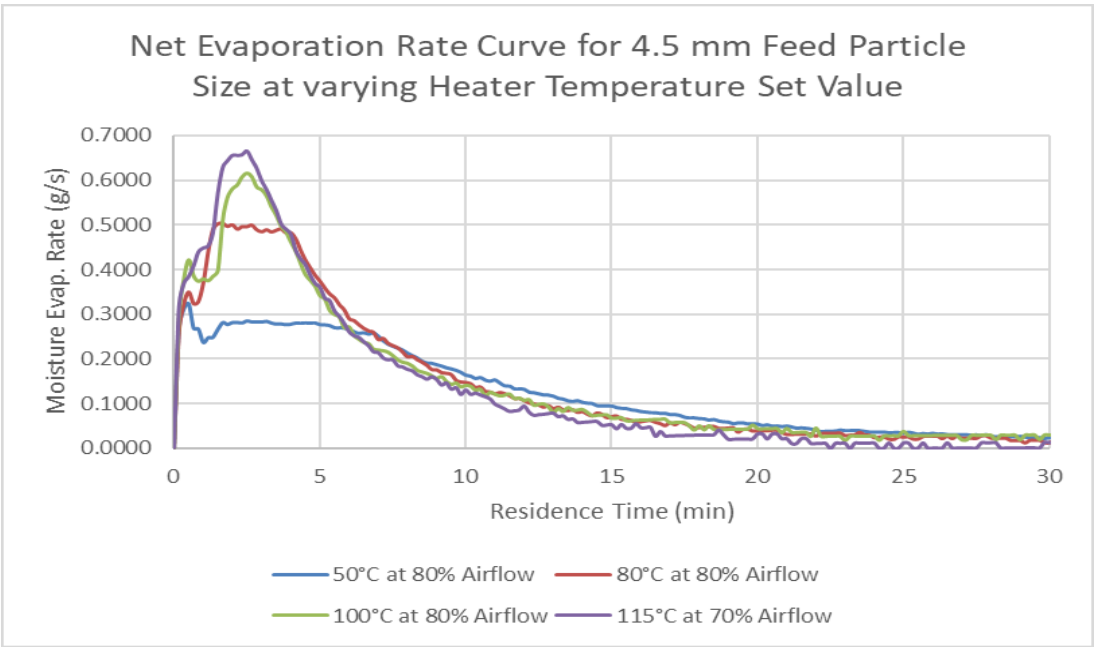

Figure I-2. Net Evaporation Rate Curve for 3.0 mm Feed Particle Size at varying Heater Temperature Set Value

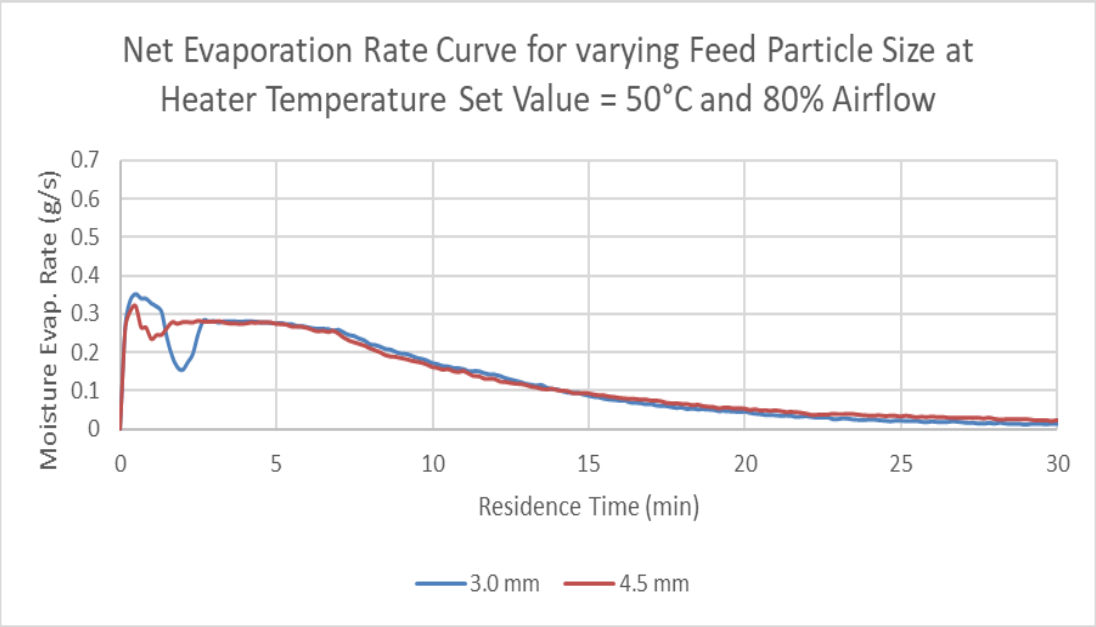

Figure I-3. Net Evaporation Rate Curve for Heater Temperature Set Value = 50°C and 80% Airflow

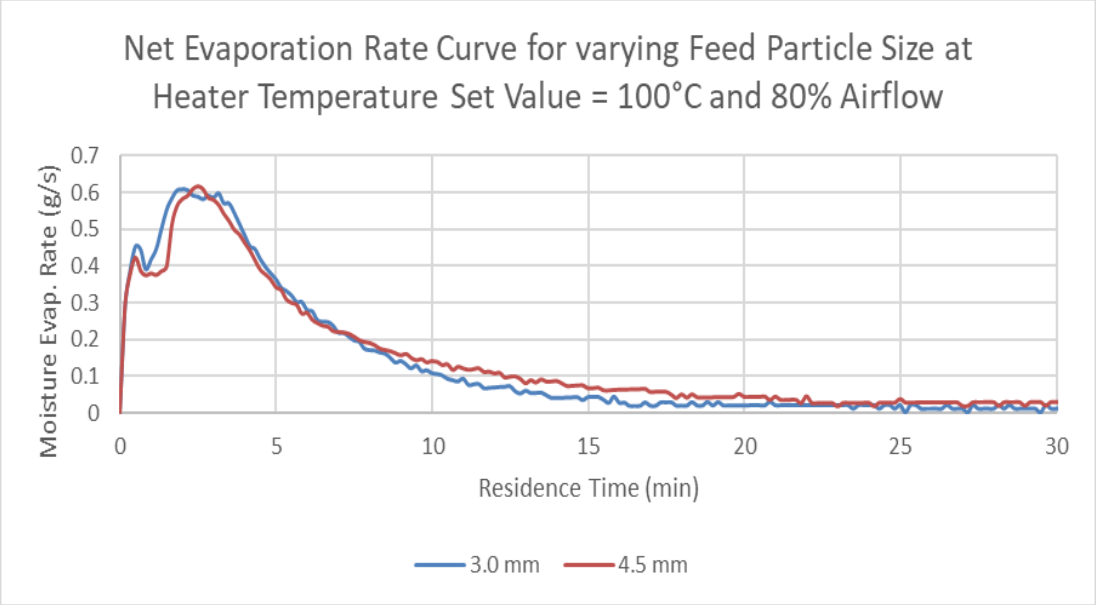

Figure I-4. Net Evaporation Rate Curve for Heater Temperature Set Value = 100°C and 80% Airflow

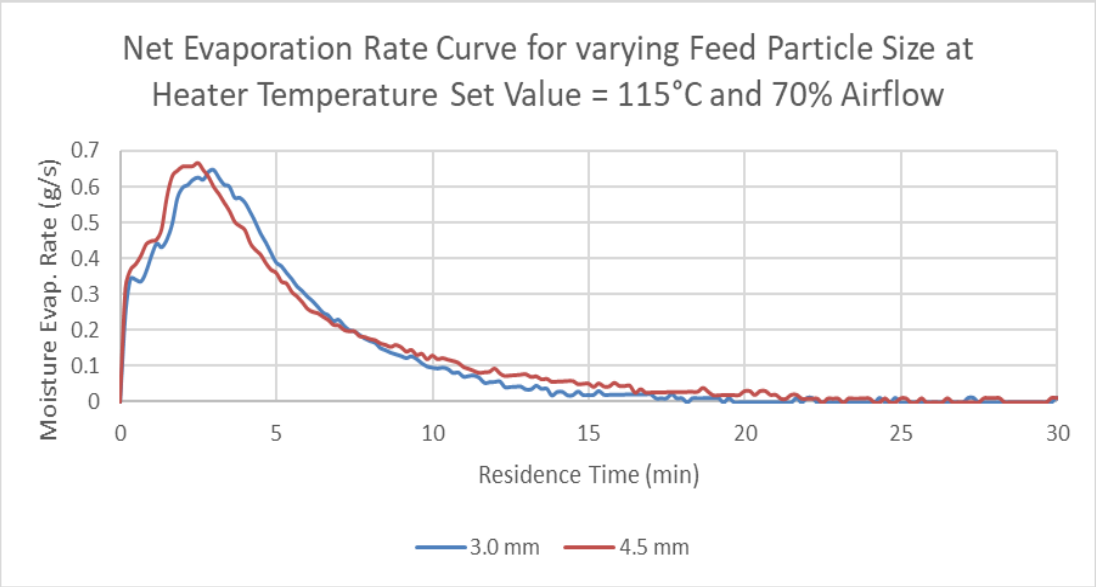

Figure I-5. Net Evaporation Rate Curve for Heater Temperature Set Value = 115°C and 70% Airflow

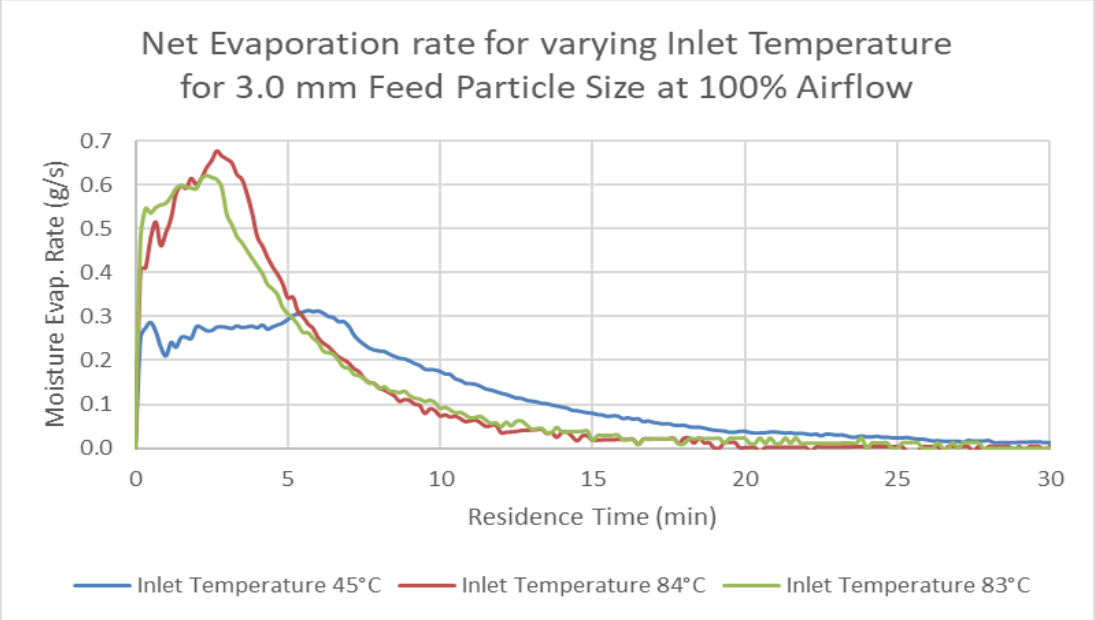

Figure I-6. Net Evaporation Rate Curve for varying Inlet temperature for Feed Particle Size = 3.0 mm at 100% Airflow

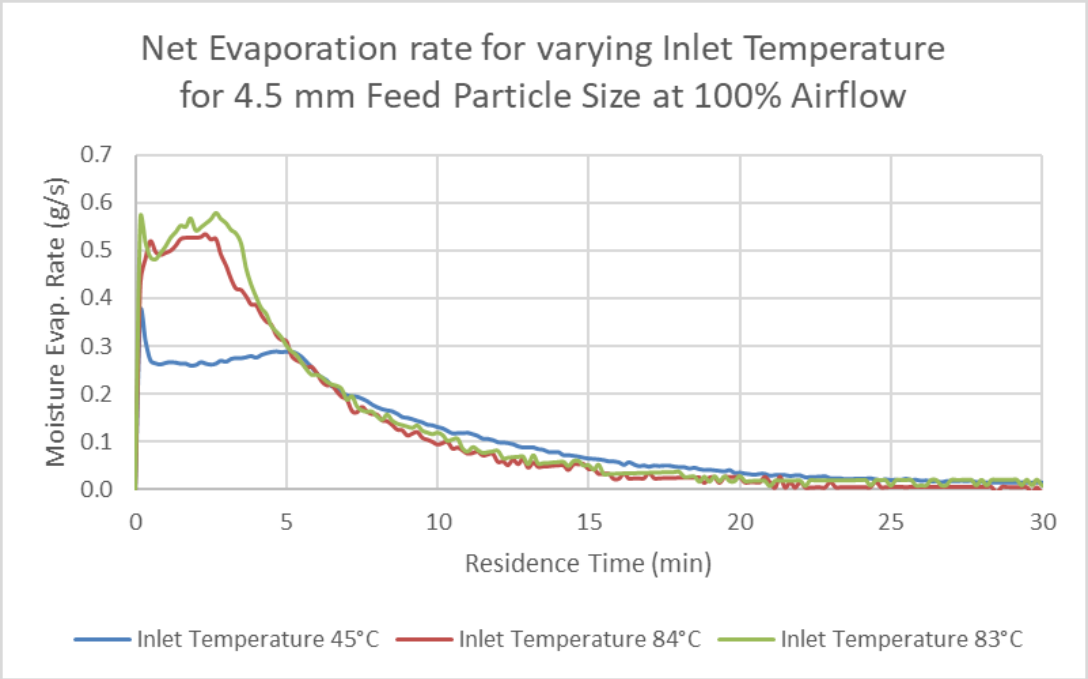

Figure I-7. Net Evaporation Rate Curve for varying Inlet temperature for Feed Particle Size = 4.5 mm at 100% Airflow

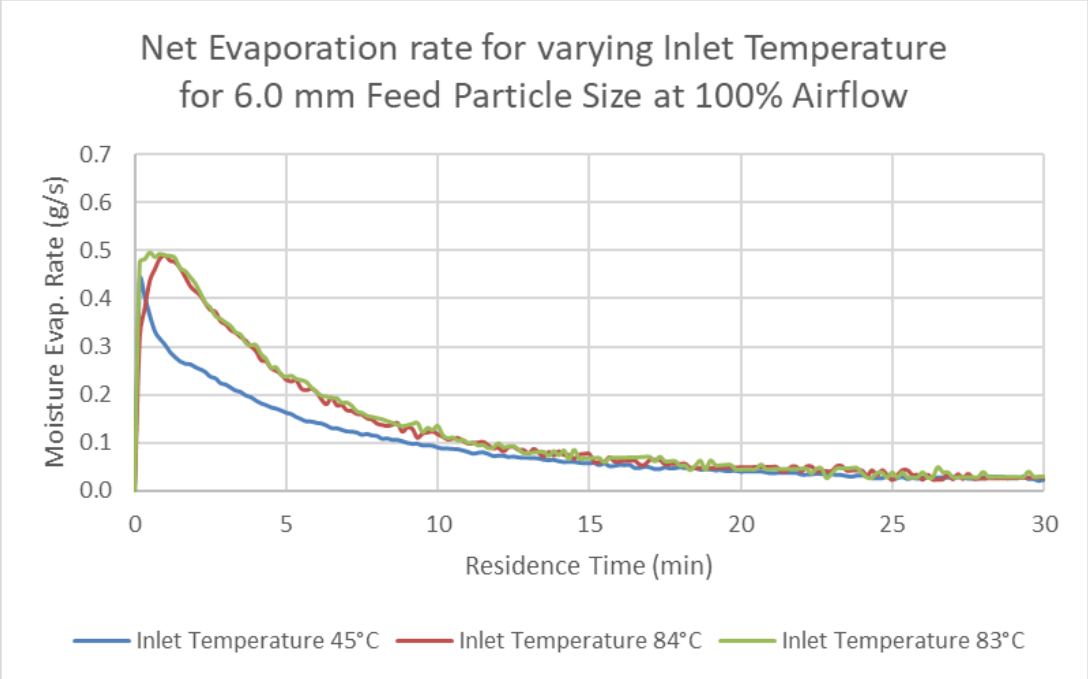

Figure I-8. Net Evaporation Rate Curve for varying Inlet temperature for Feed Particle Size = 6.0 mm at 100% Airflow

PARTICLE SIZE DISTRIBUTION AT VARYING BED LOAD

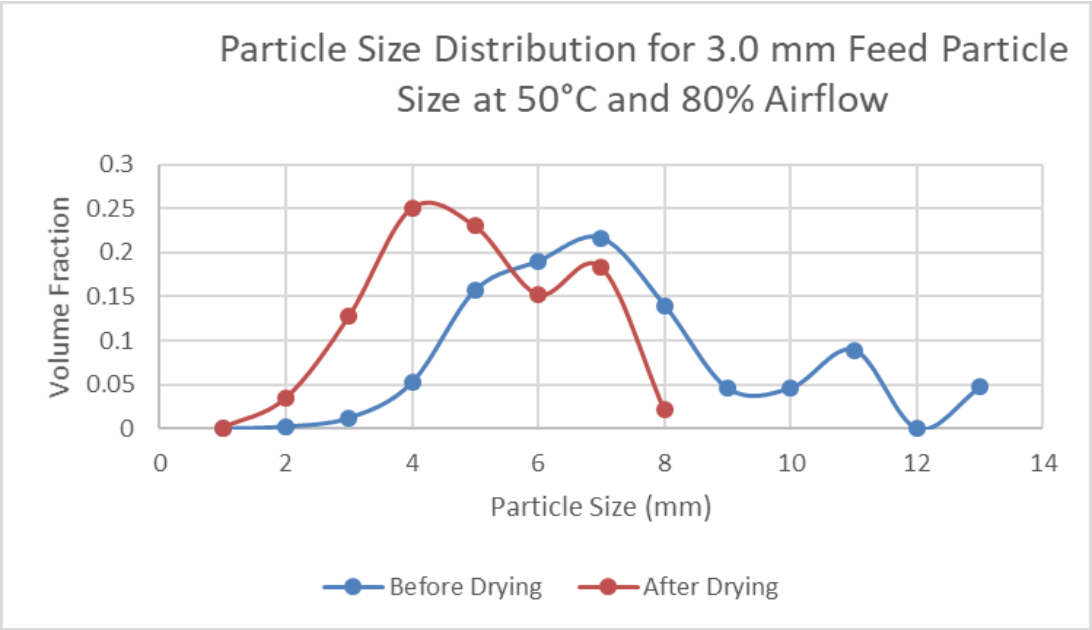

Figure I-9. Particle Size Distribution for 3.0 mm Feed Size Particle at Heater Set Value = 50°C and 80% Airflow

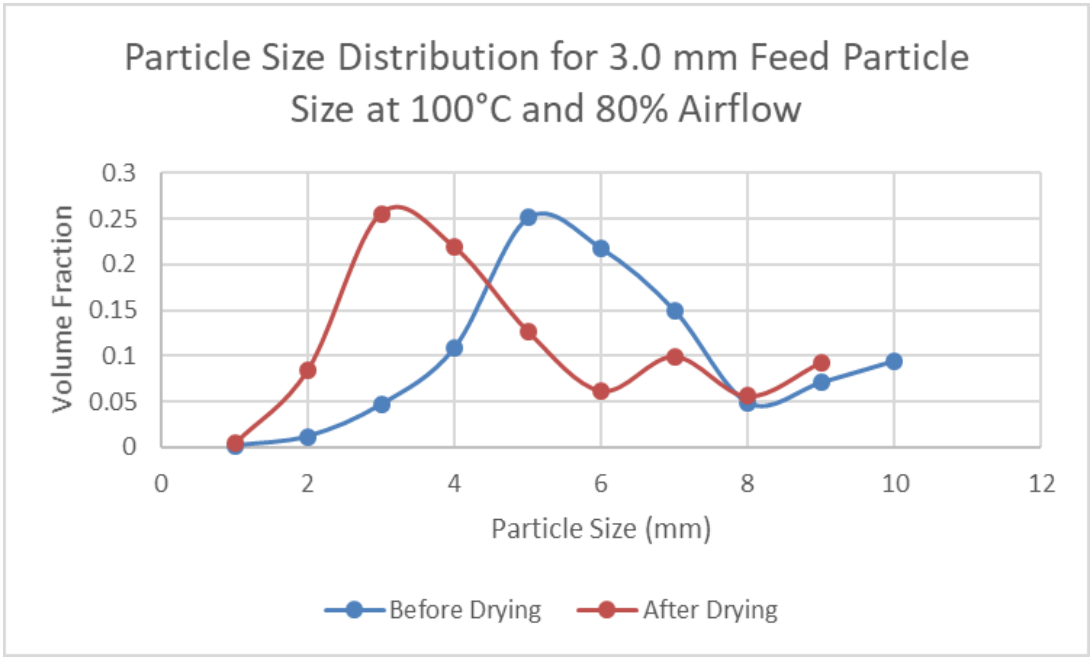

Figure I-10. Particle Size Distribution for 3.0 mm Feed Size Particle at Heater Set Value = 100°C and 80% Airflow

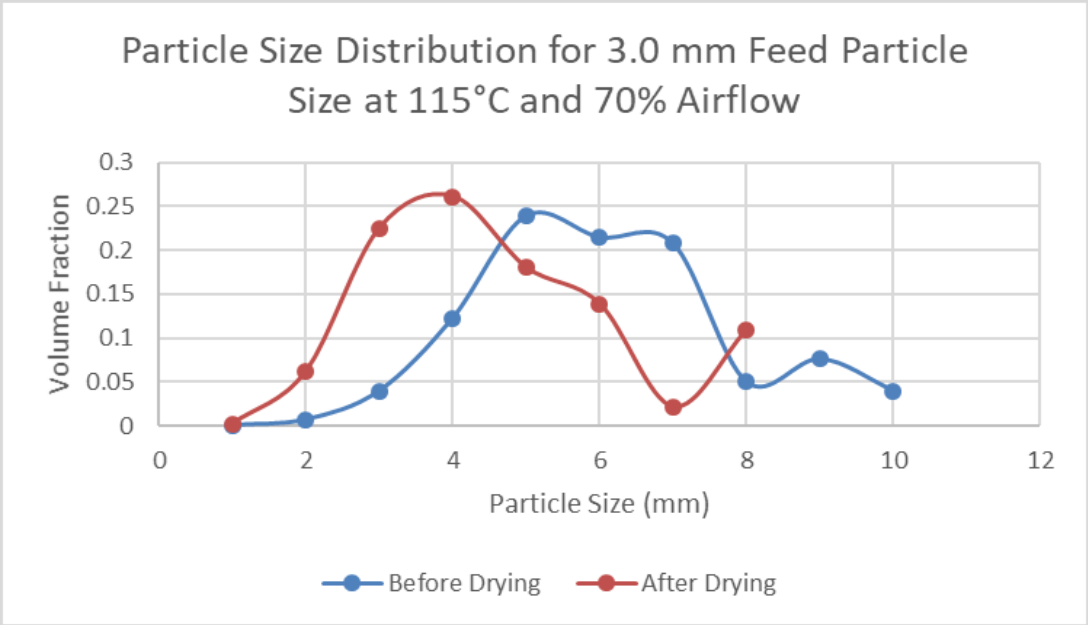

Figure I-11. Particle Size Distribution for 3.0 mm Feed Size Particle at Heater Set Value = 115°C and 70% Airflow

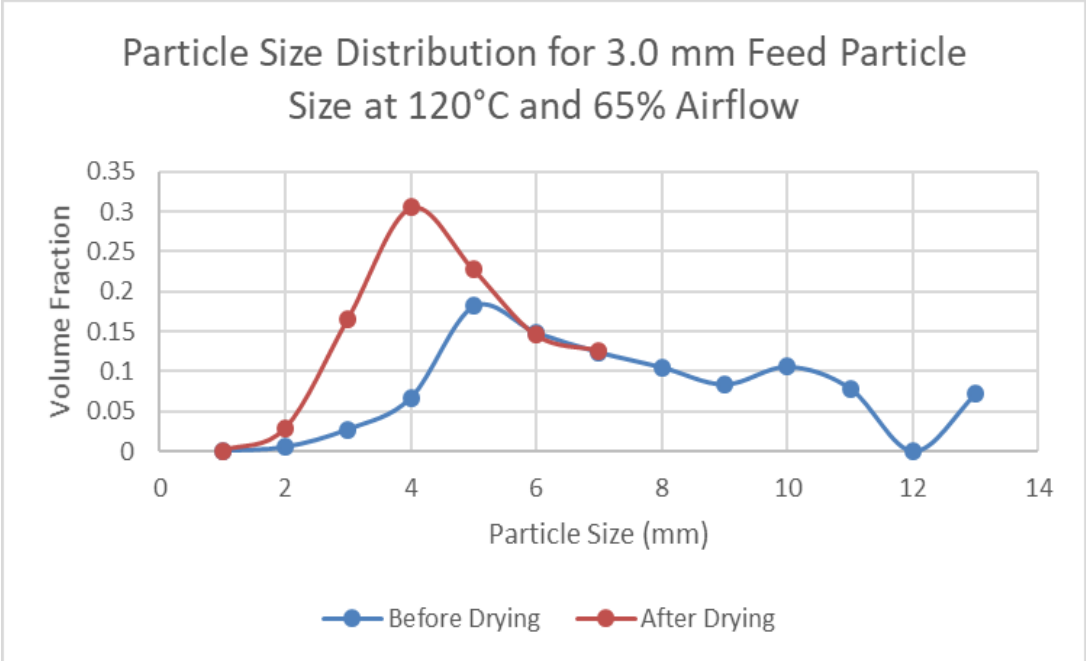

Figure I-12. Particle Size Distribution for 3.0 mm Feed Size Particle at Heater Set Value = 120°C and 65% Airflow

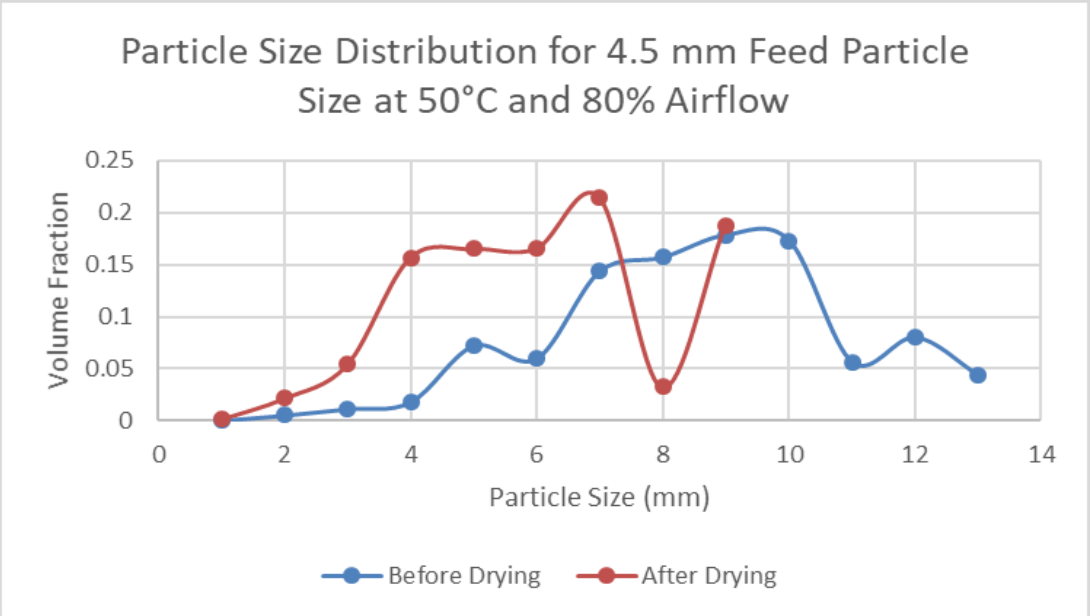

Figure I-13. Particle Size Distribution for 4.5 mm Feed Size Particle at Heater Set Value = 50°C and 80% Airflow

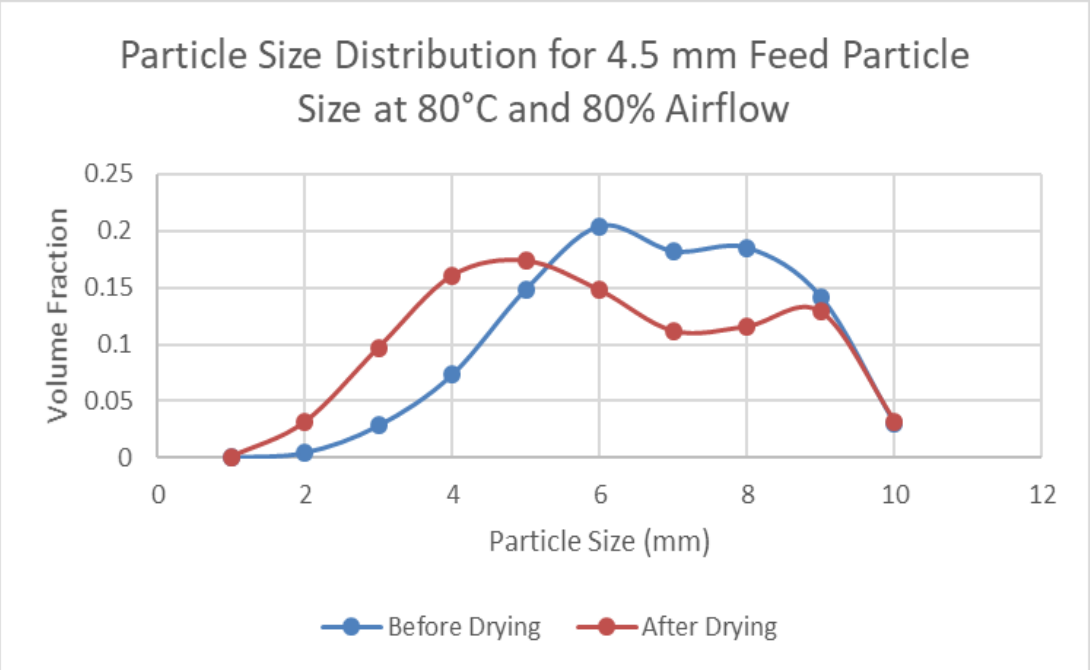

Figure I-14. Particle Size Distribution for 4.5 mm Feed Size Particle at Heater Set Value = 80°C and 80% Airflow

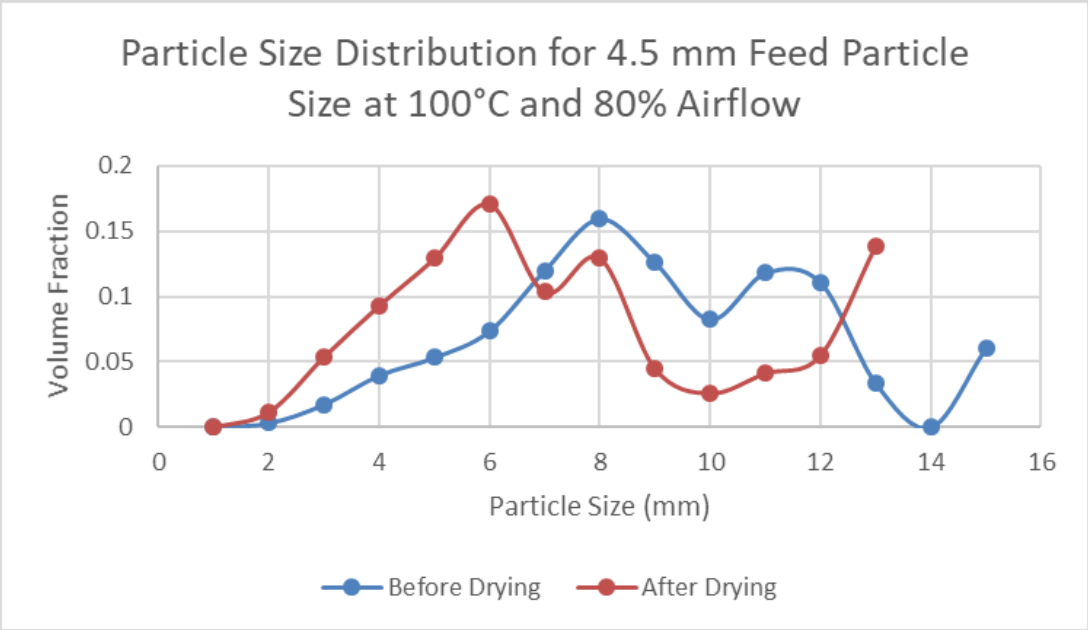

Figure I-15. Particle Size Distribution for 4.5 mm Feed Size Particle at Heater Set Value = 100°C and 80% Airflow

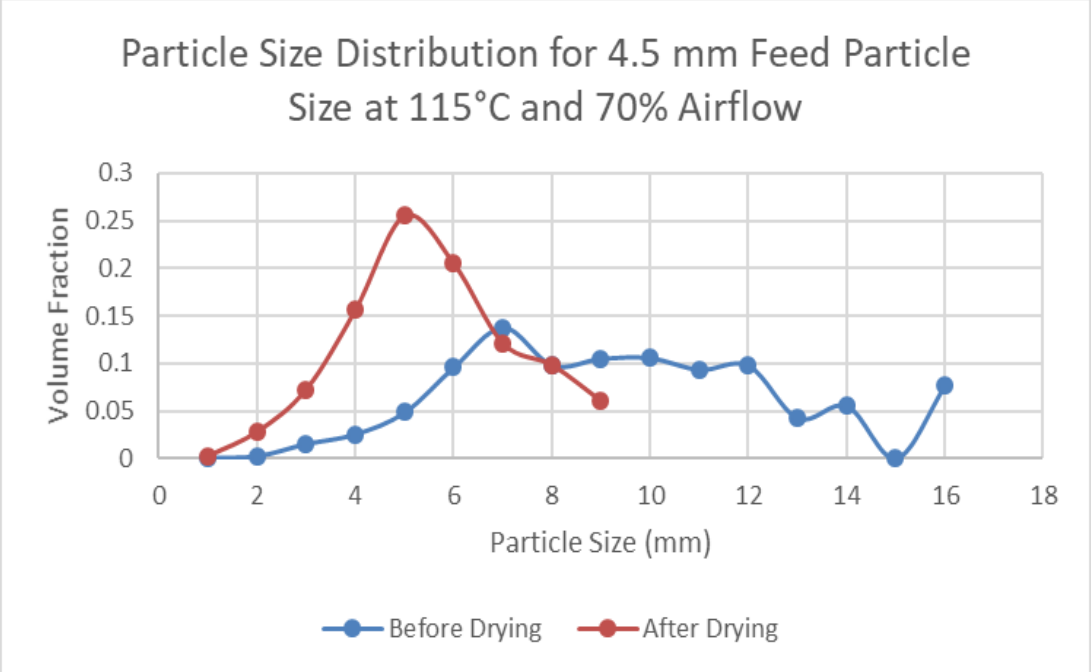

Figure I-16. Particle Size Distribution for 4.5 mm Feed Size Particle at Heater Set Value = 115°C and 70% Airflow